Uncoupling yeast growth and product formation in chemostat and retentostat cultures

Liu, Y.

DOI
10.4233/uuid:110b0119-1b0f-436d-b9a5-81445c17d542

Publication date
2020

Document Version
Final published version

Citation (APA)
Liu, Y. (2020). *Uncoupling yeast growth and product formation in chemostat and retentostat cultures*. [Dissertation (TU Delft), Delft University of Technology]. https://doi.org/10.4233/uuid:110b0119-1b0f-436d-b9a5-81445c17d542

Uncoupling yeast growth and product formation in chemostat and retentostat cultures

Dissertation

for the purpose of obtaining the degree of doctor
at Delft University of Technology,
by the authority of the Rector Magnificus Prof.dr.ir. T.H.J.J. van der Hagen,
chair of the Board for Doctorates
to be defended publicly on
Monday 28 September 2020 at 12:30 o'clock

by

Yaya LIU

Master of Science in Biochemical Engineering,
East China University of Science and Technology, China
Born in Xinyang, China

This dissertation has been approved by the

Promotor: Prof. dr. J.T. Pronk
Copromotor: Dr. W.M. van Gulik

Composition of the doctoral committee:

Rector Magnificus	chairperson
Prof. dr. J.T. Pronk	Delft University of Technology, promotor
Dr. W.M. van Gulik	Delft University of Technology, copromotor

Independent members:

Prof. dr. F.J. Bruggeman	Vrije Universiteit Amsterdam
Prof. dr. P. Osseweijer	Delft University of Technology
Dr. L. Domingues	Universidade do Minho, Portugal
Dr. ir. M.L.A. Jansen	DSM
Prof. dr. F. Hollman	Delft University of Technology, reserve member

Other member:

Prof. dr. P.A.S. Daran-Lapujade	Delft University of Technology

The research presented in this thesis was performed at the Cell Systems Engineering section, Department of Biotechnology, Faculty of Applied Sciences, Delft University of Technology, The Netherlands. The project was financed by the BE-Basic R&D Program, which was granted a FES subsidy from the Dutch Ministry of Economic Affairs.

Cover designed by Yaya Liu
Printed by Ipskamp Printing

ISBN: 978-94-6421-013-2

Contents

List of Abbreviations

G6P Glucose 6-phosphate

F6P Fructose 6-phosphate

F1,6BP Fructose 1,6-bisphosphate

GADP Glyceraldehyde 3-phosphate

DHAP Dihydroxyacetone phosphate

1,3BPG 1,3-Bisphosphoglyceric acid

3PG 3-Phosphoglyceric acid

2PG 2-Phosphoglyceric acid

PEP Phosphoenolpyruvic acid

Pyr Pyruvate

AC-CoA Acetyl coenzyme A

CoA Coenzyme A

CIT Citrate

ISOCIT Isocitrate

α-KG α-ketoglutarate

SUCCoA Succinyl-CoA

SUC Succinate

FUM Fumarate

G1P Glucose 1-phosphate

T6P Trehalose 6-phosphate

6PG 6-phosphogluconate

M6P Mannose 6-phosphate

UDP-Gluc Uridine diphosphate glucose

Ribu5P Ribulose-5-phosphate

Rib5P Ribose-5-phosphate

Xyl5P Xylulose-5-phosphate

Sed7P Sedoheptulose-7-phosphate

E4P Erythrose-4-phosphate

F6P Fructose-6-phosphate

NAD(H) Nicotinamide adenine dinucleotide

FAD(H2) Flavin adenine dinucleotide

ATP Adenosine triphosphate

ADP Adenosine diphosphate

AMP Adenosine monophosphate

GTP Guanosine triphosphate

GDP Guanosine diphosphate

MAL Malate

OAA Oxaloacetate

Ala Alanine

Val Valine

Ile Isoleucine

Ser Serine

Met Methionine

Phe Phenylalanine

Glu Glutamic acid

Asn Asparagine

Tyr Tyrosine

Trp Tryptophan

ACE Acetaldehyde

EtOH Ethanol

Gly Glycine

Leu Leucine

Pro Proline

Thr Threonine

Asp Aspartic acid

Cys Cysteine

Lys Lysine

Gln Glutamine

His Histidine

Summary

The progress of modern biotechnology has enabled the development of fermentation processes for production of fuels and chemicals from renewable feedstocks. Compared with traditional petrochemical synthesis, bio-based production processes are more sustainable and environmental friendly. In recent decades, several bio-based manufacturing plants have been established for the successful commercial production of various high-value-added compounds (e.g. pharmaceuticals, enzymes and bioplastics).

The current fermentation processes for bio-based production commonly start with a growth phase of the microorganisms followed by a production phase. This implies that biomass formation competes with the production of the desired product in terms of consumption of the feedstock. In industrial fermentations, maximizing the product yield, in other words, minimizing the substrate flux to biomass, CO_2 and byproducts is the primary goal. To reach this objective, uncoupling of microbial growth from product formation seems like a feasible approach, providing that the microbial host maintains a high productivity in the absence of growth. The latter represents a scientific challenge, as low or near-zero growth rates are generally accompanied by a low metabolic activity.

Over the past 15 years, researchers from Delft University of Technology have used the yeast *S. cerevisiae*, one of the most commonly applied microbial cell factories in industrial fermentations, as a model microorganism to study its physiology and robustness at near-zero growth rates as well as the possibility of uncoupling growth from product formation. By applying retentostat cultures, in which a filter in the effluent line ensures that the biomass is retained in the bioreactor, near-zero growth can be reached by limited supply of the carbon and energy source glucose. The results from these studies indicated that the near-zero growth yeast cells were stable, robust and metabolically active. More specifically, the cells maintained a considerable ethanol productivity during prolonged growth in anaerobic, carbon-limited retentostat cultures. In addition, a culture viability of above 80 % and a high metabolic capacity were observed during prolonged cultivation in anaerobic and as well as aerobic retentostats.

In the research presented in this thesis the zero-growth concept is developed further towards industrial application, using succinic acid as a model product. To this end, industrially relevant conditions were chosen, as reflected by aerobic cultivation at low pH and at a high dissolved CO_2 level. The main aim was to improve understanding of the physiology of yeast at near-zero growth rates and thereby provide insights for the design of industrial fermentation processes based on the zero-growth concept. Specifically, we set out to investigate the applicability of retentostat cultivation for non-catabolic products, that is, products whose synthesis from sugar requires a net input of ATP.

As mentioned above, in previous research on zero-growth cultivation, growth was limited by severely restricting the supply of the carbon and energy source glucose. When aiming at the application of zero-growth cultivations for the production of compounds of which the biosynthesis requires a net input of energy, carbon and energy limited cultivation does not seem to be an obvious choice. Therefore, it was decided for to explore options to limit growth in retentostats by nutrients other than the carbon and energy source.

Chapter 2 described the design and implementation of retentostat regimes for aerobic carbon-excess, nitrogen- or phosphorus-limited cultivation of the reference strain *S. cerevisiae* CENPK113-7D. An experimental setup was implemented that allowed for a smooth transition from low growth rate chemostat cultures to near-zero growth retentostat cultures. Addition of low concentrations of ammonium or phosphate to the reservoir media was required to compensate for loss of extracellular N- or P-containing compounds during retentostat cultivation. Near-zero growth rates ($\mu < 0.001$ h^{-1}) were successfully achieved in both N- and P-limited retentostat cultures. In these cultures, viability was maintained above 80 %. Quantifications of intracellular ATP, ADP and AMP levels indicated that under these conditions an adequate energy status was maintained and the cells were in a metabolically active state. Strongly reduced cellular contents of the growth-limiting element (N or P) were observed in both chemostats as well as retentostats and were accompanied by high accumulation levels of storage carbohydrates were shown. Compared to the previous C-limited retentostat cultures that applied a similar experimental setup, the N- and P-limited cultures showed: (1) aerobic ethanol fermentation

as a result of the Crabtree effect; (2) a partial uncoupling of catabolism and anabolism; (3) a much higher non-growth associated dissimilation rate.

As a follow up of this fundamental physiology study under N- and P- limited conditions, Chapter 3 was focused on the physiological impact of industrially relevant, harsh cultivation conditions: low pH and high CO_2 levels in both C-limited and C-excess, N-limited slow growth chemostats and retentostats of the same strain. Thes conditions to a large extent simulated the conditions of the industrial succinic acid fermentation process: slow growth, low pH and high CO_2. Under C-limited pH 3 and 50 % CO_2 condition, through near-zero growth ($\mu < 0.001\ h^{-1}$) was reached, a severe loss of culture viability was shown, in which the viability decreased from above 80 % in slow growing chemostats to only 25 % in retentostats. Furthermore, an 8-fold higher specific death rate and more than 2-fold higher maintenance energy requirement were observed compared with the aerobic C-limited pH 5 near-zero growth retentostat cultures. Further experiments showed that these effects were predominantly triggered by low pH. Growth under C-excess, N-limited conditions did not ameliorate these adverse impacts, specifically, the preceding low growth rate chemostats already showed a viability of 50 %, and after redirecting to retentostats the viability decreased to only 25 % at near-zero growth. The non-growth associated energy requirement was also much higher than observed in N-limited cultures at pH 5 (Chapter 2). Clearly, the decreased viability was not induced by the extreme nutrient limitation by carbon or nitrogen. Transcriptome analysis showed that the cellular response low pH may involve the common (MAPK-) signalling pathways, notably the cell wall integrity (CWI), high osmolality glycerol (HOG) and calcineurin pathways.

Chapter 4 integrated the findings from the previous chapters by addressing the applicability of the zero-growth concept for high-yield succinic acid (SA) production by an engineered industrial strain of *S. cerevisiae*. Firstly we investigated to which extent the SA productivity of this engineered yeast strain was coupled with growth. Therefore the strain was cultivated at specific growth rates between 0.085 and 0.005 h^{-1} in N-limited chemostat and retentostat cultures under industrially relevant conditions (pH 3 and 50 % CO_2). The specific SA production rate decreased asymptotically with decreasing growth rate and stabilized at a value of 0.75 mmol/(g viable biomass)/h at near-zero growth

rate, showing that SA production rate is associated with the growth rate but that uncoupling from growth could be achieved. Although at near-zero growth rates a non-negligible amount of glucose was converted into byproducts (mainly malate, ethanol and glycerol), these conditions resulted in the highest overall SA yield on glucose due to the virtual absence of glucose conversion into biomass. Culture viabilities of the industrial strain were above 80 % for all chemostat cultures, which was higher than observed for the reference strain (Chapter 3). However, after switching to retentostat cultivation, culture viability rapidly dropped to around the same level as the reference strain (25 %, Chapter 3), but the cultures maintained a stable cellular energy status.

This study illustrates the potential for high-yield production of non-dissimilatory products at near-zero growth rates, with growth being limited by nutrients other than the carbon and energy source. In addition, it highlights a requirement for further research into enhance strain robustness under industrial conditions, with specific attention for low-pH tolerance.

Samenvatting

De vooruitgang van de moderne biotechnologie heeft de ontwikkeling mogelijk gemaakt van fermentatieprocessen voor de productie van brandstoffen en chemicaliën uit hernieuwbare grondstoffen. Vergeleken met traditionele petrochemische synthese zijn dergelijke productieprocessen veel duurzamer en milieuvriendelijker. In de afgelopen decennia zijn er verschillende fabrieken opgericht voor de succesvolle biologische productie van onder andere geneesmiddelen, enzymen en plastics op commerciële schaal.

In de huidige fermentatieprocessen wordt de productiefase meestal voorafgegaan door een groeifase van de microorganismen. Dit houdt in dat een niet onaanzienlijk deel van de gebruikte grondstof wordt omgezet in microbiële biomassa in plaats van in het gewenste product. Echter, bij industriële fermentaties is het maximaliseren van de productopbrengst, oftewel het minimaliseren van de substraatstroom naar biomassa, CO_2 en bijproducten het primaire doel. Om dit doel te bereiken, lijkt het loskoppelen van microbiële groei en productvorming een haalbare aanpak, op voorwaarde dat de microbiële gastheer een hoge productiviteit behoudt in afwezigheid van groei. Dit laatste vormt een wetenschappelijke uitdaging, aangezien lage groeisnelheden over het algemeen gepaard gaan met een lage metabole activiteit.

Onderzoekers van de Technische Universiteit Delft hebben de afgelopen 15 jaar de gist *Saccharomyces cerevisiae*, beter bekend als bakkersgist maar ook een van de meest toegepaste microbiële werkpaarden in industriële fermentaties, gebruikt als model microorganisme om de fysiologie en robuustheid van de cellen te bestuderen bij zeer lage groeisnelheden. Doel hiervan was om de mogelijkheid om groei los te koppelen van productvorming te onderzoeken. Door het gebruik van zogenoemde retentostaten, continu doorstroomde reactoren waarbij een filter in de effluentlijn ervoor zorgt dat de microorganismen in de bioreactor blijven, kan door zeer beperkte toevoer van de koolstof- en energiebron glucose de groei vrijwel volledig worden gestopt. De resultaten van deze onderzoeken gaven aan dat in retentostaten gecultiveerde gistcellen, waarbij de groeisnelheid vrijwel gelijk aan nul was, stabiel, robuust en metabool actief waren. Verder behielden de cellen een

aanzienlijke ethanolproductiviteit tijdens langdurige cultivatie in anaerobe, koolstofbeperkte retentostaat culturen. Bovendien werden in zowel anaerobe als aerobe retentostaten een levensvatbaarheid van meer dan 80 % en een hoge metabole activiteit waargenomen tijdens langdurige cultivatie.

In het onderzoek dat in dit proefschrift wordt gepresenteerd, wordt het nulgroei-concept verder ontwikkeld naar industriële toepassing, met barnsteenzuur als modelproduct. Daarbij werd gekozen voor industrieel relevante cultivatie omstandigheden, namelijk aerobe condities, lage pH en een hoog opgelost CO_2 gehalte. Het belangrijkste doel van het onderzoek was om meer kennis te vergaren van de fysiologie van de gist in afwezigheid van groei en daardoor inzicht te verschaffen in het ontwerp van industriële fermentatieprocessen op basis van het concept van nulgroei. In het bijzonder hebben we de toepasbaarheid van retentostaat cultivatie voor niet-katabole producten onderzocht, dat wil zeggen producten waarvan de synthese uit suiker een netto input van energie in de vorm van ATP vereist.

Zoals hierboven vermeld, werd in eerder onderzoek de groei in retentostaat culturen gelimiteerd door gelimiteerde toevoer van de koolstof en energiebron glucose. Wanneer men echter het nulgroei concept wil toepassen voor de productie van verbindingen waarvan de biosynthese een netto input van energie vereist, lijkt koolstof en energie gelimiteerde cultivatie geen voor de hand liggende keuze. Daarom werd besloten om opties te onderzoeken om de groei in retentostaten door andere nutriënten dan de koolstof en energiebron te beperken.

In hoofdstuk 2 wordt het ontwerp en de implementatie van retentostaat regimes voor aerobe, stikstof (N) of fosfor (P) gelimiteerde cultivatie van de referentiestam *S. cerevisiae* CENPK113-7D beschreven. Hierbij werd een experimentele opzet geïmplementeerd die een geleidelijke transitie van chemostat culturen met lage groeisnelheid naar retentostat culturen met bijna nul groei mogelijk maakte. Toevoeging van lage concentraties ammonium of fosfaat aan de reservoirmedia was nodig om het verlies van extracellulaire N- of P-bevattende verbindingen tijdens de retentostaat cultivatie te compenseren.

Groeisnelheden van bijna nul ($\mu < 0.001\ h^{-1}$) werden met succes bereikt in zowel N- als P-beperkte retentostaat culturen. In deze culturen bleef de levensvatbaarheid boven de 80 %. Kwantificatie van intracellulaire ATP, ADP en AMP niveaus gaven aan dat onder deze omstandigheden een adequate energiestatus werd gehandhaafd en dat de cellen zich in een metabool actieve toestand bevonden. Wel bleken de cellen een sterk verminderde hoeveelheid van het groei limiterende element (N of P) te bevatten, zowel tijdens chemostaat als retentostaat cultivatie. Dit ging gepaard met hoge accumulatieniveaus van opslagkoolhydraten. Vergeleken met koolstof (C) beperkte retentostaat culturen met een vergelijkbare experimentele opzet, vertoonden de N- en P-gelimiteerde culturen: (1) aerobe ethanolfermentatie als gevolg van het Crabtree-effect; (2) een gedeeltelijke ontkoppeling van katabolisme en anabolisme; (3) een veel hogere, niet-groei-geassocieerde, energie behoefte.

Als vervolg op deze fundamentele fysiologische studie onder N- en P-gelimiteerde omstandigheden, is het onderzoek waarvan de resultaten beschreven zijn in hoofdstuk 3 gericht op de fysiologische impact van industrieel relevante cultivatie condities. Cultivaties werden uitgevoerd onder C- of N-gelimiteerde condities bij lage groeisnelheden in chemostaten en bij praktische afwezigheid van groei in retentostaten. Hierbij werden zo goed mogelijk de omstandigheden nagebootst die optreden tijdens het industriële barnsteenzuurfermentatieproces: langzame groei, lage pH en hoge opgeloste CO_2 concentratie. Bij C-gelimiteerde cultivatie onder deze condities bleek de levensvatbaarheid af te nemen van meer dan 80 % in langzaam groeiende chemostaten tot slechts 25 % in retentostaten in praktische afwezigheid van groei ($\mu < 0.001\ h^{-1}$). Bovendien werd een 8 keer hogere specifieke afsterfsnelheid en een meer dan 2-voudig hoger energieverbruik voor onderhoud van de cellen waargenomen in vergelijking met aerobe C-gelimiteerde retentostaat culturen uitgevoerd bij pH 5. Verdere experimenten toonden aan dat deze effecten voornamelijk werden veroorzaakt door de lage cultivatie pH. Groei onder N-beperkte omstandigheden en overmaat aan C-verbeterden deze nadelige effecten niet. In de N-gelimiteerde chemostaat cultivaties voorafgaand aan de retentostaat fase was de levensvatbaarheid slechts 50 %, terwijl tijdens retentostaat cultivatie de levensvatbaarheid af nam

tot slechts 25 % bij een groeisnelheid praktisch gelijk aan nul. De niet aan groei gerelateerde energiebehoefte was ook veel hoger dan waargenomen in N-beperkte culturen bij pH 5 (hoofdstuk 2). Hieruit bleek dat de verminderde levensvatbaarheid niet werd veroorzaakt door de extreme limitatie van de koolstof of stikstofbron. Transcriptoom analyse toonde aan dat de cellulaire respons op lage pH de gebruikelijke (MAPK-) signaleringsroutes kan omvatten, met name de celwandintegriteit (CWI), hoge osmolariteit glycerol (HOG) en calcineurine routes.

In hoofdstuk 4 worden de bevindingen van de voorgaande hoofdstukken geïntegreerd door de toepasbaarheid van het nulgroei-concept voor de productie van barnsteenzuur door een genetisch gemodificeerde industriële stam van *S. cerevisiae* te onderzoeken. Allereerst hebben we onderzocht in hoeverre de productiviteit van deze industriële giststam gekoppeld was met groei. Daarom werd de stam gekweekt bij specifieke groeisnelheden tussen 0.085 en 0.005 h^{-1} in N-beperkte chemostaat en retentostaat culturen onder industrieel relevante omstandigheden (pH 3 en 50 % CO_2). De specifieke barnsteenzuur productiesnelheid nam asymptotisch af met een afnemende groeisnelheid en stabiliseerde zich op een waarde van 0.75 mmol/(g levensvatbare biomassa)/uur bij een groeisnelheid van praktisch nul. Hieruit bleek dat de productiesnelheid geassocieerd is met de groeisnelheid, maar dat loskoppeling van groei kan worden bereikt. Hoewel bij groeisnelheden dichtbij nul een niet te verwaarlozen hoeveelheid glucose werd omgezet in bijproducten (voornamelijk malaat, ethanol en glycerol), resulteerden deze omstandigheden in de hoogste yield van barnsteenzuur op glucose vanwege de verwaarloosbare glucoseomzetting in biomassa. De levensvatbaarheid van de industriële stam was boven de 80 % voor alle chemostat-culturen, wat hoger was dan waargenomen voor de referentiestam (hoofdstuk 3). Echter, na het overschakelen naar retentostaat cultivatie, daalde de levensvatbaarheid van de cultuur snel tot ongeveer hetzelfde niveau als van de referentiestam (25 %, hoofdstuk 3), maar de culturen behielden een stabiele cellulaire energiestatus.

Deze studie illustreert het potentieel voor productie met hoge opbrengst van niet-dissimilatoire producten bij groeisnelheden van bijna nul, waarbij de groei wordt beperkt door een andere voedingsstof dan de koolstof en energiebron. De resultaten van dit onderzoek tonen aan dat verder onderzoek naar het

verbeteren van de robuustheid van de gist onder industriële omstandigheden vereist is, met speciale aandacht voor lage pH-tolerantie.

Chapter 1 General Introduction

Fermentative production of fuels, chemicals and pharmaceuticals from renewable feedstocks

Fuels and chemicals are traditionally produced from fossil feedstocks and, in particular, from oil. However, fossil feedstocks are non-renewable resources, and their reserves are being depleted much faster than new ones are being generated. Human society faces the potentiality of fossil-resource depletion in the coming centuries (Ahuja 2015). In recent decades, the oil price has strongly fluctuated, with major impacts on the global economy. Furthermore, large-scale combustion of fossil fuels contributes to a significant amount of CO_2 emission, which impacts global warming and ocean acidification (Choi et al. 2020; Doney et al. 2009). According to the UN's Intergovernmental Panel on Climate Change, a wholesale phasing-out of fossil feedstocks, including crude oil, needs to be completed by the end of 21st century to avoid severe, pervasive, and irreversible impacts on people and ecosystems (Goodenough 2014). Therefore, production of fuels and chemicals from alternative renewable feedstocks has attracted considerable and growing attention in recent years.

Brazil and the USA successfully produce large quantities of bioethanol by using cane sugar and corn starch, respectively (Guo 2020). However, depending on the oil price, the high price of these 'first-generation feedstocks' can make it challenging to compete with conventional gasoline in the absence of tax incentives or other support measures (Lee and Lavoie 2013; Naik et al. 2010). Lignocellulosic biomass, which is abundantly available in the form of low-value agricultural residues, is a promising alternative renewable feedstock due to its availability and low cost (Mohr and Raman 2013). However, conversion of these 'second-generation feedstocks' to liquid fuels is technically complicated and costly. Over the past decades, significant efforts have been made in developing efficient and cost-effective technologies that reduce the cost of second-generation bioethanol production. The technological feasibility of second-generation bioethanol processes is illustrated by the many cellulosic ethanol pilots and demonstration plants that have come on line over the past decade (Robak and Balcerek 2018).

An alternative to increase economic benefits from second-generation feedstocks is to develop biorefineries that produce high-value-added

compounds from lignocellulosic biomass. Over the last decades, there have been increasing activities to commercialize various microbial processes for the production of pharmaceuticals and chemicals from sugars. For instance, Novo Nordisk already started producing human insulin by application of a yeast fermentation since the 1980s (Baeshen et al. 2014). Genomatica (San Diego, USA) now commercially produces 1,4-butanediol at 30,000 ton/year (Burgard et al. 2011). DSM/Roquette, BioAmber/Mitsui, BASF/Corbion-Purac and Myriant all started producing succinic acid at a commercial scale (Jansen and van Gulik 2014) in the past decades.

Microorganisms in industrial fermentation processes

In 1674, Antonie van Leeuwenhoek, "the Father of Microbiology", was the first human to observe microorganisms by using his elegant self-made microscopes in Delft. Even before Van Leeuwenhoek's observations, mankind had been using microorganisms such as bacteria, yeasts and filamentous fungi for many millennia, predominantly for a wide range of food and beverage fermentation processes. Industrialized derivatives of some of these processes are still economically important today. For instance, alcoholic beverages and bread doughs are fermentation products of *Saccharomyces* budding yeasts (Cheng et al. 2020), while cheese and yogurt are produced using lactic acid bacteria (Ameen and Caruso 2017). Since the 1970s, genetic modification has been introduced and applied as a powerful tool for modifying the characteristics of natural microorganisms and thereby extend and improve their applications in industry. Nowadays, various enzymes (e.g. lipases, proteases and sugar hydrolases), food ingredients (e.g. plant-derived sweeteners and resveratrol), and therapeutics (e.g. antimalarial compound artemisinin, human insulin, and the key intermediate for cephalosporin active pharmaceutical ingredients (APIs) 7-ADCA.) are made with genetically engineered microbes in industrial scale fermentations (Demain and Adrio 2008; Westfall and Gardner 2011).

The yeast *Saccharomyces cerevisiae* is not only applied as microbial cell factory in a wide range of large-scale industrial processes, but is also one of the most well-studied model eukaryotes in fundamental research.

Yeast as a microbial cell factory

Saccharomyces cerevisiae, commonly known as baker's yeast, is a single-cell eukaryote. Due to its ease of cultivation and storage in the lab and excellent amenability to classical genetics and recombinant-DNA technology, *S. cerevisiae* is widely applied as model microorganism in biological and biomedical research (Attfield 1997; Botstein and Fink 2011).

In 1996, *S. cerevisiae* was the first eukaryote to have its genome completely sequenced (Clayton et al. 1997). This milestone was achieved through a worldwide effort of hundreds of researchers. Since then, detailed functional and regulatory analysis of many of the ca. 6000 yeast genes and proteins has significantly increased our fundamental understanding of cellular processes such as cell division, cell cycle, cell aging, cell death, protein purification and DNA repair. In many cases, studies key cellular processes in yeast were at the basis of the subsequent unraveling of the corresponding mechanisms in human cells, as many yeast proteins are similar in sequence with those in other eukaryotes (Botstein and Fink 2011; Miller-Fleming et al. 2008).These ground-breaking studies increasingly profited from the development, inspired by the availability of the complete *S. cerevisiae* genome sequence, of various system-wide ('omics') research approaches, including metabolome analysis, proteome analysis, metabolic flux analysis and genome-scale metabolic modelling.

Over the years the yeast molecular biology toolbox has seen spectacular improvements, which further accelerated and facilitated genetic modification. Together with the information and knowledge about its well-annotated genome, these developments resulted in many successful yeast metabolic engineering studies. Metabolic engineering strategies (Gohil et al. 2017) have, for example, been applied to overexpress rate-controlling enzymes in biosynthetic pathways, to eliminate feed-back regulation mechanisms, to inactivate competing metabolic pathways and to express heterologous enzymes to enable the use of new substrates and/or the formation of novel products. As a result, *S. cerevisiae* has been reprogrammed to convert renewable resources into multiple high-value-added products at an industrial scale and in a cost effective manner, including biopharmaceuticals, polymers, monomers, fuels, chemicals, nutraceutical ingredients and probiotics (Hong

and Nielsen 2012). The recent introduction of the powerful genome-editing tool CRISPR-Cas9 has further accelerated research by enabling the simultaneous, precise introduction of multiple genetic modifications in the yeast genome (DiCarlo et al. 2013; Mans et al. 2015). Targeted metabolic engineering studies are often complemented with evolutionary engineering, in which laboratory cultures of yeasts are subjected to carefully designed cultivation regimes to select for spontaneous mutants with industrially relevant characteristics. After laboratory evolution, resequencing the genomes of evolved strains is a powerful way to identify causal mutations (Sauer 2001).

Yeast anaerobic fermentation

The term fermentation originates from the Latin word "*fervere*", meaning "to boil". Already in ancient times, our ancestors observed that storage of crushed grapes in vessels led to the formation of gas bubbles, similar to those observed in boiling water. Later, yeast fermentation appeared in daily life when alcoholic beverages were produced by incubating fruits and grains in covered containers. It was observed that the season (temperature), fermentation time and tightness of the container all impacted the quality of the spontaneous processes that yielded fermented beverages. Specifically, if the mixture did not stay long enough in the container, very little alcohol was formed; but if it was left for too long, the beverages appeared undrinkable. In 1815, with the application of the microscope, Joseph-Louis Gay-Lussac, a French chemist, first proposed that yeast, as a kind of microorganism, was responsible for the production of alcohol during the fermentation process (Alba-Lois and Segal-Kischinevzky 2010).

Nowadays, yeast fermentation technology has been transformed from an empirical and artisanal 'craft' into rationally designed, industrial-scale processes for beer brewing and wine making, which are of great economic importance (Otero et al. 2007). In a typical alcoholic fermentation process, the yeast cells utilize the nutrients essential for growth, such as sugars, nitrogen, phosphorus and sulfur sources to form biomass, while ethanol and carbon dioxide are produced as major metabolic end products. When fermentation occurs in the absence of oxygen, it is referred to as anaerobic fermentation (van Dijken et al. 1993). Not only the above-mentioned nutrients need to be supplied

at levels sufficient to support yeast growth and fermentation, but also the cultivation temperature and pH (optimal values for *S. cerevisiae* approximately 30 ℃ and pH 5, respectively) need to be maintained in an acceptable range to ensure reproducible product formation (Mohd Azhar et al. 2017). Furthermore, the alcohol concentration in the culture should not exceed toxic levels (Piper 1995), which explains why most wines and beers have ethanol concentrations below 15 % (v/v). To achieve higher concentrations of alcohol in liquors and spirits, the fermented products must be distilled.

Yeast respiration vs fermentation

When sufficient oxygen is supplied, yeast cells are in principle able to perform fully respiratory catabolism of sugars to CO_2 and H_2O. However, in *S. cerevisiae* completely respiratory catabolism is only observed when the sugar is the growth-limited nutrient and thus the residual sugar concentration in the culture broth remains low (below approximately 1 mM) (Boles and Hollenberg 1997; Reifenberger et al. 1997). During aerobic sugar excess conditions *S. cerevisiae* shows a mixed fermentative/respiratory catabolism whereby a large part of the consumed sugar is fermented to ethanol, which is known as the Crabtree effect (De Deken 1966). It is assumed that *S. cerevisiae* has acquired this mechanism during evolution, to outcompete other microorganisms when growing on grapes where sugar is available in excess but nitrogen is scarce (Ibstedt et al. 2015).

The three possible modes of glucose catabolism in *S. cerevisiae* are shown below (Figure 1.1).

Alcoholic fermentation: $C_6H_{12}O_6 \rightarrow 2\ C_2H_6O + 2\ CO_2 + 2\ ATP$

Respiratory catabolism: $C_6H_{12}O_6 + 6\ O_2 \rightarrow 6\ CO_2 + 6\ H_2O + 16\ ATP$

Mixed respiratory/fermentative: $C_6H_{12}O_6 + (6 - 3\alpha)\ O_2 \rightarrow \alpha\ C_2H_6O + (6 - 2\alpha)\ CO_2 + (6 - 3\alpha)\ H_2O + (16 - 7\alpha)\ ATP$

Figure 1.1 The three possible modes of glucose catabolism in *S. cerevisiae*. $0 \leq \alpha \leq 2$, when $\alpha = 2$ and $\alpha = 0$, it results to alcoholic fermentation and respiratory catabolism, respectively.

Regardless of the mode of glucose catabolism, *S. cerevisiae* initially breaks down the glucose molecules in the cytosol via the glycolytic pathway whereby energy (ATP) and electrons (NADH) are released. Glycolysis is a series of enzyme-catalysed reactions, which can be separated into a preparatory phase

wherein ATP is consumed and a pay-off phase wherein ATP is produced. In the preparatory phase, one molecule of glucose is converted into one molecule of GADP and one molecule of DHAP thereby consuming two molecules of ATP and is thus also known as the investment phase. The pay-off phase converts the two triose sugars (GADP and DHAP) to two pyruvate and yields two NADH and four ATP molecules. Therefore the result of glycolysis is the conversion of one glucose into two pyruvate, two ATP and two NADH, wherein the ATP is produced through substrate-level phosphorylation (Figure 1.2). It should be noted that glycolysis is an oxygen independent pathway. Approximately 4.3 billion years ago, when oxygen was still absent in the atmosphere, the first bacterial life forms already showed anaerobic metabolism whereby sugars were converted to pyruvate through (variants of) glycolysis and the Entner-Doudoroff pathways.

In *S. cerevisiae,* depending on the availability of the external electron acceptor oxygen, there are two different ways to continuously re-oxidize the produced NADH back to NAD^+ and ensure the glycolytic pathway to continue (Figure 1.2). Under fully anaerobic conditions, the two NADH produced in glycolysis are re-oxidized in the conversion of the produced two pyruvate into two ethanol. During aerobic growth, pyruvate is converted to Acetyl-CoA through pyruvate dehydrogenase and then enters the TCA cycle where the carbon is released as CO_2 and all electrons are captured in the form of NADH and FADH, which are subsequently transferred to oxygen in the respiratory chain. The TCA cycle yields eight NADH, two FADH and two GTP from two pyruvate. Therefore, fully aerobic catabolism via glycolysis and the TCA cycle converts one glucose to four ATP and twelve NADH equivalents. With O_2 as the external electron acceptor and assuming a P/NADH ratio of 1 in *S. cerevisiae* (Vanrolleghem et al. 1996; Verduyn et al. 1991), the oxidation of the twelve NADH to H_2O in the respiratory chain results in the formation of twelve ATP. In summary, when one glucose is completely catabolized aerobically, sixteen ATP is produced, four through substrate-level phosphorylation and twelve through the oxidative phosphorylation (Figure 1.1). Therefore, the ATP yield of full respiratory metabolism is 8-fold higher than that of fermentation, which also explains that

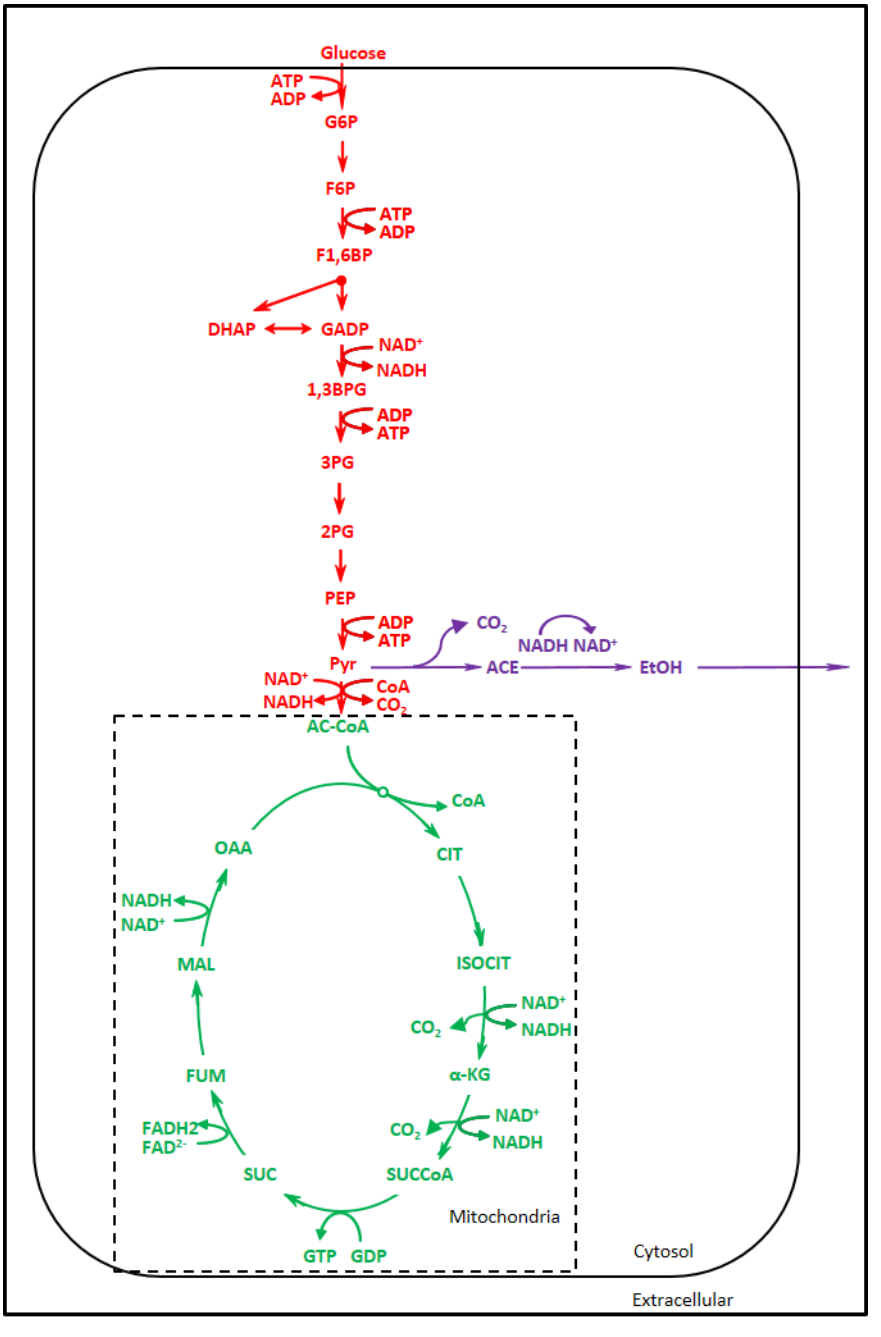

Figure 1.2 Yeast metabolism. In Glycolysis (red font), 1 glucose yields 2 pyruvate, 2 ATP and 2 NADH; Alcoholic fermentation produces 1 ethanol from 1 pyruvate (purple font); the TCA cycle yields 4 NADH, 1 FADH2 and 1 GTP from 1 pyruvate (green font).

aerobic cultivation of yeast cells is preferred for the production of ATP-demanding compounds in industrial fermentations, for example succinic acid, farnesene and proteins.

Although respiratory catabolism of glucose yields much more ATP than fermentation, the maximum rate of fermentative ATP generation in *S. cerevisiae* is approximately 2-fold higher than the maximum rate of respiratory ATP generation (Sonnleitner and Käppeli 1986). These observations underlie a rate/yield trade-off hypothesis, according to which ATP can either be produced fast (but with a low efficiency) or efficiently (but at a lower maximum rate) (Pfeiffer et al. 2001).

In *S*. *cerevisiae*, not only the sugar concentration but also relatively high specific growth rates (higher than 0.3 h^{-1}) trigger alcoholic fermentation under fully aerobic conditions (van Hoek et al. 1998). In spite of the higher ATP yield of aerobic glucose catabolism, the ATP production rate during aerobic glucose limited cultivation at high growth rates cannot satisfy the ATP requirement for anabolism anymore and above a certain "critical growth rate" additional ATP has to be produced via the faster fermentative catabolism. In contrast to this, *S. cerevisiae* was found to shift towards a more respiratory metabolism at extremely low growth rates under glucose excess conditions (Liu et al. 2019). This trade-off may contribute to an evolutionary advantage, because cells with a high growth rate but low yield of ATP production may gain a selective advantage when competing for shared energy resources (Pfeiffer et al. 2001).

Catabolism vs Anabolism

The energy released from catabolism is used to drive anabolism, wherein complex molecules are synthesized from simple ones by a series of biochemical reactions. Amongst these are compounds essential for cell proliferation such as proteins, lipids, polysaccharides, but in some cases also non-essential compounds such as secondary metabolites (Beekwilder et al. 2006; Chemler et al. 2006; Kazemi Seresht et al. 2013). Anabolism and catabolism are coupled in living beings, whereby the energy released from catabolism provides the energy required for anabolism, thus forming a tightly connected network of metabolic pathways (Figure 1.3). Both cell proliferation as well as biosynthesis of certain desired compounds rely on this network.

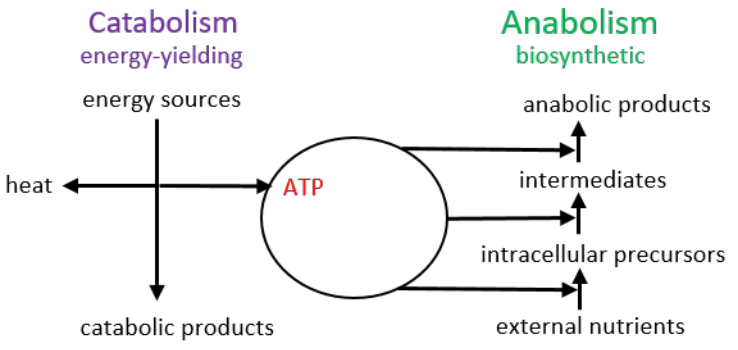

Figure 1.3 The coupling of catabolism and anabolism. In catabolism energy sources are broken down into smaller catabolic products whereby energy is released. This energy is used to drive anabolism wherein macromolecules are synthesized from small molecules.

Catabolic and anabolic products derived from yeast

According to the classification of microbial metabolism, microbial products can be subdivided into catabolic and anabolic products. Taking *S. cerevisiae* as an example, biomass itself is a typical anabolic product, which can be used as a leavening agent in bread dough, as well as ingredients for flavoring soups and sauces (Cheng et al. 2020). Representatives of anabolic products produced in yeast are heterologous proteins, isoprenoids, flavonoids, human insulin, fatty acids and resveratrol (Beekwilder et al. 2006; Chemler et al. 2006; Kazemi Seresht et al. 2013). Ethanol is a typical example of a catabolic product, as conversion of sugars to ethanol can serve as the sole source of energy (stored as ATP) for growth and maintenance of the cells under fully anaerobic conditions (Mohd Azhar et al. 2017).

Substrate distribution over growth, product formation and maintenance

The availability of a carbon and energy source is a necessity for all organisms to grow. In a microbial fermentation process the growth medium should contain all the nutrients essential for growth, such as sources of carbon, nitrogen, phosphorus and sulfur and is carefully designed for the microorganism to be cultivated. In principle each of these essential nutrients can be chosen as the growth limiting nutrient to control the growth rate of the microorganism. In 1949, Jacques Monod proposed an empirical equation to describe the growth

rate (μ) of a microorganism as a function of the concentration of a growth-limiting nutrient (Cs) (Monod 1949) (Equation (1.1)).

In this equation, μ_{max} presents the maximum specific growth rate that a microorganism can reach under the given cultivation conditions (e.g. temperature, pH etc.), Cs is the concentration of the growth-limiting nutrient and Ks is the growth-limiting nutrient concentration at $\mu = ½\ \mu_{max}$. The value of μ_{max} can be experimentally determined from a batch culture in which all the nutrients are initially supplied in excess, that is, their concentrations are much higher than Ks. After one of the nutrients is depleted the microorganisms stop growing. The classical Monod equation can be reformulated to obtain a relation for the biomass-specific substrate consumption rate (q_s) as a function of the growth-limiting substrate concentration (Cs), as shown in Equation (1.2). Ks represents the growth-limiting nutrient concentration at which $q_s = ½\ q_s^{max}$. The parameter q_s^{max} can also be experimentally determined from an unlimited batch culture where $\mu = \mu_{max}$.

Pirt proposed an empirical linear equation which describes the relation between the biomass-specific substrate consumption rate (q_s) and the specific growth rate (μ) (Equation (1.3), Figure 1.4) (Pirt 1997). Note that this equation is only valid for carbon and energy limited growth whereby biomass itself and catabolic products are formed. This equation contains two parameters, $Y_{x/s}^{max}$ represents the theoretical maximum growth yield on the growth-limiting substrate and m_s is the growth-independent maintenance energy requirement. m_s represents the specific rate of substrate consumption for cellular survival, for instance, the energy requirement to maintain intracellular homeostasis, cellular damage repair, macromolecule turnover, etc. (van Bodegom 2007). Both $Y_{x/s}^{max}$ and m_s are microorganism-dependent parameters and their values depend on the cultivation environment (e.g. pH, temperature etc.) (Tijhuis et al. 1993).

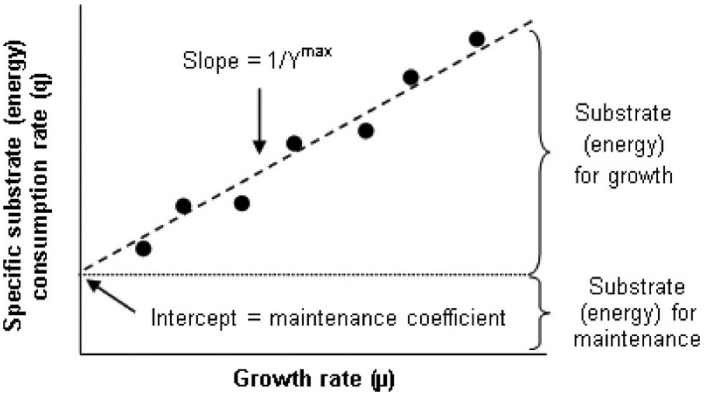

Figure 1.4 Plot of the biomass specific substrate consumption rate (q_s) as a function of the specific growth rate (μ) (Ercan et al. 2015). The intercept (extrapolation to a zero-growth condition) represents the maintenance energy requirement (m_s), the slope of the plot (dashed line) is the inverse of the maximum biomass yield on substrate (Equation 1.3, Pirt equation).

If an anabolic product is produced in a fermentation process, the Pirt equation can be extended (Equation (1.4)), known as the Herbert-Pirt equation, in which an additional drain of carbon and energy source is incorporated to produce an anabolic product (Beekwilder et al. 2006). $Y_{p/s}^{max}$ represents the theoretical maximum product yield on the growth-limiting nutrient in the absence of growth and maintenance.

$$\mu = \mu_{\max} \frac{c_s}{c_s + k_s} \tag{1.1}$$

$$q_s = q_s^{\max} \frac{c_s}{c_s + k_s} \tag{1.2}$$

$$q_s = \frac{\mu}{Y_{x/s}^{\max}} + m_s \tag{1.3}$$

$$q_s = \frac{\mu}{Y_{x/s}^{\max}} + \frac{q_p}{Y_{p/s}^{\max}} + m_s \tag{1.4}$$

Industrial fermentation metrics: Titer, Rate and Yield

A first requirement for an industrial fermentation process is that it is economically viable. To determine this, a proper estimation needs to be made

of the total costs to produce a certain amount of product in such a process. In general the overall costs of a fermentative production process can be divided into variable, fixed and downstream processing costs. The variable costs are directly related to the amount of product produced (typically the costs to purchase the substrate and other nutrients, electricity to drive compressors and stirrers, waste disposal etc.). Fixed costs include for example the expenses for buildings and equipment, labour, maintenance and depreciation. Downstream processing costs are determined by the kind of product produced, the product concentration in the fermentation broth, the desired purity, etc. Over the years, Titer (maximum product concentration in the fermentation broth), Rate (amount of product produced per amount of fermentor volume per time) and Yield (amount of product produced per amount of substrate consumed) (TRY) have been regarded as key metrics of industrial fermentation processes (Gong et al. 2017). Increasing the product titer improves the efficiency (and thus decreases the costs) of the downstream processing, a high volumetric production rate reduces the operational expenses (both variable and fixed costs), and a high product yield decreases the feedstock costs.

Without changes in rate and yield, the product titer can be increased by process optimization, that is increasing the concentration of the biocatalyst (cells) and/or the fermentation time. Thereby it should be realized that at some point product inhibition and/or product recycling could occur, resulting in a decreased productivity and/or yield (Wahl et al. 2017). Increasing the biomass density will at the same time result in an increased volumetric production rate. Another way to increase the volumetric production rate is to improve the organism, that is increase the specific productivity of the production strain.

Increasing the product yield can only be achieved by improving the production organism, i.e. through metabolic engineering efforts to improve the stoichiometric and energetic efficiency of product formation and knocking out by-product formation.

Uncoupling of microbial growth and product formation: near-zero growth

In most fermentation processes product formation is accompanied with cell growth, whereby a non-negligible part of the supplied feedstock is converted

into biomass. Therefore, the highest product yield is achieved in the absence of growth, as can also be inferred from the Herbert-Pirt equation (Equation (1.4)). So to maximize the product yield, the flux from substrate to biomass should be minimized. This requires innovative fermentation processes wherein the producing organism converts the substrate into the desired product at an extremely low or preferably zero growth rate. To establish such processes, uncoupling of microbial growth (μ) and product formation (q_p) is required. This represents a major and industrially relevant scientific challenge, since slow growing or stationary-phase cultures of microorganisms are generally characterized with progressive loss of viability and low productivity (Longo et al. 2012).

Achievement of near-zero growth in retentostat cultures

The traditional fermentation modes are batch, fed-batch and chemostat cultivation. Of these, fed-batch and chemostat cultures enable to control the growth rate. For research purposes the chemostat is preferred, because well-defined steady state conditions can be achieved wherein the cells experience constant and time independent environmental conditions. However, to achieve very low specific growth rates (lower than 0.025 h^{-1}) chemostat cultivation is less suited. Very low to near-zero specific growth rates can be reached successfully in a retentostat culture, which is a continuous cultivation system with full biomass retention (Boender et al. 2009). A retentostat can be considered as a modified chemostat, wherein fresh medium is supplied continuously to the bioreactor while effluent is removed through an internal/external filter module, which results in retention of the biomass.

By limited supply of one growth-essential compound, the specific growth rate can be controlled and brought close to zero in the retentostat cultivations. Therefore, retentostat cultivation enables the study of microbial physiology at extremely low to zero specific growth rates and is for example very well suited to determine maintenance energy requirements.

Table 1.1 Comparison of the physiological parameters of different microorganisms cultivated in near-zero growth retentostat cultures. Data were derived from (Ercan et al. 2015)

Microorganism	Time in retentostat (d)	Specific growth rate (h^{-1})	m_s (mmolS/(g biomass)/h)	Reference
L. lactis KF147	42	0.00011	1.11	(Ercan et al. 2013)
L. lactis FM03-V1	37	< 0.001	0.36	(van Mastrigt et al. 2018)
L. plantarum WCFS1	45	0.00006	0.65	(Goffin et al. 2010)
B. subtilis 168	42	0.00006	1.43	(Overkamp et al. 2015)
A. niger N402	10	0.003	~	(Jørgensen et al. 2010)
S. cerevisiae CENPK113-7D	22	0.00063	0.5	(Boender et al. 2009)
S. cerevisiae CENPK113-7D	20	< 0.001	0.039	(Vos et al. 2016)

In recent years studies on the retentostat cultivation of several industrially relevant microorganisms such as *Lactobacillus plantarum, Lactococcus lactis, Bacillus subtilis* and *Aspergillus niger* have been carried out (Table 1.1). In all cases extremely low specific growth rates could be achieved, thereby maintaining cellular integrity and activity. Observed physiological responses of these microorganisms during near-zero growth cultivation include increased stress tolerance, robustness, and a down regulation of genes involved in protein synthesis (Ercan et al. 2015).

With respect to yeast, research has been carried out over the past 15 years on carbon limited retentostat cultivation of the laboratory yeast strain *S. cerevisiae* CENPK113-7D under anaerobic and aerobic conditions. Hereby the cells were supplied with just enough carbon and energy source for maintenance, but not for growth. Quantitative physiology, robustness and maintenance energy requirements have been investigated accurately (Boender et al. 2009; Vos et al. 2016). Hereby, Boender et al. (Boender et al. 2009) studied the physiology of this yeast strain at near-zero growth rates under fully anaerobic conditions. During a 22-days retentostat cultivation the specific growth rate decreased to

values below 0.001 h^{-1}, while the viability was maintained at about 80 %. Under fully anaerobic conditions ATP-generation is coupled with ethanol production and thus measuring the ethanol production rate enables to accurately estimate the cellular ATP requirement for maintenance (Boender et al. 2009).

Vos et al. (Vos et al. 2016) applied a similar experimental set-up to explore the physiology of the same yeast strain under aerobic conditions. Also in these cultivations the specific growth rate reached values below 0.001 h^{-1} while a viability of ca. 80% was maintained over a 20-days culture period. In the absence of growth, the biomass-specific substrate consumption rate equals the maintenance-energy requirement, which was observed to be approximately 30 % lower than that estimated from the anaerobic retentostat cultures.

Aim and outline of the thesis

The major elements present in yeast biomass are carbon, hydrogen, oxygen, nitrogen, phosphorus and sulphur. Of these, carbon, nitrogen, phosphorus and sulphur are elements which are essential for growth and thus have to be supplied in the cultivation medium. Main sources of these elements could be for example glucose, ammonium, phosphate and sulphate. In principle, growth limitation can be achieved by limiting the supply of at least one of these nutrients. Previous studies have focused on the physiological response of retentostat cultured yeast under glucose limited conditions. It was observed in these studies that when near-zero growth was achieved, the yeast was capable to maintain cellular vitality, robustness and metabolic activity.

So far, little is known about the physiological response of extremely slow to non-growing yeast cells if the growth is limited by the supply of nutrients other than the carbon and energy source, whereby the latter is present in excess. In principle, carbon and energy excess is expected to be beneficial to produce compounds whose synthesis from sugar requires a net input of ATP.

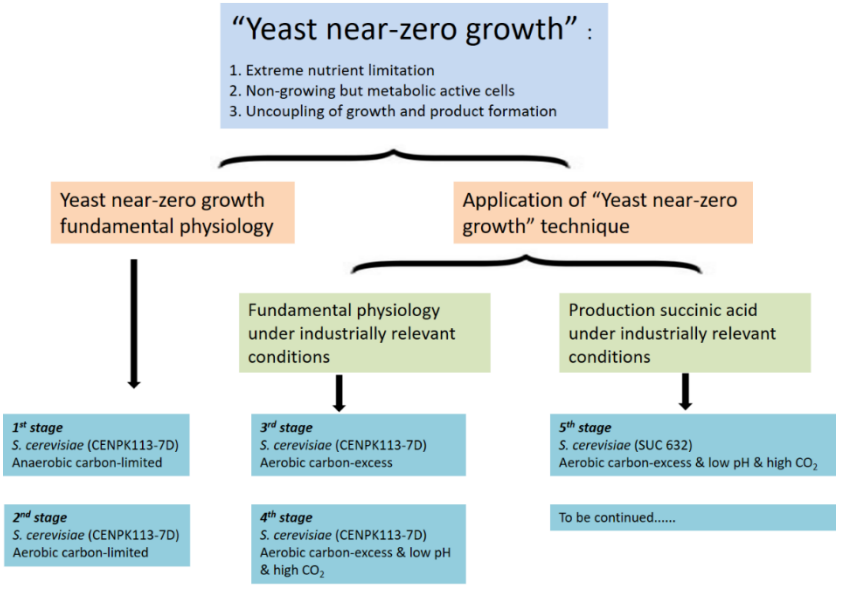

Figure 1.5 The diagram of "Yeast near-zero growth" project

For the research described in this thesis, succinic acid (SA) was chosen as the model product. By applying retentostat regimes, the quantitative physiology of a non-producing yeast strain (*S. cerevisiae* CENPK113-7D*)* and an industrial SA producing yeast strain (SUC632) were studied. The aim of the research was to explore the physiological response of the producing and non-producing strains at near-zero growth conditions, thereby investigating the possibility of uncoupling cell proliferation from SA production.

Chapters 2 and 3 focus on the physiology of the non-producing strain *S. cerevisiae* CENPK113-7D (Figure 1.5) under near-zero growth conditions in retentostat cultures. In the research described in Chapter 2, both ammonium- and phosphate-limitation were applied to examine the possibility of reaching near-zero growth conditions under other than glucose-limited conditions. To prevent a sudden change in supply of the growth limiting nutrient upon the switch between the preceding chemostat phase and the retentostat phase, and thus a sudden drop in the growth rate, a smooth transition between the supply of the chemostat and the retentostat medium was achieved by using two computer controlled feed pumps. Cellular robustness, biomass composition and metabolic flux distributions were analysed and compared with previously obtained data from carbon-limited chemostat and retentostat cultures.

Low pH and elevated CO_2 are industrially relevant, harsh conditions for succinic acid production. Chapter 3 describes the growth of the reference non-producing *S. cerevisiae* CENPK113-7D strain in chemostat and retentostat cultures under industrially relevant conditions. Two cultivation conditions were applied independently: (1) glucose-limited, pH 3 and 50 % CO_2 ; (2) ammonium-limited, carbon-excess and pH 3. These two conditions were compared with previous aerobic glucose-limited (Vos et al. 2016) and ammonium-limited retentostat cultures (Chapter 2), respectively. Quantitative analysis of rates, yields, and culture viability was carried out to dissect the physiological impacts of low pH and high CO_2. Furthermore, transcriptome analysis was employed to elucidate the regulatory responses to these conditions.

The research described in Chapter 4 aims at investigating whether the biomass specific SA production rate of the industrial strain depends on the growth rate and if so, what could be the underlying mechanism. This should provide leads on how strain engineering could be applied to achieve high productivity in the absence of growth (Figure 1.5). Based on the obtained knowledge with respect to the physiological responses of the reference *S. cerevisiae* CENPK113-7D, the design and subsequent cultivation of the industrial SA producing strain in ammonium limited chemostat and retentostat cultures under industrially relevant conditions (pH 3, 50 % CO_2) was carried out. Cellular physiology in terms of viability and death rate, productivity, metabolic activity and metabolomics was explored.

Chapter 2 Quantitative physiology of non-energy-limited retentostat cultures of *Saccharomyces cerevisiae* at near-zero specific growth rates

This chapter has been published in Applied and Environmental Microbioliology.2019, 85:e01161-19. https://doi.org/10.1128/AEM.01161-19

Abstract

So far, the physiology of *Saccharomyces cerevisiae* at near-zero growth rates has been studied in retentostat cultures with a growth-limiting supply of the carbon and energy source. Despite its relevance in nature and industry, the near-zero growth physiology of *S. cerevisiae* under conditions where growth is limited by the supply of non-energy substrates remains largely unexplored. This study analyses the physiology of *S. cerevisiae* in aerobic chemostat and retentostat cultures grown under either ammonium or phosphate limitation. To compensate for loss of extracellular nitrogen- or phosphorus-containing compounds, establishing near-zero growth rates ($\mu < 0.002$ h^{-1}) in these retentostats required addition of low concentrations of ammonium or phosphate to reservoir media. In chemostats as well as in retentostats, strongly reduced cellular contents of the growth-limiting element (nitrogen or phosphorus) and high accumulation levels of storage carbohydrates were observed. Even at near-zero growth rates, culture viability in non-energy-limited retentostats remained above 80 % and ATP synthesis was still sufficient to maintain an adequate energy status and keep cells in a metabolically active state. Compared to similar glucose-limited retentostat cultures, the nitrogen- and phosphate-limited cultures showed aerobic fermentation and a partial uncoupling of catabolism and anabolism. The possibility to achieve stable, near-zero growth cultures of *S. cerevisiae* under nitrogen- or phosphorus-limitation offers interesting prospects for high-yield production of bio-based chemicals.

Importance

The yeast *Saccharomyces cerevisiae* is a commonly used microbial host for production of various bio-chemical compounds. From a physiological perspective, biosynthesis of these compounds competes with biomass formation in terms of carbon and/or energy equivalents. Fermentation processes functioning at extremely low or near-zero growth rates would prevent loss of feedstock to biomass production. Establishing *S. cerevisiae* cultures in which growth is restricted by the limited supply of a non-energy substrate could therefore have a wide range of industrial applications, but remains largely unexplored. In this work we accomplished near-zero growth of *S. cerevisiae* through limited supply of a non-energy nutrient, namely the

nitrogen or phosphorus source and carried out a quantitative physiological study of the cells under these conditions. The possibility to achieve near-zero-growth *S. cerevisiae* cultures through limited supply of a non-energy nutrient may offer interesting prospects to develop novel fermentation processes for high-yield production of bio-based chemicals.

Key words: yeast physiology, near-zero growth, retentostat, non-energy limitation, carbon excess

Introduction

The yeast *Saccharomyces cerevisiae* is an established microbial host for production of a wide range of bio-chemical compounds (Jansen and van Gulik 2014; Nielsen and Keasling 2016). Current aerobic processes for production of ATP-requiring ('anabolic') products are typically biphasic, with separate growth and production phases. Complete uncoupling of growth and product formation could enable a further reduction of the loss of feedstock to biomass production. In theory, such a complete uncoupling can be achieved in continuous processes performed at very low or near-zero specific growth rates. In practice, however, its implementation requires processes and microorganisms that, over prolonged periods of time, ensure a high viability and a high biomass-specific product formation rate (q_p) in the absence of growth.

For laboratory studies near-zero specific growth rates are usually achieved in retentostats (Ercan et al. 2015). A retentostat is a modification of the chemostat, in which effluent removal occurs through an internal or external filter module that causes complete biomass retention. Retentostats enable studies on microbial physiology at near-zero growth rates that are technically difficult to achieve in conventional chemostats, while their use avoids complete starvation by maintaining a constant supply of essential nutrients.

When growth in retentostat cultures is limited by the energy substrate, biomass accumulates in the reactor until the biomass-specific substrate consumption rate (q_s) equals the energy-substrate requirement for cellular maintenance (m_s). Aerobic and anaerobic, glucose-limited retentostat cultures of *S. cerevisiae* were shown to retain a high viability, as well as an extremely high heat-shock tolerance, over periods of several weeks (Bisschops et al. 2014; Boender et al. 2009; Vos et al. 2016). Consistent with a growth-rate-independent requirement of ATP for cellular maintenance (Pirt 1982) observed values of q_s at near-zero growth rates ($\mu < 0.002$ h^{-1}) were in good agreement with estimates of m_s derived from measurements in glucose-limited chemostat cultures grown at a range of specific growth rates (Boender et al. 2009; Vos et al. 2016).

From an applied perspective, it seems illogical to apply severely energy-limited cultivation regimes for production of compounds whose synthesis from sugar requires a net input of ATP. In nature, *S. cerevisiae* seems to have primarily

evolved for growth in sugar-rich environments where, instead of the energy substrate, the nitrogen source is growth limiting (Brice et al. 2018; Ibstedt et al. 2015). Also in industrial substrates for *S. cerevisiae* such as wine must or brewing wort, sugar is typically present in abundance, while growth becomes limited by the nitrogen source (Taillandier et al. 2007). As an alternative to nitrogen-limited cultivation, growth under extreme phosphate limitation may offer interesting options to uncouple growth from product formation. For example, *S. cerevisiae,* a non-oleaginous yeast, has been reported to accumulate high levels of specific fatty acids when availability of phosphate is restricted (Kolouchova et al. 2016).

Studies in exponentially growing chemostat cultures have revealed an extensive reprogramming of the yeast transcriptome, proteome and fluxome in response to nitrogen and phosphorus limitation (Boer et al. 2010; Boer et al. 2003; Gutteridge et al. 2010; Tai et al. 2005). In addition, nitrogen- and phosphorus-limited growth of resulted in lower contents of protein and phospholipids, respectively, in yeast biomass (Acquisti et al. 2009; Ramsay and Douglas 1979). In contrast to the wealth of data on the effects of different nutrient limitation regimes in actively growing cultures, information on aerobic *S. cerevisiae* cultures grown at near-zero growth rates is scarce. In anaerobic cultures, nitrogen-limited cultivation with biomass recycling has been explored to maximize ethanol yields (Taniguchi et al. 1983; Wada et al. 1981). Brandberg and coauthors (Brandberg et al. 2007), who investigated the impact of severe nitrogen limitation on ethanol production by *S. cerevisiae,* used incomplete cell recycling under anaerobic and micro-aerobic conditions.

The goal of the present study is to design and implement retentostat regimes for aerobic, nitrogen- and phosphate-limited growth of *S. cerevisiae* at near-zero specific growth rates and to use the resulting cultures for a first experimental exploration of its quantitative physiology under these scientifically interesting and industrially relevant conditions. To this end, experimental setups were tested that allowed for a smooth transition from low growth rate chemostat cultures to near-zero growth rate retentostat cultures. Metabolic fluxes, biomass composition and cellular robustness were analyzed and compared with previously obtained data from glucose-limited chemostat and retentostat cultures.

Materials and Methods

Yeast strain and media

The prototrophic, haploid yeast strain *Saccharomyces cerevisiae* CENPK 113-7D was used in this study (Nijkamp et al. 2012). Working stocks were obtained by cultivation in YPD medium (10 g/L Bacto yeast extract, 20 g/L Bacto peptone and 20 g/L D-glucose). After addition of 30 % (v/v) glycerol, culture aliquots were stored in sterilized Eppendorf tubes at -80°C.

Ammonium- and phosphate-limited (N- and P-limited) pre-culture and batch culture media were prepared as described by Boer (Boer et al. 2003). For N-limited batch cultivation, the medium contained the following components: 1.0 g of $(NH_4)_2SO_4$, 5.3 g of K_2SO_4, 3.0 g of KH_2PO_4, 0.5 g of $MgSO_4.7H_2O$, and 59 g of glucose per liter. For P-limited batch cultivation, the medium contained 5.0 g of $(NH_4)_2SO_4$, 1.9 g of K_2SO_4, 0.12 g of KH_2PO_4, 0.5 g of $MgSO_4.7H_2O$, and 59 g of glucose per liter. In addition, 1 mL/L trace element solution, 1 mL/L vitamin solution and 0.2 g/L Pluronic 6100 PE antifoaming agent (BASF, Ludwigshafen, Germany) were added. Trace element and vitamin solutions were prepared as described by Verduyn (Verduyn et al. 1992). The compositions of media for N- and P-limited chemostat cultivation were as described above, except that the glucose concentration was increased to 120 g/L. For N-limited retentostat cultivation, the $(NH_4)_2SO_4$ concentration in the medium feed was decreased to 0.1 g/L and the glucose concentration was 60 g/L. To maintain the same sulfur concentration, the K_2SO_4 concentration was increased to 6.46 g/L, the concentrations of the other compounds were the same as in the chemostat medium. For P-limited retentostat cultivation, the KH_2PO_4 concentration was lowered to 0.014 g/L and the glucose concentration was 60 g/L.

Bioreactor set up

Bench-scale, turbine-stirred 7 L bioreactors (Applikon, Delft, The Netherlands) equipped with a single six-bladed Rushton turbine impeller with a diameter of 85 mm, were used in this study. The working volume was controlled at 5 L by placing the bioreactor on an electronic balance (Mettler Toledo, Columbus, Ohio, USA). During continuous cultivation, effluent was removed with a peristaltic pump to an effluent vessel, which was placed on an electronic balance for measurement of the dilution rate ($D = 0.025\ h^{-1}$). The culture

temperature was maintained at 30 ± 0.1°C and the stirrer speed at 500 rpm. Aerobic conditions were maintained by sparging 0.5 vvm compressed air, controlled by a mass flow controller (Brooks 5850 TR, Hatfield, PA, USA). The dissolved oxygen concentration was measured on-line with a DO sensor (Mettler-Toledo GmbH, Greinfensee, Switzerland) and remained above 30 % of air saturation in all experiments. Culture pH was controlled at 5.00 ± 0.05 by automated addition of either 2 M KOH or 2 M H_2SO_4, using a Biostat Bplus controller (Sartorius BBI Systems, Melsungen, Germany). Exhaust gas was cooled to 4°C by an in-line condenser and dried by a Nafion dryer (Permapure, Toms River, USA) before entering a combined paramagnetic/infrared NGA 2000 off-gas analyzer (Rosemount Analytical, Anaheim, USA) for analysis of O_2 and CO_2 concentrations. Off-gas data were acquired with MFCS/win 3.0 software (Sartorius BBI Systems, Melsungen, Germany).

Pre-culture, batch, chemostat and retentostat cultures

Pre-cultures, grown in 500 mL shake flasks containing 200 mL medium, were inoculated with 2 mL of stock culture and grown at 30°C and at 200 rpm for 8 h in a B Braun Certomat BS-1 incubator (Sartorius, Melsungen, Germany). Bioreactor batch cultures were started by transferring 400 mL of preculture to a bioreactor containing 4.6 L of medium. After approximately 24 h of batch cultivation, a sharp decrease of the CO_2 concentration in the off-gas and a corresponding increase of the dissolved oxygen concentration indicated that ammonium or phosphate was depleted. The bioreactors were then switched to chemostat cultivation mode and operated at a dilution rate of 0.025 h^{-1}. Steady-state was assumed to be achieved after 5 volume changes, in which stable (less than 3 % difference over 2 volume changes) off-gas CO_2 and O_2 concentrations, culture dry weight and cell counts were observed. At that stage, bioreactors were switched from chemostat to retentostat mode by redirecting the culture effluent through a filtration probe assembly (Applikon, Delft, The Netherlands). Each probe was fitted with a 0.22 μm tubular micro-filtration polypropylene membrane (TRACE Analytics, Brunswick, Germany). Because of the limited flow rate capacity of each filter, four filtration probes were installed in each bioreactor. Before mounting on the filtration probe and autoclaving, membranes were hydrophilized overnight in 70 % (v/v) isopropanol.

To avoid a sudden decrease of substrate concentrations during the switch from chemostat to retentostat mode, a gradual transition from chemostat to retentostat medium was accomplished by using two feed pumps. The resulting time-dependent concentrations of glucose and of the growth-limiting nutrient ($(NH_4)_2SO_4$ or KH_2PO_4) in the medium are described by the following Equation (2.1):

$$C_s = \frac{e^{-t/\tau} \cdot F_{in,ch} \cdot C_{s,ch} + \left(1 - e^{-t/\tau}\right) \cdot F_{in,re} \cdot C_{s,re}}{e^{-t/\tau} \cdot F_{in,ch} + \left(1 - e^{-t/\tau}\right) \cdot F_{in,re}} \quad (2.1)$$

In this equation, τ is the time constant for the transition which was set to a value of 16.67 h. $C_{s,ch}$, $C_{s,re}$, $F_{in,ch}$, $F_{in,re}$, correspond to the nutrient concentrations in the chemostat and retentostat media and the feed rates from the corresponding medium reservoirs, respectively. Profiles of the resulting concentrations of the limited nutrient and of glucose in the retentostat feed media during the transition are provided in Supporting information Figure S2.1. The actual medium feed rates during the chemostat and retentostat phases for each experiment were calculated from the weight increase of the effluent vessels and the addition rates of base.

Biomass and viability assays

Culture dry weight assays were carried out through a filtration, washing and drying procedure as described previously (Postma et al. 1989). Total cell counts were quantified with a Z2 Coulter counter (50 µm aperture, Beckman, Fullerton, CA). Cell viabilities were determined through a FungaLight™ Yeast CFDA, AM/Propidium Iodide Vitality Kit (a cellular membrane integrity indicator) by flow cytometry and colony-forming-unit counts (Vos et al. 2016).

Quantification of (by)products and residual substrates

Cell-free effluent samples were harvested from a sample port connected to the retentostat filters, immediately frozen in liquid nitrogen and stored at -80°C until analysis. Effluent concentrations of glucose, ethanol and by-products (glycerol, lactate, acetate, and succinate) were quantified with HPLC using a Bio-Rad HPX-87H 300 column (7.8 mm). The column was eluted with phosphoric acid (1.5 mM, 0.6 mL/min). The detection was performed with a refractometer (Walters 2414) and a UV dector (Walters 484, 210 nm). Concentrations of

ammonium and phosphate were quantified with an ammonium cuvette test (0.02-2.5 mg/L NH_4^+) and a phosphate trace cuvette test (0.03-1.5 mg/L PO_4^{3-}), respectively (Hach Lange GmbH, Düsseldorf, Germany).

Balances and rate calculations

Biomass-specific glucose and oxygen consumption rates, and biomass-specific production rates of ethanol, carbon dioxide and by-products were calculated based on primary measurements of substrates/products concentration and flow rates in gas and liquid phases. Data reconciliation was performed as described previously (Lameiras et al. 2015). The consistencies of the thus obtained rates were evaluated by calculation of carbon and degree of reduction recoveries. Ethanol evaporation via the off-gas of the reactor was quantified as described previously (Cueto-Rojas et al. 2016) and was taken into account in calculation of ethanol production rates.

Assuming only the viable biomass can replicate and lyse, the specific growth rates and death rates in retentostat cultures were calculated with Equation (2.2) and (2.3).

$$\mu = \frac{dc_{x,total}/dt}{c_{x,viable}} \tag{2.2}$$

$$k_d = \frac{dc_{x,dead}/dt}{c_{x,viable}} \tag{2.3}$$

Analysis of biomass composition

Around 250 mg of lyophilized biomass was used to determine the elemental (C, H, N, O, P, S) composition through complete combustion and subsequent gas analysis (carbon dioxide, water vapour and nitrogen mass fractions), gas chromatography (oxygen) and ICP-MS (phosphorus and sulphur) (Energy Research Centre, Petten, The Netherlands). Biomass protein was quantified with the Biuret method as described previously (Lange and Heijnen 2001). The trehalose content of the biomass was directly quantified by GC-MS/MS (Niedenfuhr et al. 2016) in intracellular metabolite samples prepared as described below. Glycogen content was quantified through an enzymatic hydrolysis method (Vos et al. 2016).

Quantification of intracellular metabolites

A rapid sampling device connected to the bioreactor was used to rapidly withdraw broth samples for intracellular metabolite measurements (Lange et al. 2001). Approximately 1.2 g broth was taken and instantaneously quenched in pre-cooled pure methanol (-40°C), followed by a washing procedure with 80 % aqueous methanol (v/v) solution pre-cooled to -40°C. Metabolite extraction was performed with 75 % (v/v) ethanol (95°C, 3 min), followed by rapid vacuum evaporation until dryness. A detailed protocol has been described previously (Lameiras et al. 2015). Metabolite concentrations were quantified by isotope dilution mass spectrometry (LC-IDMS/MS and GC-IDMS) using U-^{13}C-labeled yeast cell extract as internal standard (Wu et al. 2005). Metabolites from glycolysis, the TCA cycle and the pentose-phosphate pathway as well as amino acids were quantified according to published protocols (Cipollina et al. 2009; Seifar et al. 2009; van Dam et al. 2002). Intracellular adenine nucleotide contents (ATP, ADP, AMP) were measured according to (Seifar et al. 2009). The adenylate energy charge (AEC) was calculated with Equation (2.4):

$$\mathrm{AEC} = \frac{\mathrm{ATP} + 0.5 \cdot \mathrm{ADP}}{\mathrm{ATP} + \mathrm{ADP} + \mathrm{AMP}} \tag{2.4}$$

Metabolic flux analysis

Intracellular flux distributions during steady-state chemostat and pseudo-steady-state retentostat cultivation were calculated using a slightly modified version of a previously published stoichiometric model (Daran-Lapujade et al. 2004), in which the biomass composition was adapted according to the measurements of the biomass elemental compositions. The input variables used for the flux analysis are summarized in Supporting information Table S2.1A.

Results

Design of carbon-excess retentostat regimes

To study the physiology of *S. cerevisiae* at near-zero growth rates under non-energy-limited conditions, retentostat regimes were designed in which growth was prevented by a severely limited supply of ammonium or phosphate. To avoid starvation, any loss of nitrogen or phosphate from such cultures, either by cell lysis or by excretion of N- or P-containing compounds from viable cells,

should be compensated for. As a first approximation of the rates of N and P release by *S. cerevisiae* at near-zero growth rates, concentrations of N- and P-containing compounds were quantified in the outflow of an aerobic, glucose-limited retentostat culture. From these measurements, biomass-specific release rates of 8.3 µmol N/(g biomass)/h and 5.2 µmol P/(g biomass)/h were calculated (Supporting information Table S2.2). These rates were used to estimate required supply rates of ammonium and phosphate in non-growing retentostat cultures limited by either of these two nutrients. For a target biomass concentration in the retentostats of 5 g/L at a dilution rate of 0.025 h^{-1}, 0.1 g/L $(NH_4)_2SO_4$ was included in the medium feed of the ammonium-limited cultures, while 0.014 g/L KH_2PO_4 was used for phosphate-limited retentostat cultivation.

Aerobic growth of *S. cerevisiae* at non-limiting concentrations of glucose leads to aerobic alcoholic fermentation (De Deken 1966). Based on trial experiments, glucose concentrations in the influent of ammonium- and phosphate-limited retentostats were set at 120 g/L and 60 g/L, respectively. These concentrations of the growth-limiting nutrients resulted in residual glucose concentrations of ca. 15 g/L. Ethanol concentrations did not exceed 20 g/L, which is well below the value of 5 % (v/v) that has been reported to cause stress responses (Piper 1995).

Growth and viability in ammonium- and phosphate-limited retentostat cultures

Retentostat cultures were started by redirecting the effluent of steady-state ammonium- or phosphate-limited chemostat cultures, grown at a dilution rate of 0.025 h^{-1}, through a membrane filter unit placed inside the reactor (see Materials and Methods). Replicate ammonium-limited retentostats were operated for 220 h with full biomass retention, after which fouling caused the membrane filters to clog. Membrane fouling was not observed in the phosphate-limited retentostats, which were operated with full biomass retention until, after 400 h, the biomass concentration had reached a stable value.

Irrespective of the nutrient limitation regime, the onset of retentostat cultivation led to a gradual increase of the biomass concentration (Figure 2.1A and 2.1B). In ammonium-limited retentostats, the biomass concentration

stabilized at ca. 14 g/L after 150 h, while stabilization in the phosphate-limited cultures at ca. 18 g/L occurred after 300 h. The increase in biomass concentration in the ammonium-limited retentostats mainly reflected an increase of the dry mass per cell, which was initially smaller than in the phosphate-limited retentostats. Conversely, the biomass increase in phosphate-limited retentostats predominantly reflected an increase of the cell number (Figure 2.1C and 2.1D).

Culture viability was estimated by plate counts of colony-forming units (CFU) and by flow cytometry after CFDA/propidium iodide (PI) staining (Supporting information Table S2.3). We observed a consistently lower viability in the CFU assays than in the CFDA/PI stains. A similar difference has previously been attributed to loss of viability of retentostat-grown cells during plating (Boender et al. 2009; Vos et al. 2016). Based on PI staining, the viability of the ammonium- and phosphate-limited retentostat cultures towards the end of the experiments did not decrease below 80 % and 90 %, respectively (Figure 2.1A and 2.1B, Supporting information Table S2.3).

During retentostat cultivation, specific growth rates progressively decreased, reaching final values of 0.00056 ± 0.00010 h^{-1} and 0.00043 ± 0.00012 h^{-1} for the ammonium- and phosphate-limited cultures, respectively, corresponding to doubling times of 55 and 67 days (Figure 2.1E and 2.1F). Based on these observations, death rates of 0.0018 ± 0.0001 h^{-1} and 0.0012 ± 0.0001 h^{-1} were calculated for prolonged ammonium- and phosphate-limited retentostat cultures, respectively, which are somewhat higher than the value of 0.00047 h^{-1} reported for carbon limited aerobic retentostat cultures (Vos et al. 2016). The resulting gradual decrease of culture viability partially explained the difference between the observed biomass accumulation and the targeted values in the experimental design.

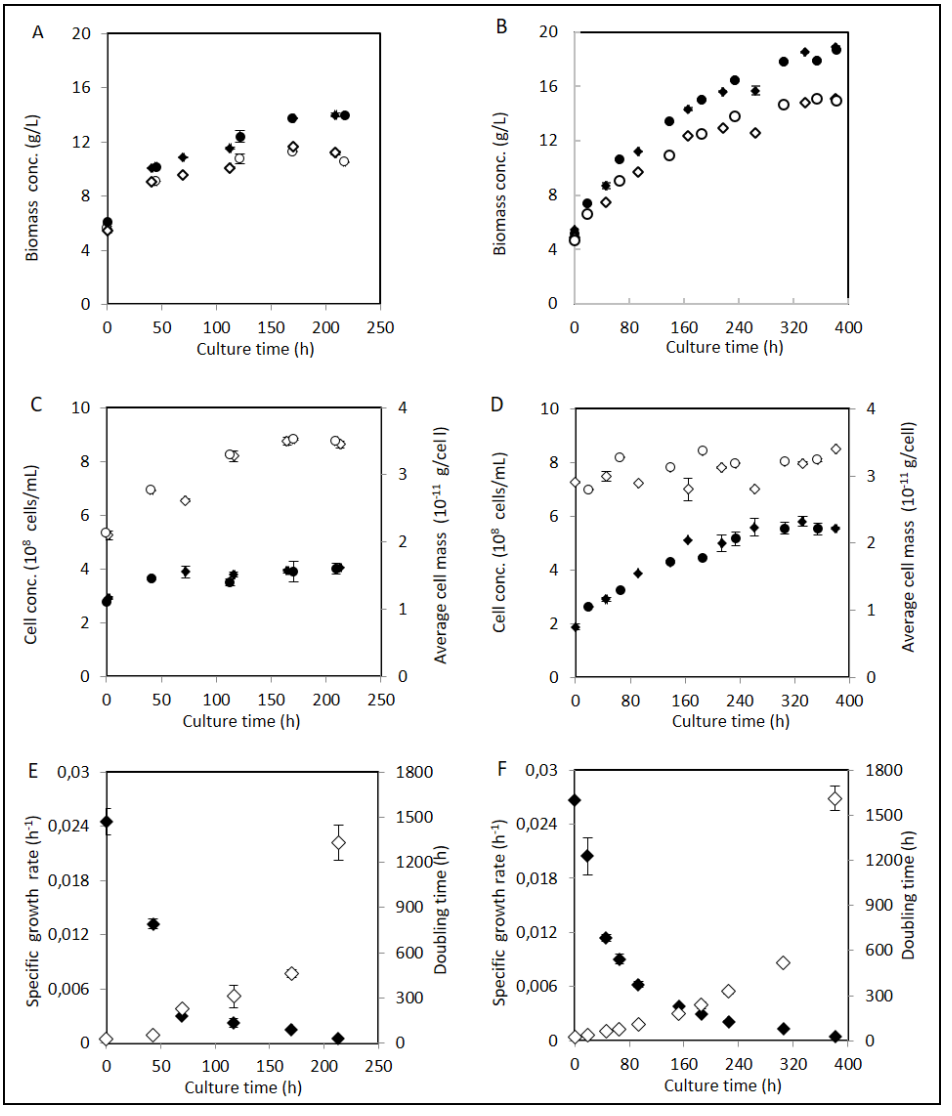

Figure 2.1 Biomass accumulation, cell counts and specific growth rates in aerobic ammonium- and phosphate-limited retentostat cultures of *S. cerevisiae* CEN.PK113-7D. Data of Figure A, B, C, and D obtained from independent duplicate cultures are shown as circles and diamonds, and error bars indicate standard errors of analytical replicates on samples from the same culture. Data of Figure E and F represent the averages and standard errors of measurements on duplicate retentostat cultures. A, B: Total biomass (closed symbols), viable biomass (open symbols) and percentage of viable biomass in ammonium-limited (A) and phosphate-limited (B) retentostat cultures. C, D: Cell numbers (closed symbols) and average mass per cell (open symbols) in ammonium-limited (C) and phosphate-limited (D) retentostat cultures. E, F: Specific growth rate

(closed symbols) and doubling time (open symbols) in ammonium-limited (E) and phosphate-limited (F) retentostat cultures.

Quantitative physiology under extreme ammonium and phosphate limitation

During retentostat cultivation, the biomass-specific consumption rates of glucose and oxygen and production rates of ethanol and CO_2 asymptotically decreased over time and stabilized after approximately 100 h in the ammonium-limited cultures and after approximately 200 h in the phosphate-limited cultures (Supporting information Figure S2.2). At this stage, the specific growth rate of the cultures was lower than 0.002 h^{-1}, growth stoichiometries became constant (Figure 2.1E and 2.1F) and cells were assumed to be in a metabolic pseudo steady state. Physiological parameters obtained from the preceding, slowly growing steady-state chemostat cultures (μ = 0.025 h^{-1}) and from the pseudo-steady-state, near-zero growth retentostat cultures (μ < 0.002 h^{-1}) are summarized in Table 2.1. As anticipated, the concentrations of the limiting nutrients (ammonium or phosphate) were below the detection limit, whereas glucose concentrations were between 10 and 20 g/L in all cultures (Table 2.1). Carbon- and degree-of-reduction balances yielded recoveries close to 100 % (Table 2.1), indicating that no major metabolites had been overlooked in the analyses.

In the slow-growing (μ = 0.025 h^{-1}) chemostat cultures the biomass-specific rates of glucose and oxygen consumption as well as ethanol and carbon dioxide production, were consistently higher in the phosphate-limited cultures than in the ammonium-limited cultures (Table 2.1). In line with these observations, the phosphate-limited cultures showed a lower biomass yield and higher ethanol yield on glucose. Respiratory quotients (RQ, ratio of CO_2 production and O_2 consumption rate) were identical for the two nutrient limitation regimes, indicating that the difference in biomass yield of the chemostat cultures was not caused by different contributions of respiratory and fermentative metabolism. Furthermore, the sum of the specific production rates of the four minor byproducts (glycerol, succinate, lactate and acetate), which accounted for less than 4 % of the consumed glucose, were not significantly different for the two limitation regimes and were also not responsible for the observed difference in biomass yield.

Table 2.1 Physiological parameters of *S. cerevisiae* CEN.PK113-7D cultured in aerobic ammonium- and phosphate-limited (N- and P-limited) slow growth (SG) (μ = 0.025 h^{-1}) steady-state chemostats and near-zero growth (NZG) (μ < 0.002 h^{-1}) pseudo-steady-state retentostats. Data represent averages, with their standard errors, calculated from multiple measurements obtained from duplicate experiments.

Culture condition	Biomass specific net conversion rates								
	$q_{glucose}$[a]	$q_{ethanol}$	q_x[b]	$q_{glycerol}$	$q_{succinate}$	$q_{lactate}$	$q_{acetate}$	q_{O2}	q_{CO2}
N-limited at SG	14.0 ± 0.0	6.1 ± 0.2	0.96 ± 0.09	0.10 ± 0.01	0.40 ± 0.06	0.070 ± 0.001	0.017 ± 0.002	1.7 ± 0.0	5.5 ± 0.2
P-limited at SG	16.6 ± 1.2	7.9 ± 0.3	0.99 ± 0.04	0.18 ± 0.00	0.15 ± 0.01	0.065 ± 0.001	0.21 ± 0.01	2.1 ± 0.0	6.6 ± 0.3
N-limited at NZG	3.4 ± 0.1	1.5 ± 0.0	---[c]	0.18 ± 0.01	0.30 ± 0.01	0.048 ± 0.002	0.026 ± 0.001	0.71 ± 0.03	1.5 ± 0.0
P-limited at NZG	3.1 ± 0.1	1.1 ± 0.1	---	0.14 ± 0.03	0.15 ± 0.00	0.000 ± 0.000	0.049 ± 0.005	0.94 ± 0.02	1.6 ± 0.1

Culture condition							Residual nutrient concentrations		
	viability	RQ[d]	$Y_{x/s}$[e]	$Y_{p/s}$[f]	carbon recovery	reduction recovery	glucose	NH_4^+	PO_4^{3-}
	%				%	%	g/L	mM	mM
N-limited at SG	93 ± 0	3.1 ± 0.0	0.059 ± 0.000	0.32 ± 0.12	95 ± 1	95 ± 1	16.48 ± 0.2	BD[g]	18.4 ± 0.92
P-limited at SG	91 ± 0	3.1 ± 0.1	0.052 ± 0.000	0.36 ± 0.00	99 ± 6	99 ± 3	18.21 ± 0.7	40.5 ± 2.0	BD
N-limited at NZG	80 ± 0	2.1 ± 0.1	---	0.33 ± 0.02	101 ± 2	98 ± 3	14.99 ± 2.01	BD	18.2 ± 0.90
P-limited at NZG	90 ± 0	1.7 ± 0.0	---	0.28 ± 0.03	98 ± 2	99 ± 1	10.30 ± 0.15	53.5 ± 2.7	BD

Notes: a: Biomass-specific rates were expressed in the unit of mCmol/(g viable biomass)/h.

b: biomass specific production rate. "X" represents "biomass".

c: Not calculated.

d: RQ, respiratory quotient (q_{CO2}/q_{O2}).

e: $Y_{x/s}$, Yield of biomass (g biomass/(g glucose consumed)).

f: $Y_{p/s}$, Yield of ethanol (g ethanol/(g glucose consumed)).
g: BD, below detection limit of assay.

In the pseudo-steady-state near-zero growth retentostat cultures, the observed ethanol yields on glucose (Table 2.1) were respectively 71 % and 53 % of the theoretical maximum (0.51 g ethanol/(g glucose)) for the ammonium- and phosphate-limited regimes. Consistent with this observation, significant oxygen consumption occurred in these cultures and their RQ values were significantly lower than those of the preceding chemostat cultures. For the phosphate-limited cultures the difference was most pronounced. These observations indicate that near-zero growth achieved by phosphate limitation leads to a more respiratory metabolism than was observed in the preceding slowly growing, phosphate-limited chemostats. Formation of byproducts accounted for 16 % and 11 % of the supplied glucose in the ammonium- and phosphate-limited near-zero growth cultures, respectively. Glycerol and succinate were the main contributors, with succinate accounting for 9 % of the consumed glucose in the ammonium-limited culture.

Biomass composition under extreme ammonium and phosphate limitation

To analyse the impact of extreme ammonium and phosphate limitation on biomass composition, biomass samples from slow growing, steady-state chemostat cultures and from near-zero growth rate pseudo-steady-state retentostat cultures were analysed for their elemental and macromolecular compositions (Table 2.2). In the chemostat cultures as well as in the retentostat cultures, the content of the growth-limiting element in the biomass was strongly reduced relative to that of the culture grown under the other nutrient limitation (Table 2.2). This difference was even more pronounced in the retentostat cultures than in the preceding chemostat cultures. The nitrogen content of biomass from ammonium-limited retentostat cultures was ca. 2-fold lower than that of the corresponding phosphate-limited retentostats, while the phosphorus content of biomass from the phosphate-limited retentostats was 3.5-fold lower than that of biomass from the ammonium-limited retentostats. Both in phosphate-limited chemostats and retentostats, a low phosphorus content was accompanied by a 2-3 fold higher sulfur content than in the corresponding ammonium-limited cultures. The increased sulfur content in phosphate-limited cultures may be due to sulfate uptake by high-affinity

phosphate transporters (Tai et al. 2005). Compared with glucose-limited chemostat cultures of the same *S. cerevisiae* strain at a similar dilution rate (D= 0.022 h^{-1},Table 2.2), the biomass protein content and the total nitrogen content of cells grown in the ammonium-limited chemostat cultures were over 60 % and 50 % lower, respectively. Similarly, in the phosphate-limited chemostat cultures, the phosphorus content of the biomass was ca. 50 % lower.

Table 2.2 Biomass elemental compositions of *S. cerevisiae* CEN.PK113-7D cultured in aerobic ammonium- and phosphate-limited (N- and P-limited) slow growth (SG) (μ = 0.025 h^{-1}) steady-state chemostats and near-zero growth (NZG) (μ < 0.002 h^{-1}) pseudo-steady-state retentostats. Data represent averages, with standard errors, of measurements from duplicate cultures and are compared with published values from aerobic glucose-limited (C-limited) chemostat culture of the same strain (Lange and Heijnen 2001).

Culture condition	μ	f_C	f_H	f_N	f_O	f_P	f_S	sum	C-mol[a] weight
	h^{-1}	%	%	%	%	%	%	%	g
N-limited	0.025	47.0 ± 0.0	7.2 ± 0.0	3.5 ± 0.1	39.5 ± 0.4	1.3 ± 0.0	0.16 ± 0.01	98 ± 0	25.56 ± 0.00
P-limited	0.025	44.0 ± 0.2	7.0 ± 0.1	5.3 ± 0.0	36.9 ± 0.3	0.50 ± 0.01	0.39 ± 0.03	94 ± 0	24.27 ± 0.25
N-limited	< 0.002	49.5 ± 0.4	7.6 ± 0.0	2.5 ± 0.0	39.5 ± 1.1	1.1 ± 0.0	0.11 ± 0.01	100 ± 1	27.33 ± 0.22
P-limited	< 0.002	47.3 ± 0.1	7.2 ± 0.0	4.6 ± 0.1	37.4 ± 0.0	0.29 ± 0.00	0.27 ± 0.01	97 ± 0	25.42 ± 0.08
C-limited	0.022	45.6	6.8	6.6	37.3	1.0	0.22	97	26.4

Note: a: The amount of biomass (g) containing 1 mol of carbon

Consistent with their low nitrogen content, ammonium-limited chemostat and retentostat cultures showed a ca. 2.5-fold lower biomass protein content than the corresponding phosphate-limited cultures, with the lowest protein content (9.6 %) measured in the ammonium-limited retentostats (Figure 2.2A). Conversely, glycogen contents were higher (5.8 fold in chemostats and 1.8 fold in retentostats) in ammonium-limited cultures than in phosphate-limited cultures, while trehalose contents were only 30-40 % higher in the ammonium-limited cultures (Figure 2.2B). When analysed throughout the retentostat experiments, glycogen contents in the ammonium-limited cultures remained consistently high, while they increased with declining specific growth rate in the

phosphate-limited cultures (Figure 2.2C). For both nutrient limitation regimes, the trehalose content reached a maximum at a specific growth rate of ca. 0.01 h^{-1} (Figure 2.2D).

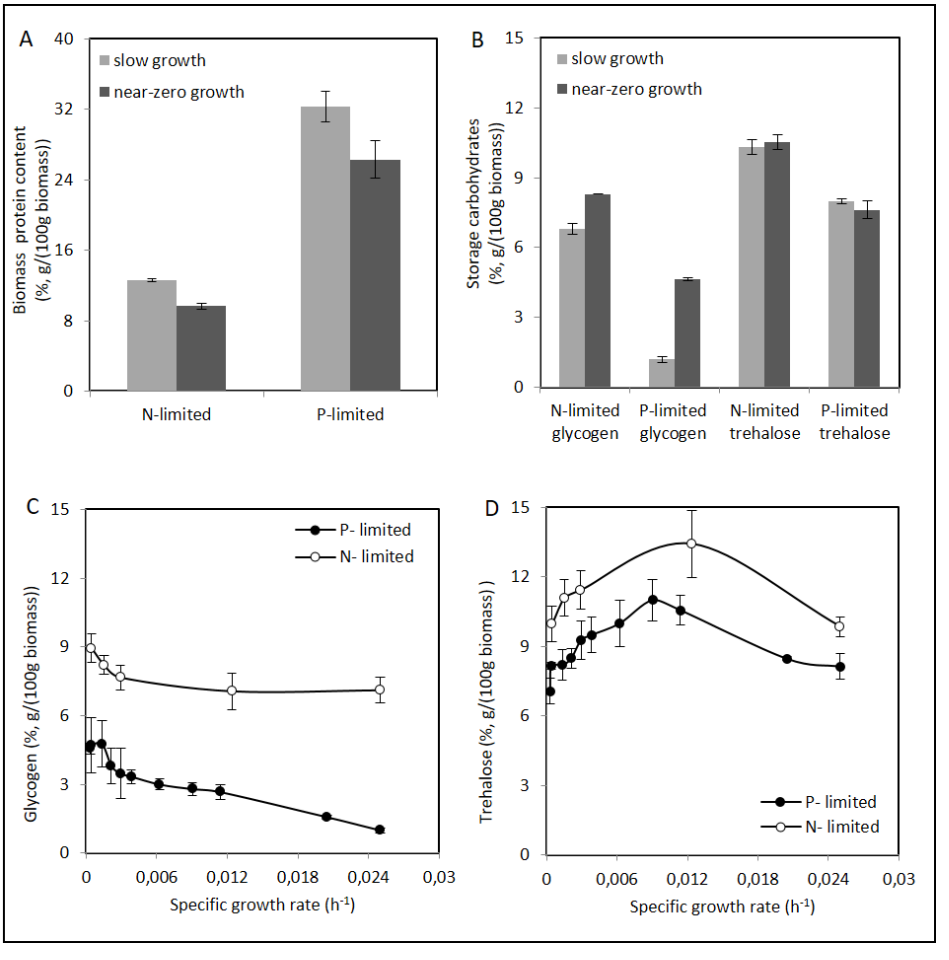

Figure 2.2 Biomass protein and storage carbohydrates (glycogen and trehalose) contents in aerobic ammonium- and phosphate-limited (N- and P-limited) cultures of *S. cerevisiae* CEN.PK113-7D. Data represent the averages and standard errors of multiple measurements on duplicate cultures. A, B: Biomass protein (A) and storage carbohydrates (glycogen and trehalose) (B). Samples were withdrawn from the steady-state, slow growth (μ = 0.025 h^{-1}) chemostat cultures, and the pseudo-steady-state, near-zero growth (μ < 0.002 h^{-1}) retentostat cultures. C, D: Glycogen (C) and trehalose (D) contents vs. the specific growth rate in the prolonged retentostat cultures.

Metabolic flux analysis

To further investigate the physiological differences between extreme ammonium and phosphate limitation, metabolic flux analysis was performed for both the slow growing, steady-state chemostat cultures ($\mu = 0.025\ h^{-1}$) and near-zero growth, pseudo-steady-state retentostat cultures ($\mu < 0.002\ h^{-1}$) (Figure 2.3, Supporting information Table S2.1B). At a specific growth rate of $0.025\ h^{-1}$, fluxes through glycolysis, pyruvate decarboxylase and alcohol dehydrogenase were significantly higher while the TCA cycle flux was slightly higher in the phosphate-limited cultures than in the ammonium-limited cultures. This observation indicated a higher contribution of catabolism in the phosphate-limited cultures. Assuming a P/O ratio of 1 (Verduyn et al. 1990), biomass-specific rates of ATP turnover were ca. 1.3-folder higher in the phosphate-limitated chemostat cultures than in the corresponding ammonium-limited cultures (Figure 2.3).

In the retentostats, fluxes through the pentose-phosphate pathway (PPP) were extremely low, which is consistent with the strictly assimilatory role of this central metabolic pathway in *S. cerevisiae* (Steel et al. 2001). The glycolytic flux was nearly identical for the two nutrient limitations. Conversely, distribution of pyruvate over alcoholic fermentation and the TCA cycle were different. Consistent with their lower RQ, phosphate-limited retentostat cultures channeled a higher fraction of the pyruvate into the TCA cycle than the ammonium limited retentostat cultures. Estimated non-growth-associated ATP consumption was higher in the phosphate-limited retentostats (3.4 ± 0.2 mmol ATP/(g viable biomass)/h) than in the ammonium-limited retentostats (2.9 ± 0.1 mmol ATP/(g viable biomass)/h) (Figure 2.3).

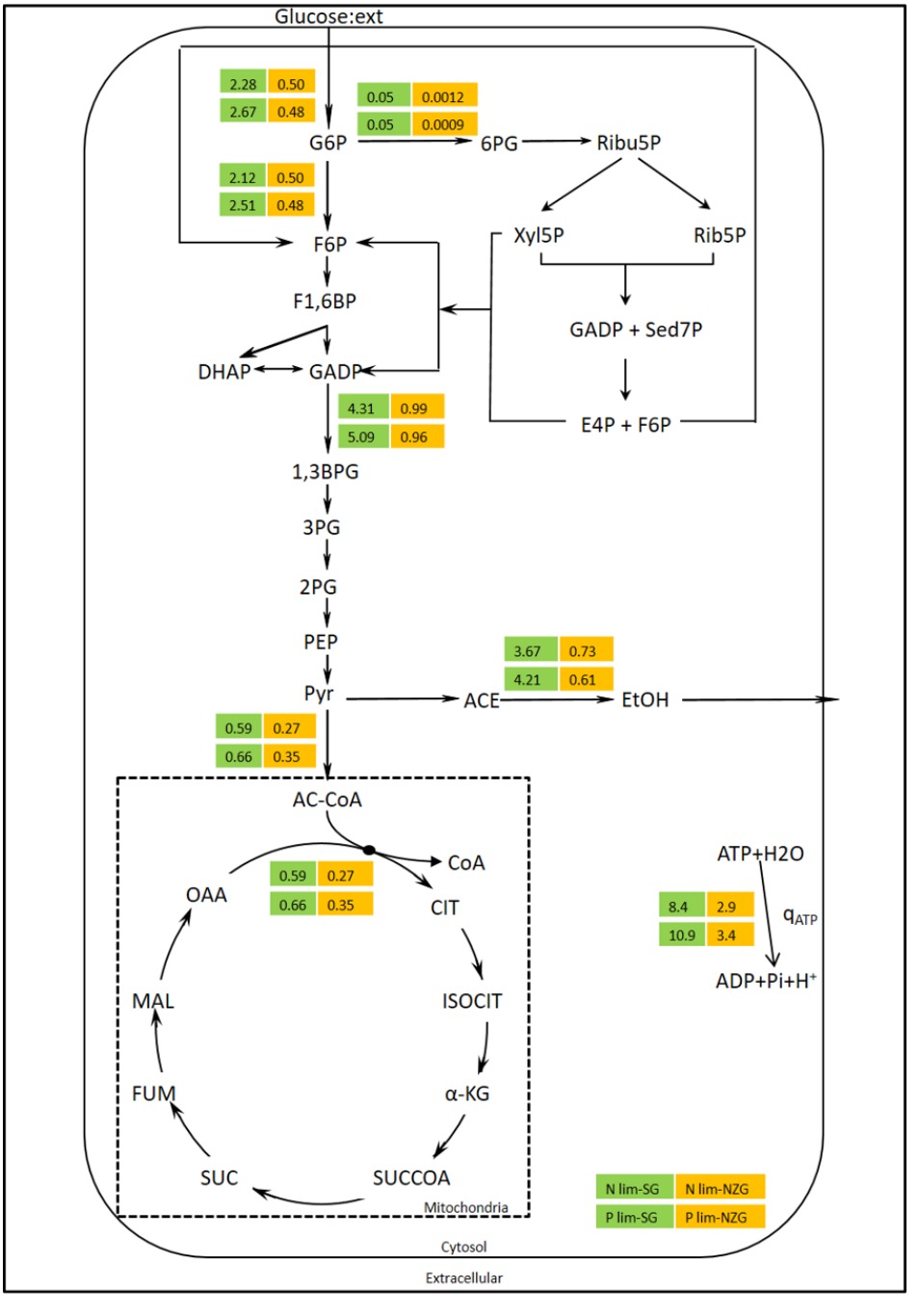
Glucose:ext
2.28 0.50
2.67 0.48
0.05 0.0012
0.05 0.0009
G6P
6PG
Ribu5P
2.12 0.50
2.51 0.48
F6P
Xyl5P
Rib5P
F1,6BP
GADP + Sed7P
DHAP
GADP
4.31 0.99
5.09 0.96
E4P + F6P
1,3BPG
3PG
2PG
PEP
3.67 0.73
4.21 0.61
Pyr
ACE
EtOH
0.59 0.27
0.66 0.35
AC-CoA
CoA
0.59 0.27
0.66 0.35
OAA
CIT
ATP+H2O
8.4 2.9
10.9 3.4
qATP
ADP+Pi+H+
MAL
ISOCIT
FUM
α-KG
SUC
SUCCOA
Mitochondria
N lim-SG
N lim-NZG
P lim-SG
P lim-NZG
Cytosol
Extracellular

Figure 2.3 Metabolic flux analysis in aerobic ammonium- and phosphate-limited (N- and P-limited) cultures of *S. cerevisiae* CEN.PK113-7D. Flux values present the steady-state, slow growth (SG) ($\mu = 0.025\ h^{-1}$) chemostat cultures (numbers on green background), and the pseudo-steady-state, near-zero growth (NZG) ($\mu < 0.002\ h^{-1}$) retentostat cultures (numbers on orange background). Data are expressed in millmoles of per gram viable biomass per hour and represent the averages of duplicate cultures. Complete flux analysis values and standard errors were presented in Supporting information Table S2.1B.

Energetics under extreme ammonium and phosphate limitation

Nitrogen and phosphate limitation can both be characterized as non-energy-limited cultivation regimes. However, because phosphate plays a vital role in cellular energy metabolism and energy status, the intracellular nucleotide levels (ATP, ADP and AMP) and corresponding adenylate energy charge and ATP/ADP ratios were quantified for both chemostat and retentostat conditions (Figure 2.4). Intracellular levels of all three adenine nucleotides were consistently higher in the chemostats than in the retentostats. Comparing these two limitations, both in slow-growth and near-zero growth cultures, intracellular ATP and AMP levels were consistently lower under phosphate limitation than under ammonium limitation. In addition, phosphate-limited near-zero growth cultures also showed ca. 40 % lower ADP levels than the corresponding ammonium-limited cultures, while ADP levels were identical in phosphate- and ammonium-limited, slow-growing chemostat cultures (Figure 2.4A).

Neither the ATP/ADP ratios nor the energy charge in the retentostat cultures differed from those in the corresponding slow-growing chemostat cultures (Figure 2.4B and 2.4C). However, ATP/ADP ratios in the phosphate-limited cultures were 30-35 % lower than in the corresponding ammonium-limited cultures. A similar, less pronounced difference was observed for the adenylate energy charge. These results show that phosphate limitation indeed significantly affected cellular energy status.

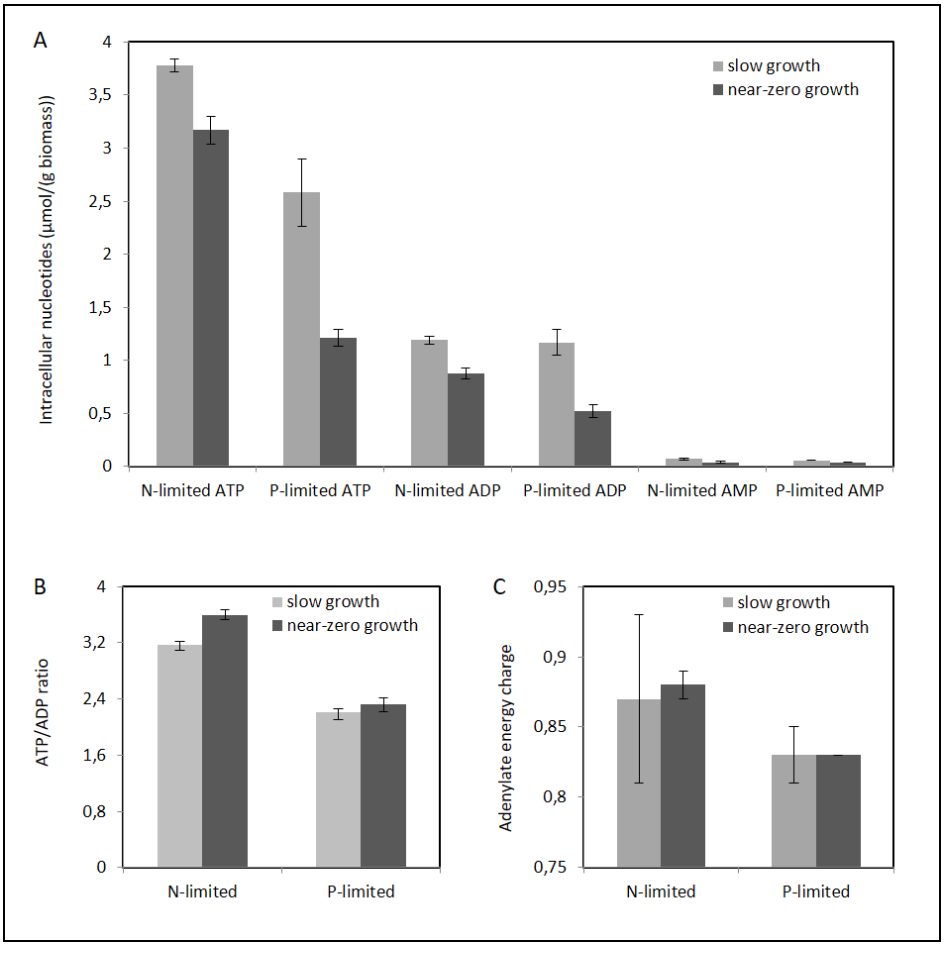

Figure 2.4 Intracellular adenosine phosphate concentrations (A), ATP/ADP ratio (B), and energy charge (C) in aerobic ammonium- and phosphate-limited (N- and P-limited) cultures of *S. cerevisiae* CEN.PK113-7D. Data represent the averages and standard errors of multiple measurements from duplicate cultures. Samples were withdrawn from the steady-state, slow growth (μ = 0.025 h^{-1}) chemostat cultures, and the pseudo-steady-state, near-zero growth (μ < 0.002 h^{-1}) retentostat cultures.

Discussion

Prolonged near-zero growth of S. cerevisiae under non-energy-limited conditions

Retentostat cultivation of heterotrophic microorganisms typically involves a constant, growth-limiting supply rate of the carbon and energy substrate (Ercan et al. 2015). The amount of viable biomass in such energy-limited retentostats

asymptotically increases to a constant value, while the specific growth rate asymptotically approaches zero. In the resulting pseudo steady states, biomass-specific substrate supply rates closely match cellular maintenance-energy requirements (Ercan et al. 2015). The retentostat regimes explored in this study, in which growth was restricted by supply of the nitrogen or phosphorus source, represented a fundamentally different scenario. While biomass also asymptotically increased to a constant value, the corresponding constant biomass-specific ammonium or phosphate consumption rates were not related to maintenance-energy metabolism. Instead, they represented release of nitrogen- or phosphorus-containing compounds, which were removed via the cell-free effluent.

Excretion of nitrogen- or phosphorus-containing compounds by severely ammonium- or phosphate-limited yeast cultures appears counter intuitive. Instead, release of these compounds probably occurs by cell death and/or lysis. *S. cerevisiae* can express a range of specific and non-specific amino acid permeases (Gournas et al. 2016), while di- and tri-peptides can be imported by Prt2p (Melnykov 2016). Presence of amino acids in culture supernatants is therefore likely to reflect the kinetics of such transporters, rather than a complete inability for amino-acid reconsumption by viable cells. Consistent with this hypothesis, extracellular concentrations of amino acids in the ammonium-limited retentostats were lower than the K_m values of the corresponding high-affinity *S. cerevisiae* amino-acid permeases (Supporting information Table S2.4).

Biomass concentrations in the ammonium- and phosphate-limited retentostats reached values that were approximately 3-fold higher than the target value of 5 g/L on which design of growth media and operating conditions were based. This difference could only partially be attributed to accumulation of non-viable biomass. In addition, strongly reduced contents of the growth limiting element in the retentostat-grown biomass could explain this large discrepancy to a large extent.

As previously reported for glucose-limited cultures (Brandberg et al. 2007), ammonium- and phosphate-limited cultivation of *S. cerevisiae* at low to near-zero growth rates led to increased intracellular levels of glycogen and trehalose. This observation confirms that glycogen and trehalose accumulation is a

universal physiological response of *S. cerevisiae* at near-zero growth conditions. Also in faster growing chemostat cultures, nitrogen limitation has been shown to lead to higher storage carbohydrate levels than other nutrient-limitation regimes (Hazelwood et al. 2009). Intracellular reserves of glycogen and trehalose enable survival during carbon and energy source starvation and can fuel cell cycle progression under carbon- and energy-source limitation (Silljé et al. 1999). Additionally, upregulation of genes involved in synthesis, metabolism and degradation of trehalose has been implicated in the extreme heat-shock tolerance of glucose-limited retentostat cultures of *S. cerevisiae* (Petitjean et al. 2015; Vos et al. 2016).

Energy metabolism of S. cerevisiae under extreme ammonium and phosphate limitation

Despite strongly reduced phosphate content and low intracellular levels of adenosine nucleotides, the adenylate energy charge of 0.83 of the phosphate-limited chemostat and retentostat cultures was within the normal physiological range of 0.7 to 0.95 (De la Fuente et al. 2014). Also the adenylate energy charge of 0.88 for the corresponding ammonium-limited cultures indicated that cells were able to maintain their energy status under extreme nutrient restriction.

Consistent with the well-known tendency of *S. cerevisiae* to exhibit aerobic alcoholic fermentation when exposed to excess glucose (De Deken 1966) respiratory quotients (RQs) of all ammonium- and phosphate-limited cultures were above 1. RQ values were lowest at near-zero growth rates (Supporting information Table S2.5), indicating that the contribution of fermentative metabolism decreased with decreasing specific growth rate. Even though *S. cerevisiae* has a low P/O ratio, respiratory catabolism of glucose yields much more ATP than fermentation (van Gulik and Heijnen 1995). However, its maximum rate of fermentative ATP generation is approximately 2-fold higher than its maximum rate of respiratory ATP generation (Sonnleitner and Käppeli 1986). These observations underlie a rate/yield trade-off hypothesis, according to which ATP can either be produced fast (but with a low efficiency) or efficiently (but at a lower maximum rate) (Pfeiffer et al. 2001). The shift towards a more respiratory metabolism in the near-zero growth rate retentostat cultures is entirely in line with this hypothesis.

Non-growth associated rates of ATP turnover in the aerobic, non-energy-limited cultures were significantly higher than maintenance-energy requirements estimated from aerobic and anaerobic energy-limited retentostat studies with the same *S. cerevisiae* strain (Supporting information Figure S2.3). While a similar uncoupling of anabolic energy demand and catabolic energy conservation has been reported for nitrogen-limited chemostat cultures, the underlying mechanism has not been elucidated (Boer et al. 2003; Brandberg et al. 2007; Larsson et al. 1997; Larsson et al. 1993; Lidén et al. 1995; Varela et al. 2004). Quantification of the in *vivo* cytosolic concentrations of ammonium and ammonia recently showed that, in ammonium-limited chemostat cultures of *S. cerevisiae* grown at pH 5, cytosolic ammonia concentrations exceeded extracellular concentrations (Cueto-Rojas et al. 2017). Diffusion of ammonia from the cells, combined with reuptake of ammonium cation by the high-affinity uniporter Mep2 (Marini et al. 1997) and expulsion of its associated proton by the plasma-membrane H^+-ATPase Pma1 could lead to a futile cycle.

Extreme phosphate-limited growth of *S. cerevisiae* induces expression of *PHO84*, which encodes a high-affinity phosphate/proton symporter and vacuolar synthesis of inorganic polyphosphate (Ogawa et al. 2000). By acting as a phosphorus sink, polyphosphate sustains phosphate uptake at low extracellular concentrations (Gerasimaitė and Mayer 2016; Ogawa et al. 2000). Its synthesis in yeast requires activity of the vacuolar H^+-ATPase (V-ATPase) to maintain a proton-motive force across the vacuolar membrane (Ogawa et al. 2000). Although high-affinity phosphate import and subsequent vacuolar polyphosphate synthesis must have resulted in increased ATP requirements, these are negligible compared to the observed non-growth associated ATP requirements in the phosphate-limited retentostat cultures. Unless very significant turnover of the polyphosphate pool has occurred, these additional ATP requirements are likely to have been caused by other, yet unknown processes.

Possible application of severe ammonium or phosphate limitation for industrial processes

Metabolic engineering of *S. cerevisiae* has enabled the production of a wide range of compounds whose biosynthesis from sugars requires a net input of ATP (Borodina and Nielsen 2014). The specific rate of formation of such

'anabolic' products is determined by the capacities and regulation of the enzymes of the product pathway and connected primary metabolic pathways, as well as by the continuous (re)generation of cofactors such as NAD(P)H, Coenzyme A and ATP. To optimize yields of such products, allocation of sugar to growth should be minimized. At the same time, ATP availability should not limit product formation rates. Theoretically, these goals can be reconciled by near-zero-growth-rate cultivation under non-energy-limited conditions. This study shows that, under ammonium limitation as well as under phosphate limitation, glucose-sufficient, near-zero-growth retentostat cultures of a laboratory strain of *S. cerevisiae* are able to maintain a normal energy charge and showed only a modest loss of culture viability. The extremely low protein content of biomass grown in the nitrogen-limited retentostats is likely to represent a disadvantage for high-level expression of heterologous product pathways. Moreover, nitrogen limitation is intrinsically poorly suited for production of proteins and other nitrogen-containing compounds. Extreme phosphate limitation did not affect biomass protein levels. However, relative to glucose-limited retentostats, both the ammonium- and phosphate-limited cultures showed increased rates of non-growth associated ATP dissipation. This increase is undesirable in industrial contexts, as the resulting increased rate of sugar dissimilation would go at the expense of the product yield. Future research should therefore aim at identifying the causes of non-growth associated ATP dissipation and on their elimination, either by alternative nutrient limitation regimes, by strain engineering or by alternative approaches to restrict cell division.

Acknowledgement

This research was financed by the Netherlands Be-Basic research program (Be-Basic project: FS10-04 Uncoupling of microbial growth and product formation). We thank Cor Ras, Patricia van Dam, Silvia Marine and Johan Knoll for analytical support.

Supporting information

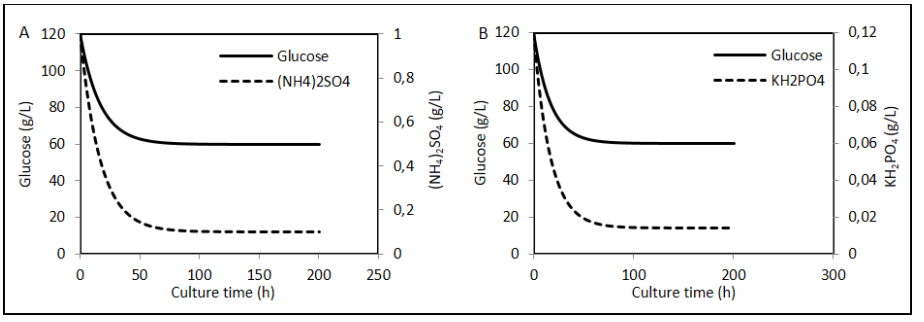

Figure S2.1 Gradual switch between chemostat and retentostat media during the start of the retentostat cultivations, (A) feed concentrations of glucose and ammonium sulfate of the N-limited retentostat cultures, (B) feed concentrations of glucose and potassium dihydrogen phosphate of the P-limited retentostat cultures vs culture time in the retentostat.

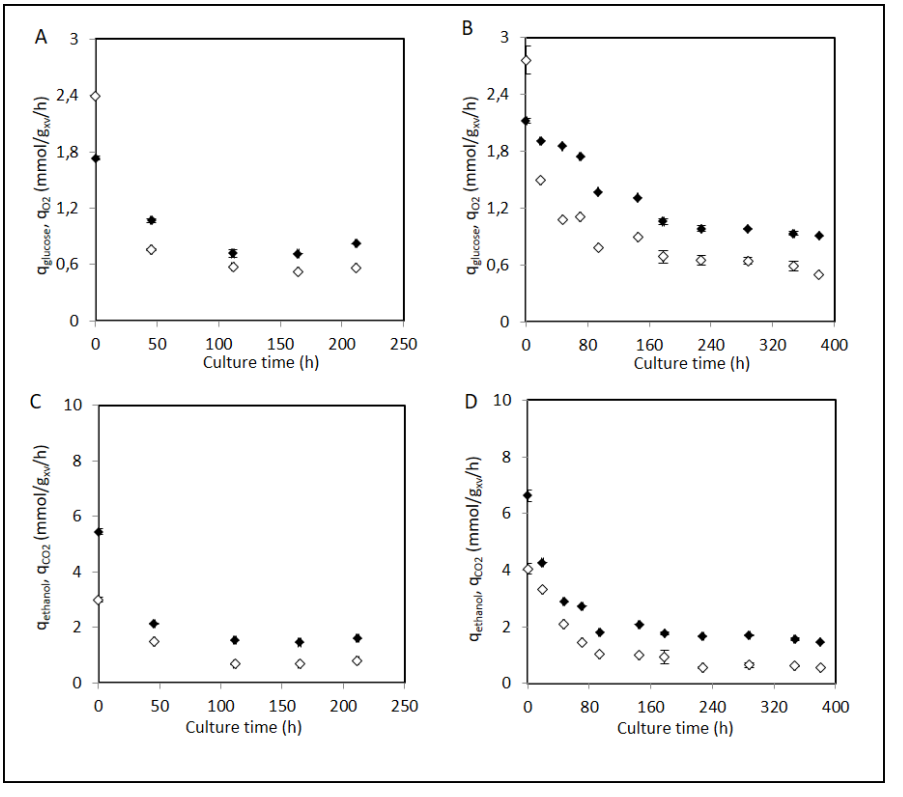

Figure S2.2 Biomass-specific consumption rates of glucose and oxygen and production rates of ethanol and carbon dioxide in aerobic ammonium- and phosphate-limited retentostat cultures of *S. cerevisiae* CEN.PK113-7D. Data represent the averages and standard errors of measurements from duplicate retentostat cultures. A, B: biomass-specific consumption rates of oxygen (closed symbols) and glucose (open symbols) in ammonium-limited (A) and phosphate-limited (B) retentostat cultures. C, D: biomass-specific production rates of carbon dioxide (closed symbols) and ethanol (open symbols) in ammonium-limited (C) and phosphate-limited (D) retentostat cultures.

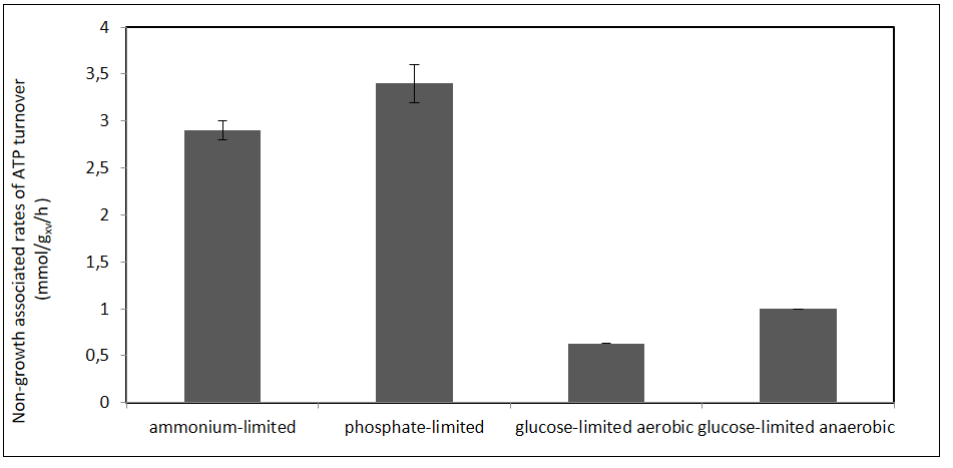

Figure S2.3 Non-growth associated rates of ATP turnover in retentostat cultures. Data from glucose-limited aerobic and anaerobic cultures were obtained from previously published work (Boender et al. 2009; Vos et al. 2016). Data from this study represent the averages and standard errors of measurements from duplicate cultures.

Table S2.1 Input parameters for metabolic flux analysis (S2.1A) and obtained flux values with their standard errors of central metabolism (S2.1B) for aerobic ammonium- and phosphate-limited (N- and P- limited) steady-state, slow growth (SG) (μ = 0.025 h^{-1}) chemostat cultures, and pseudo-steady-state, near-zero growth (NZG) (μ < 0.002 h^{-1}) retentostat cultures of *S. cerevisiae* CEN.PK113-7D.

Table S2.1A

Input parameters	Unit	N-limited at SG	N-limited at NZG	P-limited at SG	P-limited at NZG
q_X	mmol/g_{xv}/h	0.96 ± 0.09	0.022 ± 0.003	0.99 ± 0.04	0.017 ± 0.003
q_{CO2}	mmol/g_{xv}/h	5.5 ± 0.2	1.5 ± 0.0	6.6 ± 0.3	1.6 ± 0.1
$q_{ethanol}$	mmol/g_{xv}/h	3.1 ± 0.1	0.75 ± 0.00	4.0 ± 0.2	0.55 ± 0.05
$q_{glucose}$	mmol/g_{xv}/h	2.3 ± 0.0	0.57 ± 0.01	2.7 ± 0.2	0.53 ± 0.01
q_{O2}	mmol/g_{xv}/h	1.7 ± 0.0	0.71 ± 0.03	2.1 ± 0.0	0.94 ± 0.02
μ	h^{-1}	0.025 ± 0.002	0.00054 ± 0.00006	0.028 ± 0.003	0.00042 ± 0.0008
biomass protein	% (g/(100 g biomass))	12.6 ± 0.2	9.6 ± 0.4	32.3 ± 1.7	26.3 ± 2.1
Mw	g/mol	25.6 ± 0.0	24.3 ± 0.3	27.3 ± 0.2	25.4 ± 0.1
C molar formulas		$CH_{1.8}O_{0.63}N_{0.063}P_{0.011}S_{0.0013}$	$CH_{1.8}O_{0.60}N_{0.042}P_{0.0082}S_{0.0009}$	$CH_{1.9}O_{0.63}N_{0.10}P_{0.0044}S_{0.0034}$	$CH_{1.8}O_{0.59}N_{0.083}P_{0.0023}S_{0.0022}$

Table S2.1B

Metabolic Reaction	Enzyme	N-limited at SG mmol/g_{xv}/h	P-limited at SG mmol/g_{xv}/h	N-limited at NZG mmol/g_{xv}/h	P-limited at NZG mmol/g_{xv}/h
	Glycolysis				
Glucose→G6P	hexokinase	2.28 ± 0.04	2.67 ± 0.04	0.50 ± 0.01	0.48 ± 0.00
G6P→F6P	G6P isomerase	2.12 ± 0.03	2.51 ± 0.04	0.50 ± 0.01	0.48 ± 0.00
F6P→F1,6BP	phosphofructokinase	2.15 ± 0.03	2.54 ± 0.04	0.50 ± 0.01	0.48 ± 0.00
F1,6BP→DHAP+GADP	fructosebisphosphate aldolase	2.15 ± 0.03	2.54 ± 0.04	0.50 ± 0.01	0.48 ± 0.00
DHAP→GADP	triosephosphate isomerase	2.15 ± 0.03	2.54 ± 0.04	0.50 ± 0.01	0.48 ± 0.00
GADP→1,3BPG	glyceraldehyde phosphate dehydrogenase	4.31 ± 0.06	5.09 ± 0.08	0.99 ± 0.01	0.96 ± 0.01
1,3BPG→3PG	phosphoglycerate kinase	4.31 ± 0.06	5.09 ± 0.08	0.99 ± 0.01	0.96 ± 0.01
3PG→2PG	phosphoglycerate mutase	4.30 ± 0.06	5.08 ± 0.08	0.99 ± 0.01	0.96 ± 0.01
2PG→PEP	enolase	4.30 ± 0.06	5.08 ± 0.08	0.99 ± 0.01	0.96 ± 0.01
PEP→Pyr	pyruvate kinase	4.30 ± 0.06	5.07 ± 0.08	0.99 ± 0.01	0.96 ± 0.01
	PP-pathway				
G6P→6PG	G6P dehydrogenase	0.05 ± 0.00	0.05 ± 0.00	0.0012 ± 0.0001	0.0009 ± 0.0002
6PG→RIBU5P	6-phosphogluconate dehydrogenase	0.05 ± 0.00	0.05 ± 0.00	0.0012 ± 0.0001	0.0009 ± 0.0002
RIBU5P→RIB5P	ribosephosphate isomerase	0.02 ± 0.00	0.02 ± 0.00	0.0004 ± 0.0000	0.0003 ± 0.0001
RIBU5P→XYL5P	ribulosephosphate epimerase	0.03 ± 0.00	0.03 ± 0.00	0.0007 ± 0.0001	0.0005 ± 0.0001
RIB5P+XYL5P→GADP+SED7P	transketolase 1	0.02 ± 0.00	0.02 ± 0.00	0.0004 ± 0.0000	0.0003 ± 0.0001
GADP+SED7P→E4P+S6P	transaldolase	0.02 ± 0.00	0.02 ± 0.00	0.0004 ± 0.0000	0.0003 ± 0.0001
RIB5P+XYL5P→GADP+SED7P	transketolase 2	0.01 ± 0.00	0.02 ± 0.00	0.0003 ± 0.0000	0.0002 ± 0.0000

	TCA cycle				
AC-CoA+OAA→CoA+CIT	citrate synthase mitochondrial	0.59 ± 0.01	0.66 ± 0.06	0.27 ± 0.01	0.35 ± 0.02
CIT→ISOCIT	aconitase 1,2	0.59 ± 0.01	0.66 ± 0.06	0.27 ± 0.01	0.35 ± 0.02
ISOCIT→α-KG	isocitrate dehydrogenase (NAD)	0.58 ± 0.01	0.65 ± 0.06	0.27 ± 0.01	0.35 ± 0.02
ISOCIT→ α-KG	isocitrate dehydrogenase (NADP)	0.01 ± 0.00	0.01 ± 0.00	0.0002 ± 0.0000	0.0001 ± 0.0000
α-KG→SUCCoA	a-ketoglutarate dehydrogenase	0.58 ± 0.01	0.65 ± 0.06	0.27 ± 0.01	0.35 ± 0.02
SUCCoA→SUC	succinylcoa synthetase	0.58 ± 0.01	0.65 ± 0.06	0.27 ± 0.01	0.35 ± 0.02
SUC→FUM	succinate dehydrogenase	0.58 ± 0.01	0.65 ± 0.06	0.27 ± 0.01	0.35 ± 0.02
FUM→MAL	fumarate hydrase	0.58 ± 0.01	0.65 ± 0.06	0.27 ± 0.01	0.35 ± 0.02
FUM→MAL	fumarate hydrase cytosolic	0.01 ± 0.00	0.01 ± 0.00	0.0001 ± 0.0000	0.0001 ± 0.0000
MAL→OAA	malate dehydrogenase	0.59 ± 0.01	0.66 ± 0.06	0.27 ± 0.01	0.35 ± 0.02
	Pyruvate branchpoint				
Pyr→ACE	pyruvate decarboxylase	3.67 ± 0.07	4.21 ± 0.20	0.73 ± 0.00	0.61 ± 0.01
Pyr→AC-CoA	pyruvate dehydrogenase	0.59 ± 0.01	0.66 ± 0.06	0.27 ± 0.01	0.35 ± 0.02
Pyr→OAA	pyruvate carboxylase	0.02 ± 0.00	0.02 ± 0.00	0.0004 ± 0.0000	0.0003 ± 0.0001
ACE→EtOH	alcohol dehydrogenase	3.61 ± 0.06	4.14 ± 0.20	0.72 ± 0.00	0.61 ± 0.01
ACE→AC-CoA	acetyl-CoA synthase	0.06 ± 0.00	0.06 ± 0.00	0.001 ± 0.000	0.001 ± 0.000
AC-CoA→CoA	acetylcoa carboxylase cyt	0.05 ± 0.00	0.05 ± 0.00	0.001 ± 0.000	0.001 ± 0.000
ATP→ADP	**Non-growthed associated rates of ATP turnover**	8.4 ± 0.4	10.9 ± 0.5	2.9 ± 0.1	3.4 ± 0.2

Table S2.2 Determination of the required concentrations of $(NH_4)_2SO_4$ and KH_2PO_4 in the feeds of the N- and P-limited retentostats.

total N released from AAs [a] (mol/L)	total N released from protein (mol/L)	total N released rate (mol/g_{xv}/h)	total N compensation rate (based on 5 g/L biomass) (mol/g_{xv}/h)	$(NH_4)_2SO_4$ (g/L)
6.71E-03	5.71E-04	8.28E-06	4.14E-05	0.10

total P released from metabolites [b] (mol/L)	total P released rate (mol/g_{xv}/h)	total P compensation rate (based on 5 g/L biomass) (mol/g_{xv}/h)	KH_2PO_4 (g/L)
4.57E-04	5.19E-07	2.59E-06	0.014

Note: a: Measured amino acids: Ala, Gly, Val, Leu, Ile, Pro, Ser, Thr, Met, Asp, Phe, Cys, Glu, Lys, Asn, Gln, Tyr, His, Trp

b: Measured P-containing metabolites: F1,6BP, PEP, G1P, 6PG, T6P, UDP-Glc, GADP, 2PG, DHAP, 3PG, E4P, RIB5P, RIBU5P, XYL5P, M6P, F6P, G6P, SED7P, AMP, ADP, ATP, CoA, Ac-CoA

Table S2.3 Measured viabilities in steady state chemostat and pronged retentostat cultures, data present averages with their standard errors of results from duplicate experiments.

culture condition	culture time (h)	viability from CFU (%)	viability from CFDA (%)	viability from PI (%)
N-limited chemostat	136	80 ± 7	93 ± 2	95 ± 1
	184	87 ± 6	90 ± 0	93 ± 0
	256	84 ± 2	92 ± 2	92 ± 0
N-limited retentostat	0	82 ± 3	92 ± 2	92 ± 0
	43	81 ± 1	91 ± 2	90 ± 0
	70	79 ± 0	85 ± 0	88 ± 0
	117	71 ± 5	83 ± 1	87 ± 0
	170	66 ± 4	81 ± 1	84 ± 1
	213	67 ± 5	79 ± 1	78 ± 2
P-limited chemostat	103	80 ± 27	92 ± 3	93 ± 1
	153	80 ± 7	92 ±4	92 ± 0
	201	75 ± 2	87 ± 7	90 ± 2
P-limited retentostat	0	72 ± 12	89 ± 10	90 ± 0
	33	70 ± 30	89 ± 8	88 ± 2
	79	59 ± 11	84 ± 3	86 ± 1
	152	61 ± 11	83 ± 5	84 ± 2
	201	63 ± 25	80 ± 7	83 ± 1
	249	61 ± 0	82 ± 4	82 ± 1
	321	61 ± 10	77 ± 5	81 ± 1
	354	62 ± 5	76 ± 9	85 ± 0
	382	62 ± 8	76 ± 12	80 ± 0

Table S2.4 Extracellular amino acids concentration (μM) in aerobic ammonium-limited (N-limited) steady-state, slow growth (SG) ($\mu = 0.025\ h^{-1}$) chemostat cultures, and pseudo-steady-state, near-zero growth (NZG) ($\mu < 0.002\ h^{-1}$) retentostat cultures of *S. cerevisiae* CEN.PK113-7D. Data represent the averages and standard errors of multiple measurements from duplicate cultures.

	N-limited at SG	N-limited at NZG	Km from literature
Ala	17.9 ± 4.4	6.9 ± 1.3	37 (Ruiz et al. 2017)
Gly	0.90 ± 0.25	0.46 ± 0.02	~[a]
Val	2.0 ± 0.3	0.81 ± 0.06	37 (Ruiz et al. 2017)
Leu	0.47 ± 0.05	1.2 ± 0.3	37 (Ruiz et al. 2017; Schreve and Garrett 1997)
Ile	0.31 ± 0.05	0.59 ± 0.19	37 (Ruiz et al. 2017)
Pro	0.17 ± 0.03	0.10 ± 0.04	34 (Gournas et al. 2015; Tavoularis et al. 2003)
Ser	1.1 ± 0.1	1.2 ± 0.2	590 (Ruiz et al. 2017)
Thr	0.72 ± 0.09	0.57 ± 0.02	590 (Ruiz et al. 2017)
Met	~[b]	~[b]	13 (Isnard et al. 1996)
Asp	1.0 ± 0.1	1.0 ± 0.0	56 (Ruiz et al. 2017)
Phe	0.38 ± 0.03	0.92 ± 0.31	24 (Sáenz et al. 2014)
Cys	25.9 ± 3.9	4.4 ± 0.6	37, 55 (Kaur and Bachhawat 2007; Ruiz et al. 2017)
Glu	8.8 ± 0.8	4.2 ± 0.5	48 (Ruiz et al. 2017)
Lys	33.7 ± 2.2	0.52 ± 0.17	10-25 (Ghaddar et al. 2014; Ruiz et al. 2017)
Asn	~[c]	3.5 ± 0.0	590 (Ruiz et al. 2017)
Gln	4.1 ± 0.6	6.0 ± 0.3	590 (Ruiz et al. 2017; Zhu et al. 1996)
Tyr	~[d]	~[d]	160 (Omura et al. 2007)
His	~[e]	0.11 ± 0.06	10-20 (Bajmoczi et al. 1998; Ruiz et al. 2017)
Trp	~[f]	~[f]	42 (Trip et al. 2004)

Note: a: did not find in literature

b: Meth was below the detection limit of assay: 0.03 µM

c: Asn was below the detection limit of assay: 0.125 µM

d: Tyr was below the detection limit of assay: 0.03 µM

e: His was below the detection limit of assay: 0.12 µM

f: Trp was below the detection limit of assay: 0.025 µM

Table S2.5 Comparison of respiratory quotients (RQ) of aerobic ammonium- and phosphate-limited steady state, slow growth (SG) ($\mu = 0.025\ h^{-1}$) chemostat cultures and pseudo-steady-state, near-zero growth (NZG) ($\mu < 0.002\ h^{-1}$) retentostat cultures of *S. cerevisiae* CEN.PK113-7D. Data from this study represent averages with standard errors of measurements from duplicate cultures.

μ (h^{-1})	RQ		Reference
	ammonium-limited	phosphate-limited	
0.1	4.5 ± 0.2	3.4 ± 0.0	(Boer et al. 2003)
0.025	3.1 ± 0.0	3.1 ± 0.1	This study
< 0.002	2.1 ± 0.1	1.7 ± 0.0	This study

Chapter 3 Physiological responses of *Saccharomyces cerevisiae* to industrially relevant conditions: slow growth, low pH and high CO_2 levels

This chapter has been published in Biotechnology and Bioengineering.2020;117:721–735. https://doi.org/10.1002/bit.27210.

Xavier Hakkaart and Yaya Liu are joint first authors.

Abstract

Engineered strains of *Saccharomyces cerevisiae* are used for industrial production of succinic acid. Optimal process conditions for dicarboxylic-acid yield and recovery include slow growth, low pH, and high CO_2. To quantify and understand how these process parameters affect yeast physiology, this study investigates individual and combined impacts of low pH (3.0) and high CO_2 (50 %) on slow-growing chemostat and retentostat cultures of the reference strain *S. cerevisiae* CEN.PK113-7D. Combined exposure to low pH and high CO_2 led to increased maintenance-energy requirements and death rates in aerobic, glucose-limited cultures. Further experiments showed that these effects were predominantly caused by low pH. Growth under ammonium-limited, energy-excess conditions did not aggravate or ameliorate these adverse impacts. Despite the absence of a synergistic effect of low pH and high CO_2 on physiology, high CO_2 strongly affected genome-wide transcriptional responses to low pH. Interference of high CO_2 with low-pH signaling is consistent with low-pH and high-CO_2 signals being relayed via common (MAPK) signaling pathways, notably the cell wall integrity, high-osmolarity glycerol, and calcineurin pathways. This study highlights the need to further increase robustness of cell factories to low pH for carboxylic-acid production, even in organisms that are already applied at industrial scale.

Keywords: acid stress, carbon dioxide, carboxylic acid, yeast, zero-growth

Introduction

Dicarboxylic acids are attractive platform molecules for production of a wide range of chemicals (Becker et al. 2015). High-yield microbial conversion of glucose to dicarboxylic acids can be achieved through the reductive branch of the TCA cycle and requires elevated concentrations of dissolved carbon dioxide (CO_2) to promote carboxylation of pyruvate or phosphoenolpyruvate to oxaloacetate (Ahn et al. 2016; Yin et al. 2015; Zelle et al. 2010). Cost efficiency and sustainability of industrial dicarboxylic-acid production can be increased by using culture pH values well below pKa1 of the product (pKa1 values of succinic, malic and fumaric acid are 4.16, 3.51, and 3.03, respectively). Production of the free acid prevents the need for coproduction of large quantities of gypsum (Abbott et al. 2009; Chen and Nielsen 2016). In contrast to most carboxylic-acid producing prokaryotes, the yeast *Saccharomyces cerevisiae* can withstand both high CO_2 (Aguilera et al. 2005; Eigenstetter and Takors 2017; Richard et al. 2014) and low pH (Della-Bianca et al. 2014; Postma et al. 1989; Verduyn et al. 1990). However, although *S. cerevisiae* grows at high CO_2, reduced biomass yields have been reported for respiring *S. cerevisiae* cultures grown at CO_2 values of 50 % and 79 % (Aguilera et al. 2005; Eigenstetter and Takors 2017; Richard et al. 2014). Similarly, *S. cerevisiae* can grow at pH values as low as pH 2.5, but only at significantly reduced specific growth rates (Carmelo et al. 1996; Della-Bianca et al. 2014; Della-Bianca and Gombert 2013; Eraso and Gancedo 1987; Orij et al. 2009).

Heterotrophic microorganisms dissimilate their carbon and energy substrate to supply ATP for biomass formation and for cellular maintenance (Pirt 1982; Pirt 1997). In yeast strains engineered for dicarboxylic-acid production, product formation and export costs ATP and therefore directly competes with growth and maintenance processes for ATP supply (Abbott et al. 2009; Jansen and van Gulik 2014; van Maris et al. 2004). Slow growth in fed-batch cultures (typically at specific growth rates below $0.05 h^{-1}$) limits consumption of substrate for biomass formation, which benefits product yields. However, a trade-off of this strategy is that the fraction of the energy substrate allocated to cellular maintenance increases with decreasing specific growth rate, thereby leaving less substrate available for energy-dependent product formation (Hensing et al. 1995; Maurer et al. 2006; Wahl et al. 2017). Despite its industrial relevance,

quantitative understanding of maintenance-related processes in *S. cerevisiae* and their sensitivity to industrially relevant process conditions is far from complete. Previous studies showed that, while growth-rate independent (Boender et al. 2009; Vos et al. 2016), the maintenance-energy requirement (m_s; mmol glucose/(g biomass)/h) of *S. cerevisiae* can be affected by the cultivation conditions (Lahtvee et al. 2016; Liu et al. 2019; Vos et al. 2016). For example, growth at pH 2.5 substantially reduces the maximum specific growth rate in batch cultures (Carmelo et al. 1996; Della-Bianca et al. 2014; Orij et al. 2009) and increases activity of the plasma-membrane proton pumps, suggesting that low pH also affects m_s (Carmelo et al. 1996; Eraso and Gancedo 1987). Moreover, even under mildly acidic conditions, the presence of weak, membrane permeable organic acids strongly increases energy-requirements for intracellular pH homeostasis (Abbott et al. 2007; Verduyn et al. 1990).

Although elevated CO_2 and low pH are relevant industrial process conditions for dicarboxylic-acid production and have both been reported to adversely affect yeast physiology, their effects on maintenance-energy requirements and viability of slow growing *S. cerevisiae* cultures have not yet been quantitatively analyzed. To address this knowledge gap, a nonproducing *S. cerevisiae* laboratory strain was grown at low and near-zero specific growth rates using a combination of glucose-limited chemostat and retentostat cultures, at a low pH (pH 3) and elevated CO_2 concentrations (50 % CO_2). Additionally, cultures were grown under ammonium-limited, energy excess conditions at low pH. Quantitative analysis of rates, yields, and culture viability was used to dissect physiological impacts of low pH and high CO_2. Furthermore, transcriptome analysis was employed to elucidate regulatory responses to these conditions

Materials and Methods

Strain and strain maintenance

S. cerevisiae CEN.PK113-7D (Entian and Kötter 2007; Nijkamp et al. 2012) was used in this study. The strain was stored at −80°C in 1ml aliquots in YPD (10 g/L Bacto yeast extract, 20 g/L Bacto peptone, 20 g/L glucose) supplemented with 30 % (vol/vol) glycerol.

Aerobic, glucose-limited bioreactor cultures

Glucose-limited chemostat and retentostat cultures were grown in 2 L bioreactors (Applikon, Delft, The Netherlands) at a working volume of 1.4 L, essentially as described previously (Vos et al. 2016). Chemically defined medium containing 20 g/L glucose was used for chemostat and retentostat cultures. The inflowing gas (0.5 vvm) was either compressed air (0.04 % CO_2) or an in-line mix of 50 % compressed air and 50 % pure CO_2 (> 99.7 % purity, Linde Gas Benelux, Schiedam, The Netherlands). The two gas flows were precisely controlled with mass flow controllers (Brooks, Hatfield, PA) and mixed in a ratio of 1:1. A detailed description of preculture preparation, bioreactor operation, and medium composition is given in Supporting Information Appendix 1. Chemostat cultures were assumed to be in steady state when, after at least five volume changes under the same process conditions, culture dry weight (see below) changed by less than 4 % over two consecutive volume changes. Glucose-limited cultures grown at pH 3 showed oscillations of CO_2 and O_2 concentrations in the off-gas with a frequency of 5-8 h, but were sampled regardless of the oscillations. These oscillations subsided upon approaching severe calorie restriction in the retentostat phase after 3 days.

Aerobic, ammonium-limited bioreactor cultures

Ammonium-limited retentostats grown at pH 3 were preceded by a chemostat phase under the same nutrient limitation, essentially as described before (Liu et al. 2019). Details on bioreactor operation and media composition of these nitrogen-limited cultures are given in Supporting Information Appendix 1. Ammonium-limited chemostat cultures were assumed to be in steady state when, after four volume changes, biomass dry weight, CO_2 production rate and residual glucose and ethanol concentrations in the effluent differed by less than 5 % over three consecutive volume changes.

Off-gas analysis, biomass, and extracellular metabolite determinations

Concentrations of O_2 and CO_2 in the exhaust gas of bioreactors were quantified with a paramagnetic/infrared off-gas analyzer (NGA 2000, Baar, Switzerland). For glucose-limited cultures, biomass concentrations were determined by filtering duplicate, exact volumes of culture broth, diluted to an approximate concentration of 2.5 g biomass/L, over predried Supor 47 membrane filters with

a 0.45 µm pore size (Pall Laboratory, Port Washington, NY) as described previously (Postma et al. 1989). Biomass concentrations in ammonium-limited cultures were analyzed by essentially the same procedure with the exception that filters were dried in an oven instead of in a microwave. Procedures for analysis of extracellular metabolites are described in detail in Supporting Information Appendix 1.

Viability

Viability measurements in retentostats were based on colony-forming unit (CFU) counts, which indicate reproductive capacity of single cells (Vos et al. 2016). For glucose-limited chemostats, CFU counts were obtained by sorting 96 single events detected by a FACS Aria™ II SORP Cell Sorter (BD Biosciences, Franklin Lakes, NJ) on a YPD plate (in quintuplicate, see Supporting Information Appendix 1 for details). To measure viability based on membrane integrity, cells were stained with the fluorescent dye propidium iodide (PI) (Vos et al. 2016). Staining of single-cell esterase activity with 5-CFDA-AM was used to evaluate metabolic activity (Bisschops et al. 2015). Flow cytometry was done on a BD-Accuri C6 with a 488 nm excitation laser (Becton Dickinson, Franklin Lakes, NJ). For each sample, over 10,000 events in fluorescence channel 3 (670 LP) were analyzed for PI and in fluorescence channel 1 (530/30 nm) for 5-CFDA-AM. The forward-scatter height (FSC-H) threshold was set to 80,000.

Regression analysis of biomass accumulation in glucose-limited retentostats

Quantification of maintenance-energy requirements and death rate in glucose-limited retentostats was done by model-based regression analysis of biomass accumulation over time (Vos et al. 2016). The fitted model parameters were a constant first-order death rate and a growth-rate independent maintenance-energy coefficient. The maximum theoretical yield of biomass on substrate glucose ($Y_{x/s}^{max}$) was set to a fixed value of 0.5 g_x/g_s. This analysis generated quantitative estimates of specific growth rate and glucose consumption rates during the first, dynamic phase of retentostat cultivation (see Results section).

Carbon and nitrogen balances and rate calculations

Carbon and nitrogen recoveries were calculated based on measurements of substrate and product concentrations in the gas and liquid phases and gas and

liquid in- and outflow rates. Ethanol evaporation from bioreactors was quantified (Cueto-Rojas et al. 2016) and taken into account in the calculation of specific ethanol-production rates. Specific growth rates in nitrogen-limited retentostat cultures were calculated as described previously (Boender et al. 2009).

Transcriptome analysis

Detailed descriptions of sampling procedures (Mendes et al. 2013; Piper et al. 2002) total RNA extraction (Schmitt et al. 1990), mRNA enrichment and RNA sequencing (Novogene, Hong Kong, China & Baseclear, Leiden, The Netherlands), alignment (STAR) (Dobin et al. 2012) and mapping (ht-seq count) (Anders et al. 2014) of reads against the S288C genome (Engel et al. 2014), TMM-normalization (EdgeR R-package) (Robinson et al. 2009), gene set enrichment (pianoR-package) (Väremo et al. 2013) and trend analysis with the regression-based growth rate (see above) as variable (maSigPro R-package) (Conesa et al. 2006; Nueda et al. 2014) are provided in Supporting Information Appendix 1. Transcriptome data are available in Gene Omnibus (https://www.ncbi.nlm.nih.gov/geo/) under accession number GSE133136.

Biomass composition, glycogen, and trehalose determination

Biomass elemental composition and biomass protein content were quantified as described previously (Lameiras et al. 2015; Lange and Heijnen 2001). After sampling for analysis of the intracellular storage carbohydrates glycogen and trehalose (Vos et al. 2016), pellets were stored at −80°C. Samples were processed (Parrou and François 1997) and analyzed as described in Supporting Information Appendix 1.

Metabolic flux analysis (MFA)

MFA was performed as described previously (Daran-Lapujade et al. 2004) with two modifications to the stoichiometric model: biomass composition was redefined based on measured biomass elemental composition and reduction of acetaldehyde to ethanol was incorporated as ethanol was a main product of ammonium-limited aerobic cultures.

Results

Low pH and high CO_2 levels cause increased death rate and maintenance-energy requirements in glucose-limited retentostat cultures of S. cerevisiae

The physiological responses of the *S. cerevisiae* laboratory strain CEN.PK113-7D under conditions relevant for industrial dicarboxylic acid production (aerobic, 50 % CO_2, pH 3.0) were investigated at near-zero growth rates in retentostat cultures. In retentostat cultures, a filter in the effluent line enabled full biomass retention (Ercan et al. 2015). At a constant feed rate of glucose, biomass accumulates and the supplied substrate per cell gradually decreases and growth ceases until virtually all substrate is used to fulfil maintenance-energy requirements (Boender et al. 2009; Vos et al. 2016).

Because the industrially relevant conditions applied in this study were expected to increase m_s relative to standard laboratory conditions (i.e., pH 5.0 and sparging with air) (Lahtvee et al. 2016; Vos et al. 2016), the asymptotic decrease of the glucose concentration in the feed, as previously applied for laboratory conditions (Vos et al. 2016), was not applied (Figure 3.1a and 3.1b). Instead, the substrate concentration in the feed was kept constant. This higher rate of substrate supply enabled the culture dry weight to accumulate to higher concentrations (Figure 3.1c and 3.1d). Culture viability, based on membrane integrity (PI staining) and reproductive capacity (CFU) was substantially lower under the industrially relevant conditions than under standard laboratory conditions (Figure 3.1e and 3.1f). Furthermore, the lower viable biomass concentration at near-zero growth rates in the retentostat cultures grown under industrially relevant conditions indicated a higher m_s than under laboratory conditions.

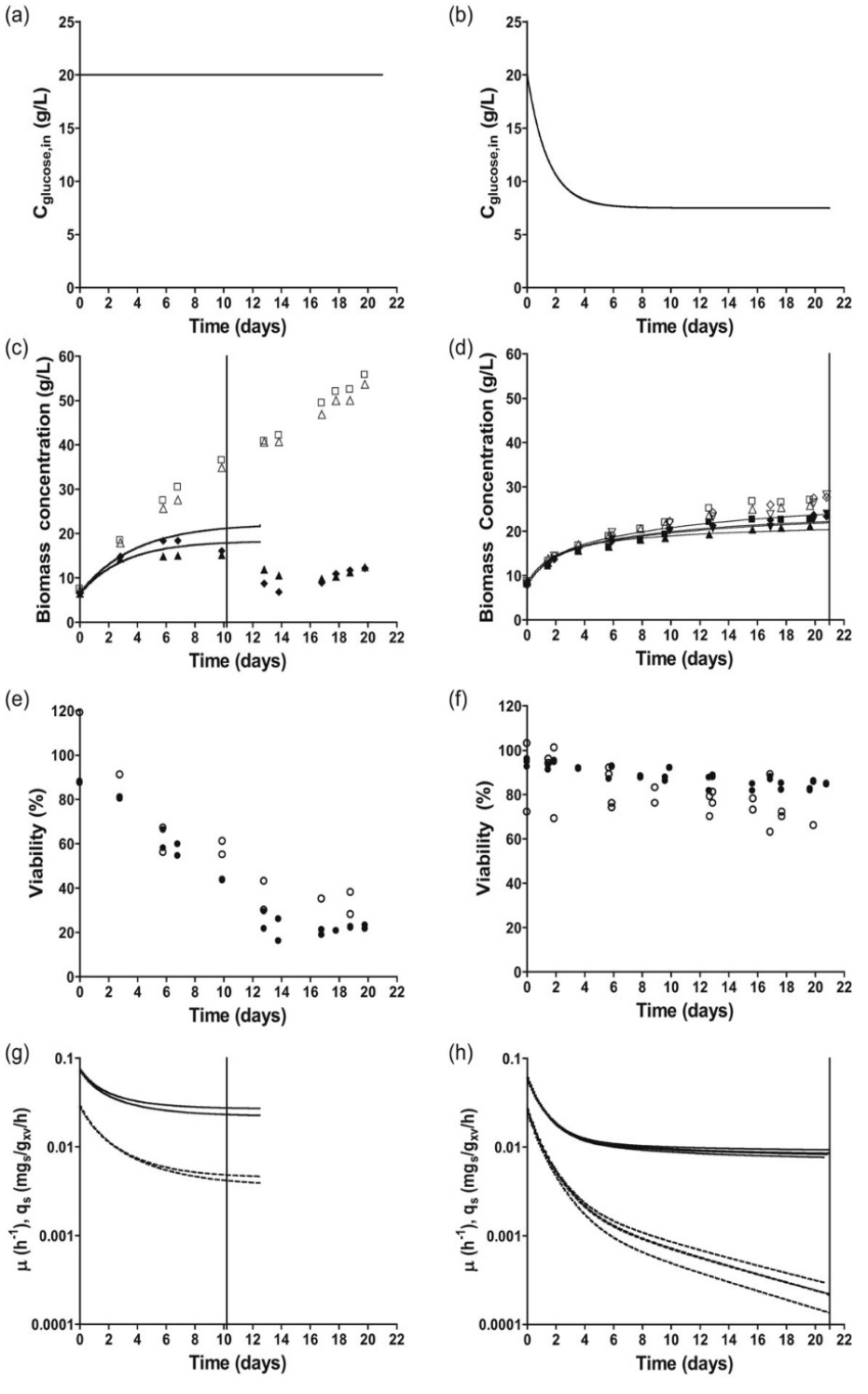
(a)
$C_{glucose,in}$ (g/L)
Time (days)
(b)
$C_{glucose,in}$ (g/L)
Time (days)
(c)
Biomass concentration (g/L)
Time (days)
(d)
Biomass Concentration (g/L)
Time (days)
(e)
Viability (%)
Time (days)
(f)
Viability (%)
Time (days)
(g)
μ (h^{-1}), q_s ($mg_s/g_{xv}/h$)
Time (days)
(h)
μ (h^{-1}), q_s ($mg_s/g_{xv}/h$)
Time (days)

Figure 3.1 Physiological characterization of *S. cerevisiae* CEN.PK113-7D in duplicate glucose-limited, aerobic retentostat cultures, grown at pH 3 and 50 % CO_2 (left column) and in quadruplicate cultures grown under reference conditions (pH 5, 0.04 % CO_2; (Vos et al. 2016)). a & b: Glucose concentration in influent during retentostat cultivation. c & d: Biomass dry weight (open symbols) and viable biomass dry weight estimated by propidium iodide (PI) staining (closed symbols). The vertical line indicates the time until which data points were included in regression analysis for biomass accumulation (see main text for detailed explanation). e & f: Viability of retentostat cultures based on PI staining (closed symbols) and CFU (open symbols). g & h: Regression-based biomass-specific growth rate (μ, gray lines) and biomass-specific glucose uptake rate (black lines) during the first 10 d of retentostat cultivation. Viable biomass concentrations used for regression analysis were based on PI staining. The vertical line indicates the time until which data points were included in the regression analysis for biomass accumulation (see main text for detailed explanation). CFU, colony-forming unit; PI, propidium iodide.

Time-dependent regression analysis of substrate and product concentrations was previously shown to enable accurate estimates of specific growth rate, specific substrate-consumption rate, first-order death rate and m_s in carbon- and energy-limited yeast retentostat cultures (Vos et al. 2016). In contrast to growth under standard laboratory conditions, growth under industrially relevant conditions caused a strong decrease of the viable biomass concentration after the first 10 days of cultivation, which prevented use of regression analysis for data obtained beyond Day 10 (Figure 3.1c and 3.1g).

Regression analysis showed that, although higher than the lowest growth rate reached under laboratory conditions (0.0008 h^{-1} , Figure 3.1h), the specific growth rate of retentostat cultures grown under the industrially relevant conditions was already extremely low at 10 days of cultivation (0.0045 ± 0.0003 h^{-1}, Figure 3.1g). This difference was partially due to an 8-fold higher death rate under industrially relevant conditions than under laboratory conditions (0.0039 ± 0.0005 h^{-1} vs 0.00047 h^{-1}; Figure 3.2). Moreover, the m_s calculated by regression analysis was more than 2-fold higher under industrially relevant conditions (0.0908 ± 0.0085 mmols/(g viable biomass)/h vs 0.039 ± 0.003 mmols/(g viable biomass)/h, Figure 3.2). Throughout retentostat cultivation, residual glucose concentrations remained between 0.01 and 0.07 mM. These results demonstrate that the combination of an extremely low growth rate, low pH and high CO_2 has marked adverse effects on the physiology of *S. cerevisiae*.

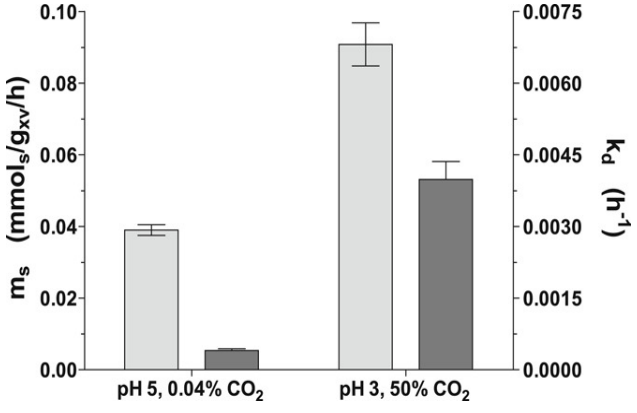

Figure 3.2 Maintenance-energy requirements and first-order death rate in pH 5, 0.04 % CO_2 reference conditions and in industrially relevant pH 3, 50 % CO_2 conditions in carbon-limited retentostat cultures of *S. cerevisiae* CEN.PK113-7D. These parameters were derived based on regression analysis of the biomass and viable biomass accumulation (see materials and methods and Supporting information Appendix 1 for details). Light grey bars and dark grey bars present maintenance energy requirements and first-order death rates, respectively.

High maintenance-energy requirements and death rates result from low pH rather than high CO_2 levels

To further explore the extreme physiological response of *S. cerevisiae* in retentostat cultures grown under industrially relevant conditions, the effects of low pH and high CO_2 concentration at low growth rates were investigated separately and in combination. These experiments were performed in glucose-limited chemostat cultures grown at the same dilution rate (0.025 h^{-1}) as the retentostats, but without cell retention. In energy-limited chemostat cultures grown at a fixed dilution rate, differences in biomass yield ($Y_{x/s}$) can provide strong indications for differences in maintenance-energy requirements (Lahtvee et al. 2016). Under laboratory conditions (low CO_2, pH 5) at 0.025 h^{-1}, *S. cerevisiae* invests ca. 20 % of the consumed glucose in cellular maintenance (Vos et al. 2016), resulting in a biomass yield of 0.416 ± 0.005 gx/gs. Despite small deviations in medium composition (higher concentrations of biotin and iron sulfate in the present study), the biomass yield of 0.419 ± 0.009 gx/gs measured in the present study was entirely consistent with the yield observed by Vos and coauthors (Vos et al. 2016).

Table 3.1 Physiology of *S. cerevisiae* CEN.PK113-7D in glucose-limited aerobic chemostat cultures grown at a dilution rate of 0.025 h^{-1}.

	pH 5		pH 3	
CO_2 in inlet gas (%)	0.04	50	0.04	50
Culture replicates	4	5	3	4
D (h^{-1})	0.026 ± 0.001	0.025 ± 0.001	0.025 ± 0.001	0.025 ± 0.000
Biomass yield (g_x/g_s)	0.419 ± 0.009	0.409 ± 0.005	0.388 ± 0.005	0.372 ± 0.004
Viability PI (%)	97 ± 1	96 ± 4	71 ± 1	85 ± 3
Viability CFDA (%)	96 ± 2	98 ± 0	81 ± 2	92 ± 2
Viability CFU-FACS (%)	92 ± 1^2	85 ± 10^5	73 ± 2^2	74 ± 1^2
μ (h^{-1})	0.027 ± 0.001	0.026 ± 0.000	0.035 ± 0.001	0.03 ± 0.001
$q_{glucose}$ (mmol/g_{xv}/h)	0.358 ± 0.016	0.357 ± 0.008	0.508 ± 0.011	0.443 ± 0.023
q_{O2} (mmol/g_{xv}/h)	1.019 ± 0.087	ND	1.361 ± 0.102	ND
q_{CO2} (mmol/g_{xv}/h^1)	1.042 ± 0.094	ND	1.394 ± 0.138	ND
$C_{glucose}$ (g/L)	0.011 ± 0.003	0.013 ± 0.001	0.005 ± 0.003	0.010 ± 0.006
Carbon recovery (%)	100.0 ± 4.1	ND	93.0 ± 4.5	ND
RQ (q_{CO2}/q_{O2})	1.023 ± 0.016	ND	1.024 ± 0.043	ND
Glycogen content (mg/g_x)	35.3 ± 3.3	32.6 ± 2.2	46.4 ± 3.2^2	30.4 ± 1.9
Trehalose content (mg/g_x)	19.4 ± 3.7	18.3 ± 1.94	12.64 ± 1.1^2	9.7 ± 1.7

Note: 'Replicates' indicates the number of biological replicates. Superscripts indicate the number of biological replicates for individual analyses when these deviate from the number presented under 'Replicates'. ND: not determined. Biomass specific rates (q values) were calculated based on viable biomass (xv), estimated by PI staining. At pH 3 the cultures showed oscillations in dissolved oxygen, exhaust CO_2 and exhaust oxygen levels, regardless of the percentage of CO_2 in the inlet gas.

Irrespective of culture pH, increasing CO_2 levels to 50 % did not significantly affect biomass yields at a dilution rate of 0.025 h^{-1} relative to those observed under standard laboratory conditions (Table 3.1). Conversely, growth at pH 3 led to a significantly lower biomass yield than at pH 5, both at standard and at elevated CO_2 levels (7.4 % and 9.7 % decrease, respectively; 0.419 ± 0.009 gx/gs vs 0.388 ± 0.005 gx/gs; $p < 0.001$ for pH 5 vs pH 3 when sparged with compressed air and 0.411 ± 0.006 gx/gs vs 0.371 ± 0.004 gx/gs; $p < 0.02$ for pH 5 vs pH 3 at 50 % CO_2). These results showed that the higher m_s in retentostat cultures grown at high CO_2 and low pH resulted from the low pH rather from the high CO_2. Measurements, by three different methods (CFU, PI, and CFDA staining, Table 3.1 and Supporting Information Appendix 2), showed that, irrespective of CO_2, low pH led to a strongly reduced viability of glucose-limited chemostat cultures. Conversely, increasing the CO_2 levels did not significantly affect culture viability. Assuming that cells measured as nonviable did not contribute to biomass formation or glucose consumption, specific rates were corrected for viability based on PI staining, resulting in higher specific growth rates (μ) and biomass-specific substrate uptake rates (Table 3.1).

Growth under ammonium-limited, energy-excess conditions does not reduce death rates at low pH and increases non-growth associated glucose consumption rates

Since glucose acts as energy substrate as well as carbon source, the high death rates and maintenance-energy requirements observed at pH 3 might reflect a cellular energy shortage. Therefore, physiological responses of *S. cerevisiae* were also investigated in near-zero growth rate retentostat cultures grown at pH 3 and pH 5 under ammonium-limited, glucose-excess conditions. These cultures were started from ammonium-limited chemostat cultures grown at a low dilution rate of 0.023 h^{-1}.

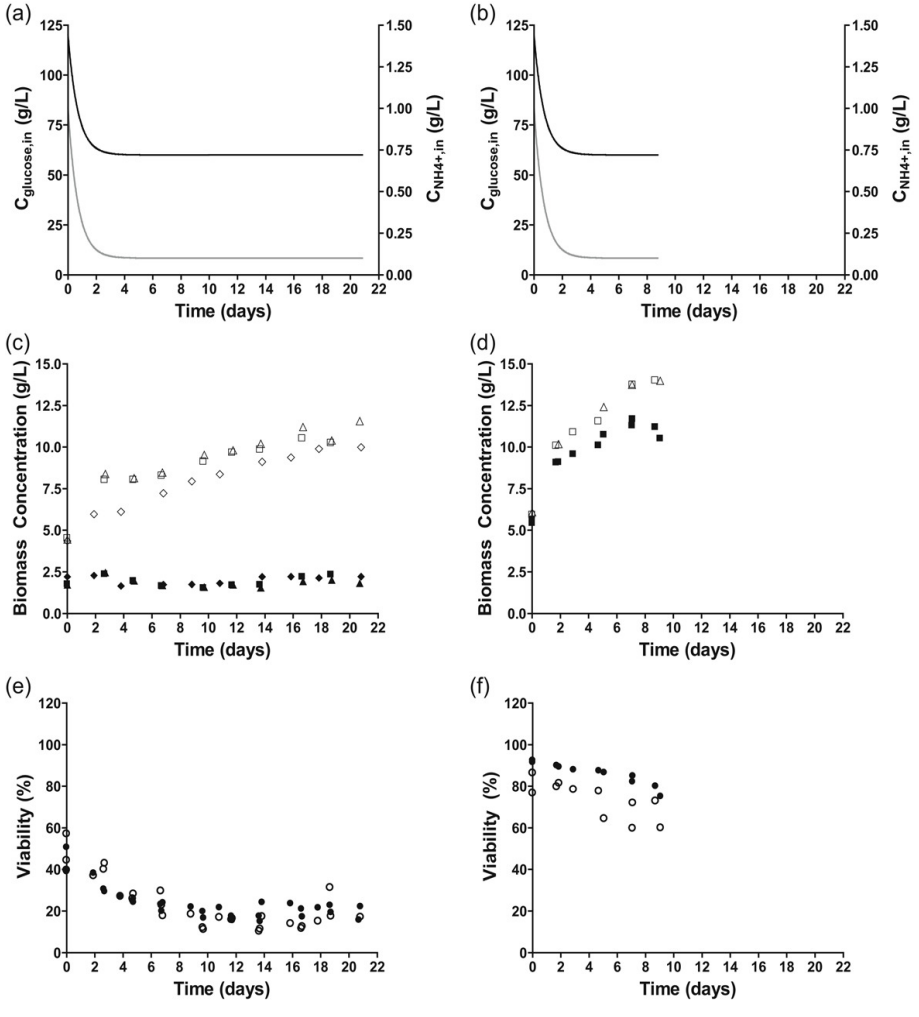

Figure 3.3 Physiological characterization of *S. cerevisiae* CEN.PK113-7D in triplicate nitrogen-limited retentostat cultures at pH 3 (left column) and in duplicate reference condition at pH 5 (Liu et al. 2019). a & b: Medium glucose (black line) and nitrogen (gray line) concentration during retentostat cultivation. c & d: Biomass accumulation for cell dry weight (open symbols) and viable biomass (closed symbols) quantified by PI staining. e & f: Viability of retentostat cultures based on PI staining (closed symbols) and CFU (open symbols). CFU, colony-forming unit; PI, propidium iodide.

The biomass concentration increased during the first 15 days of retentostat cultivation, after which it stabilized (Figure 3.3c). Culture viability in ammonium-limited chemostats grown at pH 3 (50 %; Figure 3.3e) was very low in comparison with viabilities observed in glucose- and ammonium-limited chemostat cultures grown at pH 5 (Figure 3.1f and 3.3f) and in glucose-limited cultures grown at pH 3 (Figure 3.1e). During ammonium-limited retentostat cultivation at pH 3, the total viable biomass concentration did not increase significantly (Figure 3.3c). Based on biomass and viability measurements towards the end of the retentostat experiments, the specific growth rate had decreased to 0.0006 ± 0.0001 h^{-1} (Table 3.2). As the viable biomass concentration remained virtually constant during retentostat cultivation, this growth rate equaled the death rate. The combination of nitrogen-limited growth and its associated excess availability of glucose clearly did not prevent adverse effects of low pH at near-zero growth rates. However, the substantially lower death rate in ammonium-limited retentostats indicated that growth under energy-source excess enabled *S. cerevisiae* to better survive prolonged exposure to low-pH stress than energy-source-limited growth.

Throughout the ammonium-limited retentostat cultivation, residual glucose concentrations remained above 10 g/L, confirming that cultures were not energy-limited. Ethanol concentrations remained below 15 g/L and, therefore, below reported toxic levels (Fujita et al. 2006). Residual ammonium concentrations were below detection limit (0.02 mg/L) in all samples. In ammonium-limited chemostat cultures 93 % of the supplied nitrogen was recovered in biomass. In contrast, only 35-40 % of supplied nitrogen was used for biomass formation after prolonged ammonium-limited retentostat cultivation. The remaining 60-65 % of the supplied nitrogen was lost in the effluent as proteins and peptides (Table 3.2).

Table 3.2 Physiology of *S. cerevisiae* CEN.PK113-7D in aerobic ammonium-limited chemostat and retentostat cultures at pH3

	Chemostat	**End Retentostat**
D (h^{-1})	0.023 ± 0.004	0.023 ± 0.004
μ (h^{-1})	0.053 ± 0.001	0.0006 ± 0.0001
Yield ($g_x/g_{glucose}$)	0.048 ± 0.002	0.0016 ± 0.0002
Viability PI (%)	43 ± 5	20 ± 3
Viability CFDA (%)	46 ± 3	12 ± 3
Viability CFU (%)	47 ± 7	17 ± 6
$q_{glucose}$ (mmol/g_{xv}/h)	6.1 ± 0.4	2.2 ± 0.2
q_{O2} (mmol/g_{xv}/h)	2.00 ± 0.3	0.83 ± 0.16
q_{CO2} (mmol/g_{xv}/h)	12.5 ± 0.8	4.6 ± 0.2
$q_{ethanol}$ (mmol/g_{xv}/h)	10.2 ± 0.6	4.1 ± 0.5
$q_{byproduct}$ (mmol/g_{xv}/h)	0.36 ± 0.01	0.18 ± 0.06
$Y_{ethanol/glucose}$ (mol/mol_s)	1.71 ± 0.03	1.83 ± 0.09
$C_{glucose}$ (g/L)	33.77 ± 1.09	11.22 ± 0.15
Carbon balance (%)	99 ± 1	100 ± 2
RQ value (q_{CO2}/q_{O2})	6.8 ± 1.2	5.9 ± 1.0
$q_{N,in}$ ($mmol_N/g_{xv}$/h)	0.079 ± 0.002	0.0034 ± 0.000
$q_{N,out}$ ($mmol_N/g_{xv}$/h)	0.007 ± 0.000	0.0022 ± 0.000
$q_{N,X}$ ($mmol_N/g_{xv}$/h)	0.073 ± 0.001	0.0014 ± 0.000
C_N (g/L)	BDL	BDL
Nitrogen-recovery (%)	101.0 ± 1.0	106 ± 9
Glycogen content (mg/g_x)	22 ± 2.0	66 ± 1.8
Trehalose content (mg/g_x)	35 ± 0.3	20 ± 1.0
Biomass composition	C1H1.87O0.63N0.089 P0.012S0.0016	C1H1.85O0.59N0.061 P0.012S0.0012

Note: Data present the average and standard deviation of triplicate experiments from steady-state (chemostat) and near-zero growth (retentostat) cultures. q's indicate biomass specific values. Subscripts indicate the considered compound. X, biomass; byproducts, the sum of acetate, succinic acid, lactic acid and glycerol; N,in, nitrogen consumed; N,out, sum of nitrogen excreted in the form of protein and free amino acids; N,X, nitrogen conserved in biomass. BDL: below detection limit.

The nonconstant death rate of the nitrogen-limited retentostat cultures prevented use of the regression model to estimate maintenance-energy requirements. Instead, MFA was used to derive and compare rates of ATP turnover in the absence of growth at the end of the glucose- and ammonium-limited retentostat experiments (vertical line in Figure 3.1c,d and final points in Figure 3.3c,d; input parameters used for the MFA are specified in Supporting Information Appendix 3). Because the biomass protein content was much lower in the ammonium-limited cultures, a condition-dependent biomass composition (Table 3.2) was a key input to the MFA-model. For the glucose-limited cultures, a previously reported biomass composition for glucose-limited chemostat cultures of the same strain was used (D=0.022 h^{-1}) (Lange and Heijnen 2001). Additionally, the *in vivo* P/O ratio was assumed to be 1.0 (Verduyn et al. 1991). The ATP hydrolysis rate derived from the MFA model for glucose-limited cultures at pH 5 closely matched the mATP derived from the regression model (Figure 3.2 and Figure 3.4). Under glucose limitation, a decrease in pH from 5 to 3 resulted in a 3.7 fold increase of the calculated ATP-hydrolysis rate at near-zero growth rates (0.58 and 2.13 mmolATP/(g viable biomass)/h, respectively). The differences between the ATP-hydrolysis rate at pH 3 derived from MFA (Figure 3.4) and the mATP from the regression model at pH 3 under glucose-limitation (Figure 3.2, estimated with a P/O-ratio of 1.0) can be explained by the different method of parameter estimation and the residual growth due to the high death rates under this condition. At pH 3, this nongrowth associated rates of ATP turnover was 2.9 fold higher in ammonium-limited retentostats (6.14 mmolATP/(g viable biomass)/h) than in the corresponding glucose-limited cultures (Figure 3.4).

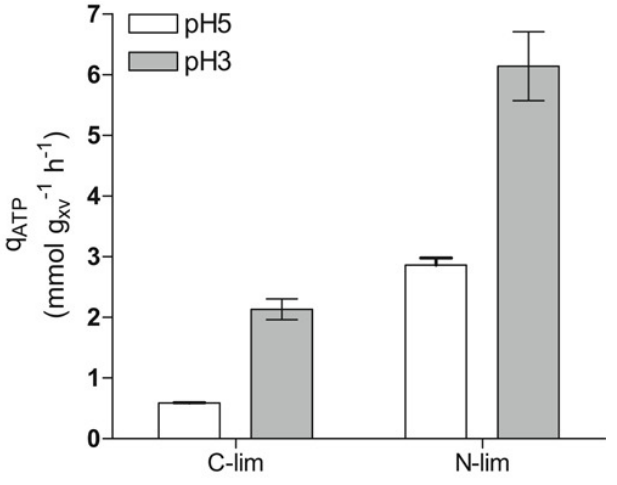

Figure 3.4 Maintenance energy requirements (glucose-limited cultures; C-lim) and non-growth associated energy requirements (ammonium-limited cultures; N-lim) of *S. cerevisiae* CEN.PK113-7D during growth at pH 5 and at pH 3 in retentostat cultures based on metabolic flux analysis. White bars: pH 5, grey bars: pH 3 (and 50 % CO_2 for glucose-limited cultures). Data for glucose-limited cultures grown at pH 5 are from (Vos et al. 2016), data for ammonium-limited cultivation at pH 5 are from (Liu et al. 2019).

Growth at low pH and/or high CO_2 cause extensive transcriptional rearrangements

Transcriptional responses of glucose-limited chemostat cultures to high CO_2, low pH or both was explored to gain further insight in the mechanisms underlying the reduced biomass yield, the increased maintenance energy requirements and increased cell death under industrially relevant conditions. Pair-wise differential gene expression analysis against the reference at pH 5 and 0.04 % CO_2 (absolute fold-change (FC)>2 and false-discovery rate (FDR)<0.005, see Section Materials and Methods) revealed large differences in yeast transcriptional responses to the different conditions for 50 % CO_2 alone (42 genes, blue), pH 3 alone (259 genes, yellow) and 50 % CO_2 and pH 3 combined (145 genes, green) (Figure 3.5a, Greek letters correspond with subsets in Figure 3.5b).

To investigate common and specific responses to high CO_2 and low pH conditions, the corresponding sets of differentially expressed genes were analyzed (Figure 3.5b, sections in Venn diagram denoted with α-ת). A set of 42 genes that were differentially expressed in response to high CO_2 only (Figure

3.5b, αβζ) did not reveal a clear enrichment for specific functional categories. The largest response was observed at pH 3, with 267 differentially expressed genes (Figure 3.5b, δεζ). This gene set showed an overrepresentation of genes involved in plasma membrane and cell-wall organization (Figure 3.5c, δεζ, yellow). The same functional categories were overrepresented among 154 genes that were differentially expressed (Figure 3.5b, βγδ) when high CO_2 and low pH were combined (Figure 3.5c, βγδ, green).

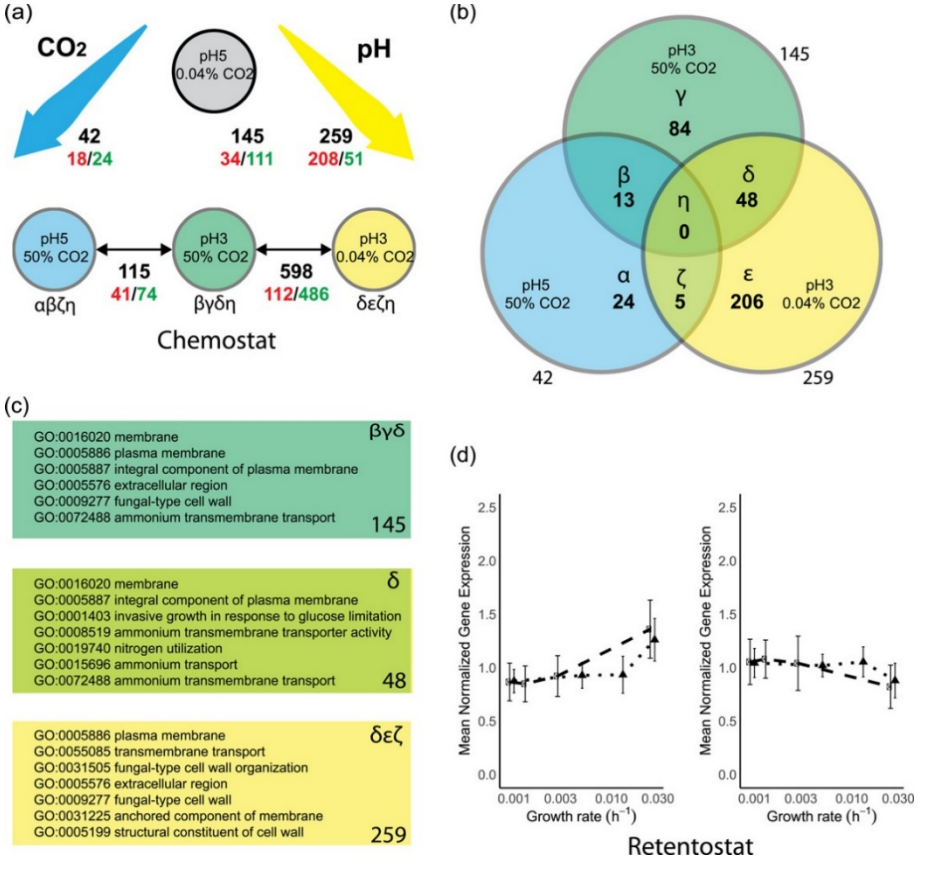

Figure 3.5 Differential Gene expression and Gene Set analysis in response to high CO_2, low pH, the combination of high CO_2 and low pH (a-c) and to near-zero growth rates (d-f). (a) Pairwise comparisons between steady-state chemostat conditions to high CO_2 (blue), low pH (yellow), its combination (green) versus a 'laboratory conditions" reference (grey), as well as against the combination of the conditions (low pH, high CO_2). Black numbers indicate total number of differentially expressed genes (|FC| >2, FDR < 0.005, see Materials and methods), red numbers indicate up-regulated genes, green numbers indicate down-regulated genes. (b) Venn diagram of total differentially expressed (DE) genes based on pairwise comparison against the "laboratory

conditions" reference, corresponding to the black numbers in panel A. Sections in the Venn diagram are indicated with Greek letters (α-η). (c) Enriched Gene Ontology sets based on Hyper-geometric distribution analysis (Bonferroni corrected $p < 0.05$ for: pH 3, 50 % CO_2 (145 genes, dark green top panel, corresponding to βγδ in panel b); the overlap between pH 3 and pH 3, 50 % CO_2 conditions (48 genes, light green middle panel; δ in panel b); low pH conditions (259 genes, yellow bottom panel, δεζ in panel b). See Supporting Information Appendix 4 for full tables. (d) Mean-normalized gene expression for genes with a positive (left) and negative (right) correlation with specific growth rate, based on Vos et al. 2016 for "laboratory conditions" (black dots, dashed line) and "industrial conditions" (black triangles, dotted line). Error bars represent standard deviation of the mean-normalized expression of the gene set. Bonferroni corrected p-values for the "laboratory conditions (pH 5, 0.04 % CO_2)" up: 1.46 E-89, down: 1.9 E-4. "industrial conditions" (pH 3, 50 % CO_2), up: 2.96 E-26, down: 9.8 E-16. DE, differentially expressed; FC, fold change; FDR, false-discovery rate.

The scale of transcriptional response to glucose limited retentostat cultivation at near-zero growth rates was similar for laboratory and industrial conditions, with 569 and 531 differentially expressed genes, respectively (Figure 3.5d). Notable differences between laboratory and industrial conditions included the regulation of PDR12, which encodes a plasma-membrane transporter in weak organic acid tolerance (Piper et al. 1998; Ullah et al. 2012), that responded in opposite directions under the two conditions, and the enrichment of genes encoding extracellular proteins and/or involved in cell wall processes among the genes whose expression was positively correlated with increasing growth rate under laboratory conditions but not industrial conditions (Supporting Information Appendix 5).

Discussion

This study was designed to quantify and dissect adverse physiological effects on *S. cerevisiae* of process conditions that are relevant for dicarboxylic acid production (low pH, high CO_2, and slow growth). Elevated CO_2 (50 %) did not, by itself, affect the biomass yield or viability of *S. cerevisiae* as compared to those under reference conditions (Table 3.1), and, accordingly, triggered only a weak transcriptional response (Figure 3.5). This result appears to contradict results from two independent previous studies on the same strain, performed at CO_2 levels of 50 % and 79 %, under fully respiratory conditions (Aguilera et al. 2005; Eigenstetter and Takors 2017; Richard et al. 2014). This apparent discrepancy may be related to the lower specific growth rates applied in the

present study (0.025 h^{-1} and below, while the cited earlier studies used 0.10 h^{-1}). Indeed, robustness of *S. cerevisiae* to various other stresses is inversely correlated with growth rate (Bisschops et al. 2017; Boender et al. 2011; Brauer et al. 2008; Lu et al. 2009). Additionally, in agreement with the present study, Eigenstetter and Takors observed a recovery from the CO_2 stress after five generations.

In contrast to the apparent insensitivity of slow-growing cultures to high CO_2, a low culture pH caused increased maintenance-energy requirements in glucose-limited cultures, both at high and at low CO_2 (Figure 3.2 and Figure 3.4). Moreover, both in glucose- and in ammonium-limited cultures, growth at low pH led to a reduced culture viability. A low extracellular pH results in a large proton gradient across the cell membrane and might increase proton influx via passive diffusion. To maintain intracellular pH homeostasis, *S. cerevisiae* can expel protons via the plasma-membrane ATPase Pma1 (Carmelo et al. 1996; Eraso and Gancedo 1987), a process that is an intrinsic part of maintenance energy metabolism (Figure 3.4). In glucose-limited chemostat cultures, no changes in the expression of genes encoding for proteins involved in proton homeostasis, including PMA1 and genes encoding subunits of the vacuolar V-ATPase, were observed. However, in glucose-limited retentostat cultures, PMA1 and PMA2 expression did show a positive correlation with specific growth rate (Figure 3.6a and 3.6b).

During ammonium-limited growth, additional mechanisms might explain the increase in nongrowth associated energy requirements (Figure 3.4). Futile cycling of ammonia and ammonium across the plasma membrane could require addition proton pumping via Pma1 (Cueto-Rojas et al. 2017; Liu et al. 2019) and might be aggravated at low pH. Additionally, presence of ethanol in the ammonium-limited cultures (up to 15 g/L) might stimulate proton leakage across the plasma membrane and thus trigger an increase in ATP-mediated proton export (Lindahl et al. 2017; Madeira et al. 2010). Together, the results of this study indicate that high death rates of slow-growing cultures at low pH cannot be directly attributed to energy-limited growth or increased maintenance energy-requirements.

Yeast transcriptional responses to near-zero growth rates in glucose-limited retentostat cultures were highly similar under laboratory and industrially

relevant conditions, indicating that the different death rates and maintenance-energy requirements under these conditions (Figure 3.1) did not trigger extensive transcriptional reprogramming. In chemostat cultures, pronounced transcriptional responses to low pH involved many genes involved in cell wall synthesis and stress. Proteins located outside the plasma membrane, including cell wall proteins, are directly exposed to the extracellular medium. As the isoelectric point (pI) of a protein determines its folding and functionality, activity of these proteins may be particularly sensitive to low extracellular pH (Schwartz et al. 2001). Failure to replace inactive extracellular proteins, either through accumulation of inactive protein or through a limited capacity for their replacement, may therefore be a key contributor to cell death, increased maintenance energy requirements or both at low pH.

While neither synergistic nor antagonistic physiological effects of low pH and high CO_2 were observed, transcriptional responses to the combination of these environmental conditions strongly differed from the transcriptional responses to either low pH or high CO_2 (Figure 3.5a). In particular, high CO_2 levels appeared to dampen the transcriptional response to low pH. Low pH stress triggers transcriptional regulation of genes under control of the cell wall integrity (CWI), high-osmolarity glycerol (HOG) and calcineurin signaling pathways (de Lucena et al. 2015) and cytosolic pH acts as a sensor for PKA-signaling (Dolz-Edo et al. 2019; Orij et al. 2012). Additionally, sensing of CO_2 is relayed through sphingolipid-mediated sensing, via the kinases Pkh1 and Pkh2, to the central nutrient sensor Sch9 (Pohlers et al. 2017). Extensive crosstalk between these signaling pathways enables cellular homeostasis (Chen and Thorner 2007; Deprez et al. 2018; Fuchs and Mylonakis 2009; Negishi and Ohya 2010; Rodríguez-Peña et al. 2010). Accordingly, genes under control of the transcription factors regulated by these signaling pathways (Skn7p, Rlm1p, Sko1p, Figure 3.6e, 3.6h, 3.6i, and 3.6j) were upregulated at pH 3, as were gene sets involved in cell wall synthesis (Lesage and Bussey 2006) and cell wall stress (Boorsma et al. 2004). However, these gene sets did not respond during growth at pH 3 at 50 % CO_2 (Figure 3.6f and 3.6g).

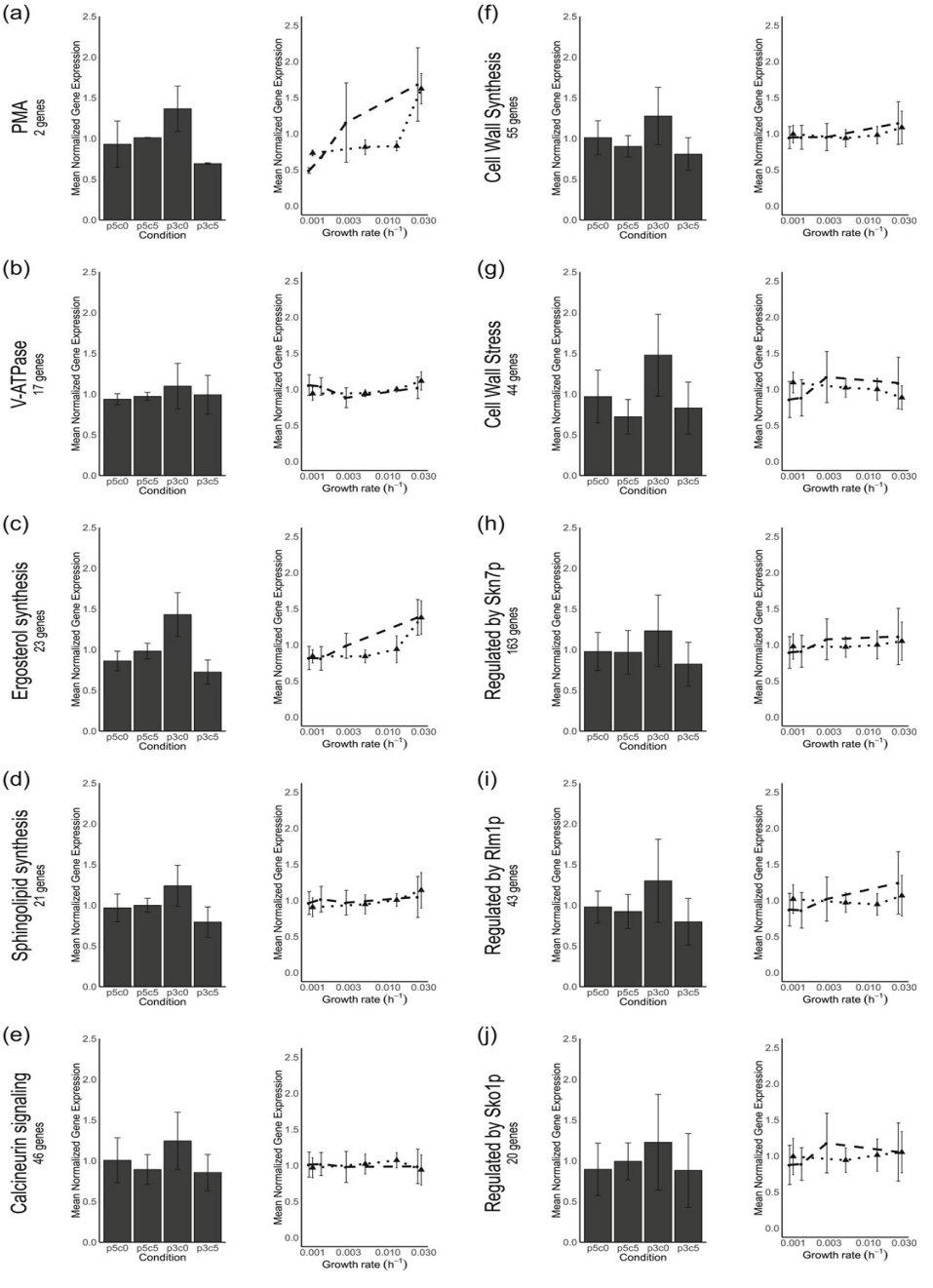

Figure 3.6 Transcriptional responses of gene sets related to proton homeostasis and diffusion (a,b,c,d), genes responsive to signaling pathways involved in low pH stress (e,h,i,j) and cell wall synthesis (f) from (Lesage and Bussey 2006) and cell wall stress (g) from (Boorsma et al. 2004). The number of genes in each gene set is indicated in the panels. Left figures indicate per gene

mean-normalized expression from chemostats. Right figures indicate the per gene mean-normalized expression versus growth rate for retentostat cultures under "laboratory" condition (black dots, dashed line) and "industrial" conditions (black triangles, dotted line). Mean-normalization was performed on the separate experiments and prohibits intercomparing the expression levels. Error bars in each plot indicate the standard deviation of the per gene mean-normalized expression of all genes in the subset.

While the present data do not enable elucidation of the precise nature of the cross-talks between pH and CO_2 signaling, in *S. cerevisiae*, two interactions between the abovementioned signaling pathways could provide further leads of investigation. First, CWI is sensed by the GPI-anchored nano-spring Wsc1 (Dupres et al. 2009), ultimately activating CWI and PKA pathways (Garcia et al. 2017). The kinases Pkh1 and Pkh2 that relay the CO_2 signal to Sch9 are also essential for Pkc1 activation of the CWI pathway (Inagaki et al. 1999; Levin 2005; Pohlers et al. 2017) and phosphorylate the kinases Ypk1 and Ypk2 that in turn phosphorylate the CWI MAP Kinase Mpk1/Stl2 (Roelants et al. 2002; Schmelzle et al. 2002). Second, at high extracellular CO_2 conditions bicarbonate accumulates intracellularly, improves buffering of the cytosol, and attenuates the cytosolic pH (Buck and Levin 2011; Eigenstetter and Takors 2017). Both the cytosolic pH and bicarbonate are direct signals for PKA signaling (Buck and Levin 2011; Dolz-Edo et al. 2019; Thomas 1976). Phosphoproteomic analysis of the proteins in the CWI, HOG, and PKA signaling pathways could prove an efficient strategy to elucidate the observed interplay of high CO_2 and low pH signaling (Mascaraque et al. 2013), which could be supported by analysis of the *in vivo* cytosolic pH at high CO_2 and low pH conditions by the pH-dependent GFP-derivative pHluorin (Orij et al. 2012).

The present study indicates that sensitivity to high CO_2 is unlikely to be a major concern for the development of robust yeast cell factories for production of dicarboxylic acids. Instead, minimizing maintenance-energy requirement and death rate at low pH was identified as a major objective for strain improvement. Even in the absence of product formation, low pH was shown to augment the trade-off, at low specific growth rates, between a reduced allocation of substrate to biomass formation and increased relative contribution of maintenance-energy requirements. The strongly increased m_s at low pH is clearly disadvantageous for industrial scale production of dicarboxylic acids and, moreover, is likely to be further enhanced in the presence of high product

concentrations. For example, high concentrations of organic acids have been shown to cause increased maintenance-energy requirements at low pH (Abbott et al. 2007; Abbott et al. 2008). From an economic perspective, the physiological impacts of low pH on *S. cerevisiae* constitute a trade-off between fermentation costs and costs for downstream processing. The complexity of the observed physiological and transcriptional responses indicates that improving robustness under industrial conditions is unlikely to be achieved by individual genetic modifications. Instead, exploration of yeast biodiversity (Palma et al. 2018), evolutionary engineering (Mans et al. 2018) and/or genome-shuffling approaches (Magocha et al. 2018; Steensels et al. 2018) may offer interesting possibilities.

Acknowledgements

This work was performed within the BE-Basic R&D Program (http://www.be-basic.org/), which was granted a FES subsidy from the Dutch Ministry of Economic Affairs, Agriculture and Innovation (EL&I). The authors would like to thank all project partners for stimulating discussions. Additionally the authors would like to thank Marcel van den Broek and Raúl Ortiz-Merino for stimulating discussions on the RNAseq analysis.

Supporting information

Additional supporting information can be found online in the Supporting Information section.

https://doi.org/10.1002/bit.27210

Appendix 1 Extended materials and methods

Appendix 2 Supplementary figures

Appendix 3 Input parameters MFA

Appendix 4 Transcriptome chemostats

Appendix 5 Transcriptome retentostats

Chapter 4 Uncoupling growth and succinic acid production in an industrial *Saccharomyces cerevisiae* strain

This chapter is under review in the journal Biotechnology and Bioengineering.

Abstract

This study explores the relation between biomass-specific succinic acid (SA) production rate and specific growth rate of an engineered industrial strain of *Saccharomyces cerevisiae*, with the aim to investigate the extent to which growth and product formation can be uncoupled. Ammonium-limited aerobic chemostat and retentostat cultures were grown at different specific growth rates under industrially relevant conditions, i.e., at a culture pH of 3 and with sparging of a 1:1 CO_2-air mixture. Biomass-specific SA production rates decreased asymptotically with decreasing growth rate. At near-zero growth rates, the engineered strain maintained a stable biomass-specific SA production rate for over 500 h, with a SA yield on glucose of 0.61 mol.mol^{-1}. These results demonstrate that uncoupling of growth and SA production could indeed be achieved. A linear relation between biomass-specific SA production rate and glucose consumption rate indicated a coupling of SA production rate and the flux through primary metabolism. The low culture pH resulted in an increased death rate, which was lowest at near-zero growth rates. Nevertheless, a significant amount of non-viable biomass accumulated in the retentostat cultures, thus underlining the importance of improving low-pH tolerance in further strain development for industrial SA production with *S. cerevisiae*.

Key words: *Saccharomyces cerevisiae,* succinic acid, near-zero growth, retentostat, high CO_2, low pH

Introduction

Succinic acid (SA), a C4 dicarboxylic acid and intermediate of the tricarboxylic acid (TCA) cycle (Tretter et al. 2016), is used as precursor for manufacturing a wide range of products in the pharmaceutical, agricultural, and food industries, including detergents, fungicides, herbicides, biodegradable polymers, flavors and food additives (Zeikus et al. 1999). Based on predicted environmental benefits, 2004 and 2010 reports of the U.S. Department of Energy (DOE) mentioned SA as one of the five most promising bio-based chemicals (Bozell and Petersen 2010; Werpy and Petersen 2004).The SA market size is expected to reach 710,000 tons by 2020, with a predicted turn-over of USD 1.1–1.3 billion in 2022 (Dessie et al. 2018; Luthfi et al. 2017). In order to supply this market, bio-based production of SA will become increasingly important as it can provide a sustainable alternative to petrochemical production (Pinazo et al. 2015).

In recent years, production of SA in industrial fermentation processes has been realized with naturally SA-producing microorganisms as well as with engineered strains (Beauprez et al. 2010; Chen and Nielsen 2013). BASF/Corbion-Purac achieved a yield of 0.75 mol of SA per mol of glucose from the natural producer *Basfia succiniproducens*, which was isolated from bovine rumen (Kuhnert et al. 2010). Myriant applied an engineered *E.coli* strain for large-scale SA production (Ahn et al. 2016). However, SA-producing bacteria may be affected by bacteriophage infection and generally require a neutral culture pH. The latter poses a requirement for alkali titration during fermentation and a subsequent acidification during downstream processing, resulting in massive waste production in the form of gypsum (Abbott et al. 2009). Fermentation at a low pH provides a way to reduce waste production and, thereby, improve process economics and sustainability.

Due to their low pH tolerance and insensitivity to phage infection, engineered yeasts have been intensively studied as microbial SA production platforms. For instance, Bioamber/Mitsui has replaced its SA producing *E.coli* strain with the yeast *Candida krusei* (Jansen and van Gulik 2014). Since 2012, DSM/Roquette has applied an engineered *S. cerevisiae* strain for industrial scale SA production (Jansen et al. 2013). To reach a high SA yield, the latter strain was genetically modified by overexpression of the reductive branch of the TCA cycle in the

cytosol, with further genetic modification focused on the glyoxylate cycle and SA export across the plasma membrane. Because SA production via the reductive part of the TCA cycle involves a net consumption of CO_2, increasing dissolved CO_2 concentrations should increase the driving force for SA biosynthesis via this pathway. It has indeed been reported that enrichment of the aeration gas with CO_2 significantly increased the rate of SA production in engineered strains of *S. cerevisiae* (Jamalzadeh 2013; Shah 2016; Zelle et al. 2010). Although the Gibbs free energy changing of the synthesis of SA from glucose is negative, the costs of active SA export (2 to 3 mol ATP per mol SA exported) (Taymaz-Nikerel et al. 2013) require a net input of ATP. Oxygen therefore needs to be supplied during yeast-based SA production to enable ATP production via respiration (Shah 2016).

In a study on product recycling across yeast membranes at high SA titers, which was based on a scaled-down industrial SA fed-batch fermentation process at low pH (Wahl et al. 2017), significant ^{13}C labeling of the TCA cycle intermediates fumarate, isocitrate and α-ketoglutarate was observed within 100 s after extracellular addition of ^{13}C labelled SA. This observation indicated that SA rapidly exchanges over the plasma membrane. In this scaled-down fed-batch process, SA production rates declined with decreasing specific growth rate. This observation was attributed to increased product degradation as well as to increased non-growth associated energy requirements at high SA titers, which left less substrate available for energy-dependent product formation.

From an industrial point of view, fermentative production of SA in the absence of cell growth would be ideal, as it would minimize formation of biomass as a byproduct and maximize the yield of product on substrate. Such an uncoupling of growth and product formation requires a producing strain which can maintain a high productivity at near-zero specific growth rates. Due to their dynamic nature, fed-batch cultures are not the best option to study relations between specific growth rate and strain performance (Hewitt and Nienow 2007). In contrast, chemostat cultivation allows studies on microbial physiology at a constant specific growth rate, under well-defined, stable process conditions. However, chemostat cultivation in laboratory bioreactors is impractical at specific growth rates below 0.025 h^{-1}, due to the long time periods needed to reach steady state. As an alternative to chemostat

cultivation, retentostat cultures have proven to be excellent tools to study growth of *S. cerevisiae* and other microorganisms at low to near-zero growth rates under various nutrient limitations (Boender et al. 2009; Ercan et al. 2015; Hakkaart et al. 2020; Liu et al. 2019; Vos et al. 2016).

The goal of the present study is to investigate whether uncoupling of growth and product formation can be accomplished in a heavily engineered, SA high-producing industrial *S. cerevisiae* strain. The strain was grown under industrially relevant conditions, i.e. at an elevated CO_2 level to increase the driving force towards SA biosynthesis via the reductive pathway and a culture pH of 3.0 to facilitate downstream processing (Hakkaart et al. 2020). Ammonium-limited cultures were used, in which glucose was present in excess, to avoid competition for glucose between growth and product formation. Ammonium-limited chemostat and retentostat cultures were used to the physiology of the industrial strain over a range of low to near-zero specific growth rates. This approach enabled a quantitative assessment of the degree to which biomass-specific production SA depends and specific growth rate are coupled and to identify goals for further strain engineering to improve uncoupling of growth and product formation in industrial SA production.

Materials and methods

Yeast strain and growth media

The engineered SA-overproducing industrial *S. cerevisiae* strain (SUC632) was kindly provided by Royal DSM B.V (Delft, the Netherlands). Properties and performance of this strain have been described previously (Jansen et al. 2013; Wahl et al. 2017). Working stocks were stored at -80 °C in 1 mL aliquots in YPD medium (10 g/L Bacto yeast extract, 20 g/L Bacto peptone, 20 g/L glucose) containing 30 % (v/v) glycerol. The pre-culture medium contained, per liter of demineralized water: 20 g galactose, 2.3 g urea, 3.0 g KH_2PO_4 , 0.5 g $MgSO_4.7H_2O$, 1 ml trace-element solution and 1 ml vitamin solution. Trace-element and vitamin solutions were prepared as described by (Verduyn et al. 1992). After filter sterilization (Millex® Syringe Filters, 0.22 µm, Merck Millipore, Massachusetts, USA), 1 ml of sterilized chalk solution (0.1 g/g $CaCO_3$) was added per 100 ml pre-culture medium. The medium for batch cultivation contained, per liter of demineralized water: 30 g galactose, 1.0 g $(NH_4)_2SO_4$, 5.3 g K_2SO_4,

3.0 g KH_2PO_4 , 0.5 g $MgSO_4.7H_2O$, 1 ml trace element solution, 1 ml vitamin solution, 1 ml of a solution containing 3 g/L $FeSO_4.7H_2O$ and 15 g/L EDTA, 1 ml of biotin solution (1 g/L), and 0.2 g Pluronic 6100 PE antifoaming agent (BASF, Ludwigshafen, Germany). The composition of the chemostat medium was the same as that of the batch cultivation medium, except for the carbon source, which was 30 g/L glucose instead of 30 g/L galactose. For retentostat cultivation concentrations of glucose and $(NH_4)_2SO_4$ were decreased to 18 g/L and 0.1 g/L, respectively.

Pre-cultures and aerobic bioreactor cultures

Pre-cultures were initiated by inoculating 500 mL Erlenmeyer flasks containing 200 mL of pre-culture medium with 2 mL of stock culture and incubated for 24 h in an orbital shaker at 30°C and at a rotation speed of 200 rpm (Sartorius BBI Systems, Melsungen, Germany).

Batch, chemostat and retentostat cultivations were carried out in 7 L bioreactors (Applikon, Delft, The Netherlands) equipped with a DCU3 control system and MFCS data acquisition and control software (Sartorius Stedim Biotech, Göttingen, Germany). The cultivation temperature was controlled at 30.0 ± 0.1°C by circulating water through the stainless-steel jacket surrounding the bottom part of the reactor vessel, using a cryothermostat (Lauda RE630, Lauda-Königshofen, Germany). For accurate measurement and control of the cultivation temperature, the water temperature of the cryothermostat was controlled by using the signal of a Pt 100 temperature sensor inside the reactor as input. The culture broth in the reactor was mixed with one 6-bladed Rushton turbine (diameter 85 mm) operated at a rotation speed of 500 rpm. Aerobic conditions were maintained by continuous gassing of the reactor, via a sparger located below the Rushton turbine. During batch cultivation, bioreactors were sparged with compressed air (0.04 % CO_2).The gas flow rate (0.5 vvm) was controlled using a mass flow controller (Brooks, 5850 TR, Hatfield, PA, USA). Before entering the reactor, the gas was sterilized by passing through a hydrophobic plate filter with a pore size of 0.2 μm (Millex, Millipore, Billerica, USA). During chemostat and retentostat cultivation, sparging of a 1:1 mixture of compressed air and pure CO_2 (> 99.7% purity, Linde Gas Benelux, Schiedam, The Netherlands) was controlled by two mass-flow controllers. The pH was

maintained at 3.00 ± 0.05 by automatic titration with 2 M KOH or 2 M H_2SO_4. The dissolved-oxygen concentration was measured using an autoclavable Clark DO sensor (Mettler-Toledo GmbH, Greinfensee, Switzerland) and remained above 30 % of air saturation. Exhaust gas from bioreactors was dried by first passing through a condenser at 4 °C and then through a Nafion dryer (Permapure, Toms River, USA). CO_2 and O_2 concentrations in the dried gas were measured with a combined paramagnetic/infrared NGA 2000 gas analyzer (Rosemount Analytical, Anaheim, USA).

Each chemostat culture was started as a batch culture. Bioreactors containing 4.6 L of batch medium were was inoculated with 400 mL of pre-culture. After approximately 24 h of batch cultivation, a sharp decrease of the CO_2 and increase of the O_2 concentrations in the off-gas and a corresponding increase of the dissolved oxygen concentration indicated that ammonium was depleted. At this point, cultures were switched to chemostat mode. During chemostat operation, the sterile feed medium was pumped into the reactor vessel at a constant flow rate using a peristaltic pump (Masterflex, Barrington, USA), such that the outflow rate of the culture broth corresponded to the desired dilution rate. The broth mass in the reactor was maintained at 5.00 ± 0.05 kg, by discontinuous removal of culture into a sterile effluent vessel, via a pneumatically operated valve in the bottom of the reactor and a peristaltic pump, which were operated by weight control (Liu et al. 2019). To this end, the complete reactor set-up was placed on a load cell (Mettler Toledo, Tiel, The Netherlands). The effluent vessel was placed on a separate load cell of which the signal was continuously logged for accurate determination of the dilution rate of the chemostat and, if required, to manually adjust the medium feed rate.

Independent duplicate chemostat cultures were carried out at dilution rates of 0.07, 0.058, 0.048, 0.035 and 0.025 h^{-1}. Steady state was assumed to be achieved when off-gas CO_2 and O_2 concentrations, biomass dry weight and cell counts changed by less than 3 % difference over 2 consecutive volume changes. After these criteria had been met, samples were withdrawn after 5, 6 and 7 subsequent volume changes for measurement of biomass dry weight, cell number, concentrations of residual substrates and (by)products and culture viability.

Retentostat cultures were started with a batch cultivation phase, followed by chemostat cultivation at a dilution rate of 0.025 h^{-1}. After reaching steady state, chemostat cultures were switched to retentostat mode by switching off the chemostat broth-removal system and activating cell-free culture removal through four filtration probes (Applikon, Delft, The Netherlands) mounted inside the reactor (Liu et al. 2019). The cell-free effluent was pumped in a sterile effluent vessel using a peristaltic pump (Masterflex, Barrington, USA) controlled by the vessel weight, such that the broth weight was kept at 5.00 ± 0.05 kg. During retentostat cultivation, dilution rate was maintained at 0.025 h^{-1} . A gradual transition from chemostat to retentostat medium was accomplished by using two feed pumps (Liu et al. 2019). Duplicate retentostats were carried out and samples were withdrawn every 48 h until cultures were terminated.

Determination of biomass dry weight, cell counts and culture viability

Biomass dry weight was quantified gravimetrically. Total cell counts were measured by a Z2 Coulter counter (50 µm aperture, Beckman, Fullerton, CA). Cell viability of culture samples was determined with a FungaLight™ Yeast CFDA, AM/Propidium Iodide Vitality Kit and flow cytometry. Detailed descriptions of the dry weight, cell counts and viability measurements were described previously (Liu et al. 2019).

Sampling for quantification of extracellular and intracellular metabolites

Cell-free effluent samples for quantification of extracellular metabolites were obtained from a sample port connected to the retentostat filter assembly. Broth samples for intracellular metabolite measurements were withdrawn by a rapid sampling device connected to the bioreactor as described previously (Liu et al. 2019).

Quantification of substrates, products and intracellular metabolites

Ammonium concentrations were analysed with a Gally Discrete Analyzer (ThermoFisher Scientific, Massachusetts, United States) with a detection limit of 0.02 mg $NH4^+$/L. Cconcentrations of glucose, succinic acid and by-products (malate, ethanol, glycerol, acetate and lactate) were quantified by HPLC, using a Bio-Rad HPX-87H 300 column (7.8 mm) as described previously (Liu et al. 2019). Intracellular metabolite concentrations were quantified by isotope

dilution mass spectrometry (LC-IDMS/MS and GC-IDMS) using U-^{13}C-labeled yeast cell extract as internal standard (Wu et al. 2005). Detailed descriptions of the mass spectrometry based quantification protocols were published previously (Cipollina et al. 2009; Seifar et al. 2009; van Dam et al. 2002). The adenylate energy charge (AEC) was calculated as described (Liu et al. 2019).

Biomass-specific rate calculations

Calculation of specific growth rates (μ, h^{-1}) and specific death rates (k_d, h^{-1}) were performed as described previously (Liu et al. 2019). Biomass-specific glucose and ammonium consumption rates and biomass-specific production rates of succinic acid, malate, ethanol, glycerol, acetate and lactate were calculated from the primary measurements of substrate and product concentrations and flow rates in gas and liquid phases using the corresponding material balances. Data reconciliation was performed as described by (Verheijen 2000).

Results

Growth and viability of S. cerevisiae SUC632 in ammonium-limited chemostat and retentostat cultures at low pH and high CO_2 levels

To investigate whether the specific SA production rate of the engineered *S. cerevisiae* strain SUC632 was related to its specific growth rate, the strain was cultivated under industrially relevant conditions (50 % CO_2, pH 3.0) in ammonium-limited cultures. Specific growth rates between 0.034 and 0.085 h^{-1} were studied in chemostat cultures, while retentostat cultures were applied to obtained quantitative data on strain performance at specific growth rates from 0.034 h^{-1} to near zero. All these continuous cultures were grown under ammonium limitation. In all retentostat and steady state chemostat cultures, concentrations of residual ammonium were below the detection limit, and residual glucose concentrations were higher than the saturation constant of high-affinity glucose transporters in *S. cerevisiae* (k_m, ca. 1 mM) (Boles and Hollenberg 1997; Reifenberger et al. 1997), indicating that ammonium was indeed the growth limiting nutrient (Supporting Information Table S4.1).

In all chemostat cultures, viability was between 80 and 90 % (Figure 4.1A). As only the viable cell fraction contributes to substrate consumption, growth and (by)product formation, specific conversion rates were expressed per g of viable

cells. The steady-state total and viable biomass concentrations slightly increased with decreasing specific growth rate to become stable below a specific growth rate of 0.042 h^{-1} (Figure 4.1C). A similar profile was observed for total cell counts, while the average dry mass per cell decreased with decreasing specific growth rate (Figure 4.1E).

As, during retentostat cultivation, the specific growth rate progressively decreased from 0.025 h^{-1} to near zero, culture viability declined from 80 % to a stable value of around 25 % between 300 and 450 h of cultivation, with a slight further decrease thereafter (Figure 4.1B). Total biomass dry weight and cell counts increased during retentostat cultivation according to similar patterns (Figure 4.1D, F). The viable biomass concentration levelled off at 2 g/L after 300 h (Figure 4.1D). The dry mass per cell was stable during retentostat cultivation (Figure 4.1F) and identical to the value observed in chemostat cultures grown at 0.034 h^{-1}.

The highest specific death rate (k_d = 0.015 h^{-1}) was observed at the highest specific growth rate of 0.085 h^{-1} applied during chemostat cultivation. In the other, slower growing chemostat cultures, k_d was approximately 0.01 h^{-1} (Figure 4.1G). From the start of the retentostat cultivations, k_d decreased from 0.01 h^{-1} to approximately 0.005 h^{-1}, meanwhile the corresponding specific growth rates (μ) also rapidly dropped and approximately stabilized at values below 0.005 h^{-1} (Figure 4.1H).

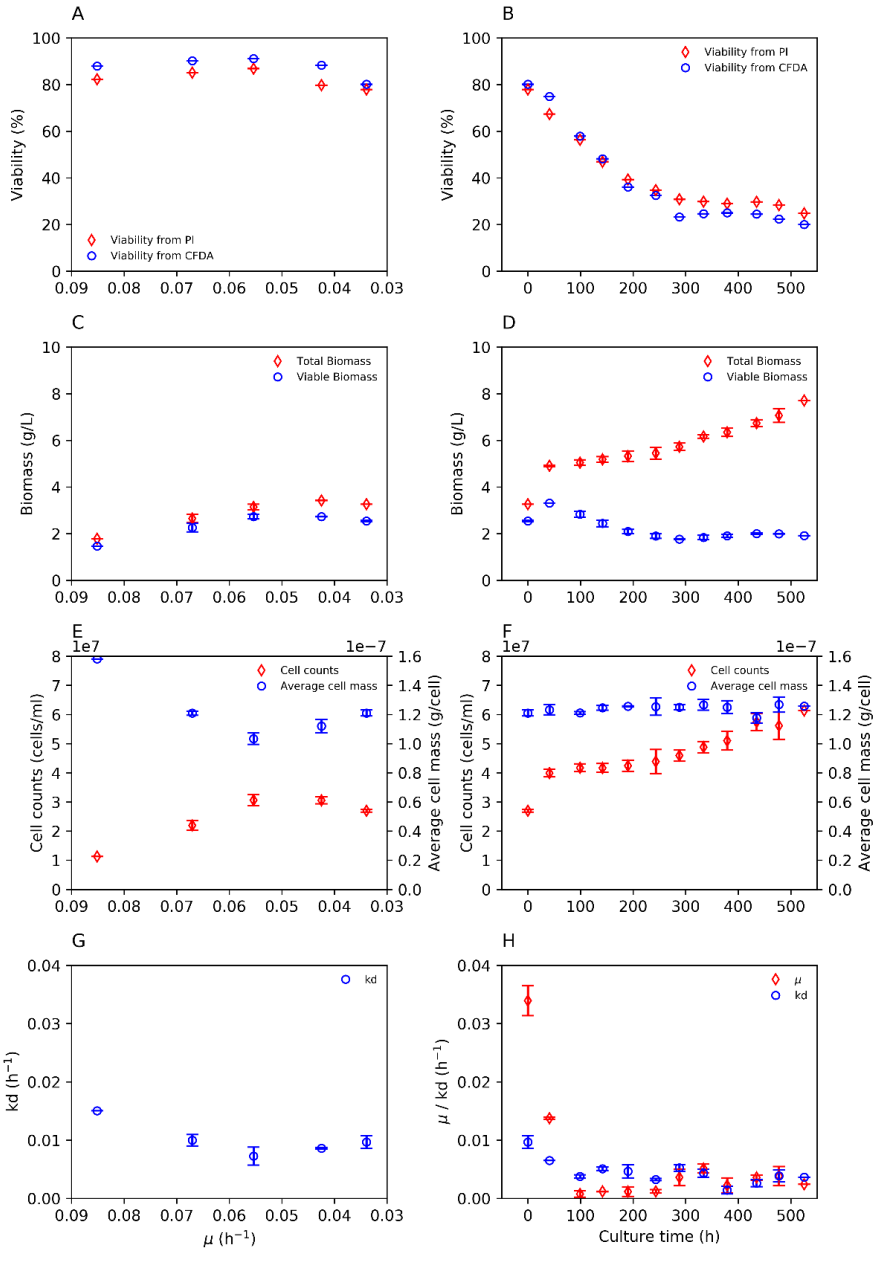
A
Viability (%)
Viability from PI
Viability from CFDA
B
Viability (%)
Viability from PI
Viability from CFDA
C
Biomass (g/L)
Total Biomass
Viable Biomass
D
Biomass (g/L)
Total Biomass
Viable Biomass
E
1e7
1e−7
Cell counts (cells/ml)
Average cell mass (g/cell)
Cell counts
Average cell mass
F
1e7
1e−7
Cell counts (cells/ml)
Average cell mass (g/cell)
Cell counts
Average cell mass
G
kd (h^{-1})
kd
μ (h^{-1})
H
μ / kd (h^{-1})
μ
kd
Culture time (h)

Figure 4.1 Culture viability (A,B), total and viable biomass concentrations (C,D), total cell counts and average cell mass (E, F), and specific growth and death rates (G,H) in aerobic, ammonium-limited chemostat and retentostat cultures of *S. cerevisiae* SUC632. Cultures were grown on glucose, at pH 3 and were sparged with a 1:1 mixture of air and CO_2. Left and right panels represent data from steady-state chemostat cultures at different specific growth rates and from retentostat cultures, respectively. In the retentostat cultures, specific growth rates decreased over time (panel H). All data represent averages ± standard errors of data from independent duplicate cultures.

Uncoupling of growth and succinic acid production

In nitrogen-limited retentostat cultures, the biomass-specific SA production rate decreased asymptotically with decreasing specific growth rate and stabilized at a value of 0.75 mmol/(g viable biomass)/h for specific growth rates between 0.008 and 0.014 h^{-1} (Figure 4.2). This result showed that the engineered strain was still capable of producing SA at near-zero specific growth rates. Apart from SA, malate, ethanol, glycerol and small amounts of acetate and lactate were formed as byproducts. The biomass-specific production rates of these by-products were combined in a "q_{byp}" term and expressed as mCmol per gram of viable biomass per h. The specific rate of byproduct formation decreased asymptotically with decreasing specific growth rate to relatively low values (1.2 mCmol/(g viable biomass)/h, Figure 4.2C). Individual production rates for each by-product are provided in Supporting Information Table S4.2.

The fraction of consumed glucose distributed to biomass, SA and byproducts formation were compared between those different specific growth rates cultures (Figure 4.3). Specifically, the fraction of the consumed glucose converted to SA was highest in the condition that growth was virtually absent (Figure 4.3). Besides, during retentostat cultivation, the yield of SA on glucose progressively decreased from almost 0.9 mol/mol (0.6 Cmol/Cmol) until, after 400 h, it reached a stable value of approximately 0.6 mol/mol (0.4 Cmol/Cmol) (Figure 4.4).

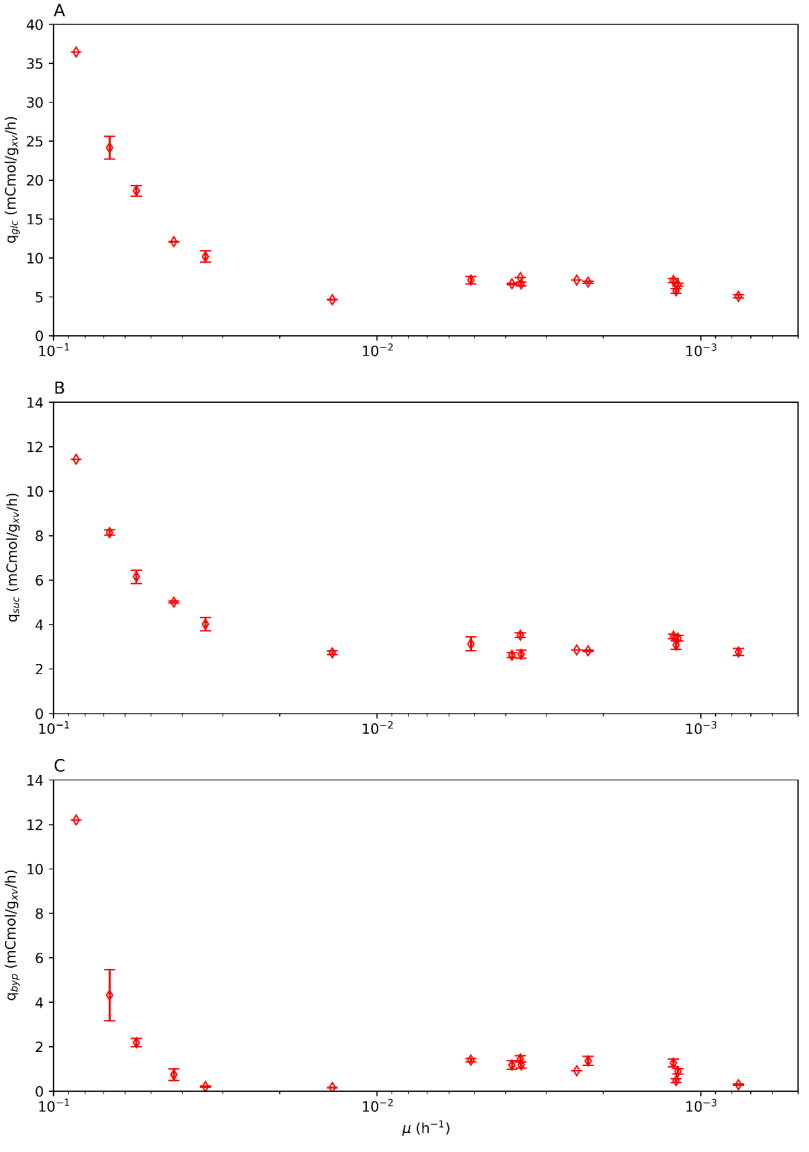

Figure 4.2 Biomass specific consumption rates of glucose (A) and production rates of succinic acid (B) and by-products (C) as a function of the specific growth rate (μ) in aerobic, ammonium-limited chemostat and retentostat cultures of *S. cerevisiae* SUC632. Cultures were grown on glucose, at pH 3 and were sparged with a 1:1 mixture of air and CO_2. q_{byp} represents the sum of the specific production rates of malate, ethanol, glycerol and acetate. All data represent averages of results from duplicate chemostat and retentostat cultures with their standard errors.

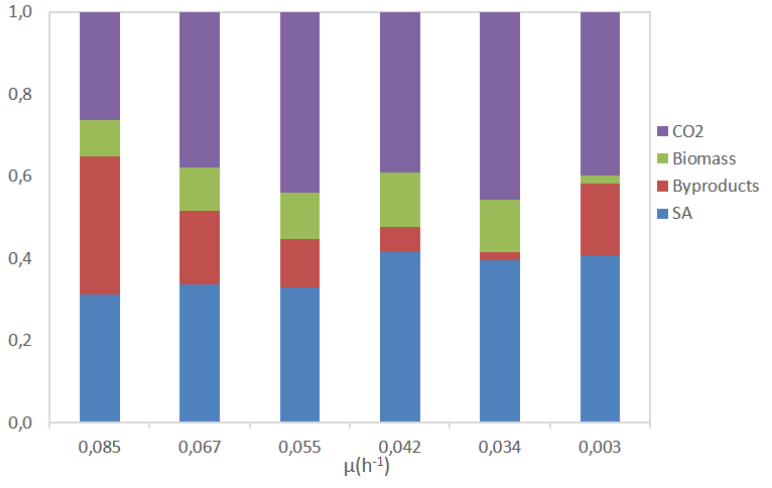

Figure 4.3 Growth rate dependent division of consumed substrate between growth, succinic acid and byproducts formation in aerobic, ammonium-limited chemostat and retentostat cultures of *S. cerevisiae* SUC632, at different specific growth rates. Cultures were grown on glucose, at pH 3 and were sparged with a 1:1 mixture of air and CO_2. The division of substrate was calculated on Cmol basis.

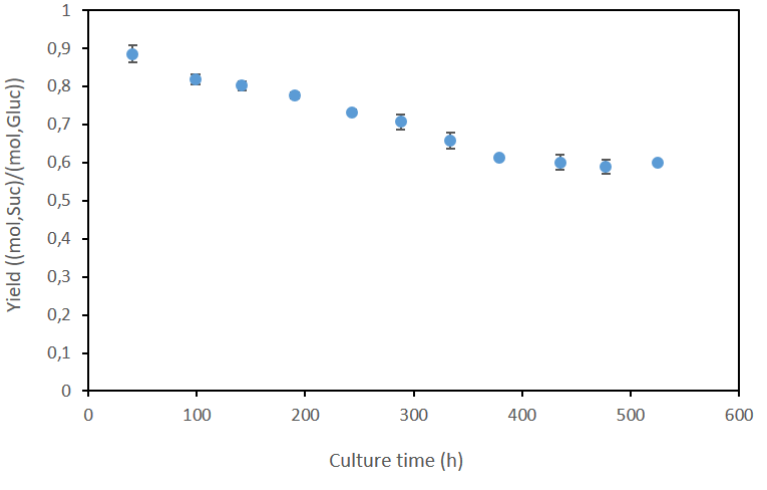

Figure 4.4 Succinic acid yield on glucose during ammonium-limited aerobic retentostat cultivation. Retentostat cultures were grown on glucose, at pH 3 and were sparged with a 1:1 mixture of air and CO_2. Specific growth rates at the time points indicated are shown in Figure 4.1H. All data represent averages with standard errors obtained from duplicate retentostat cultures.

Cellular energy status during near-zero growth cultivation

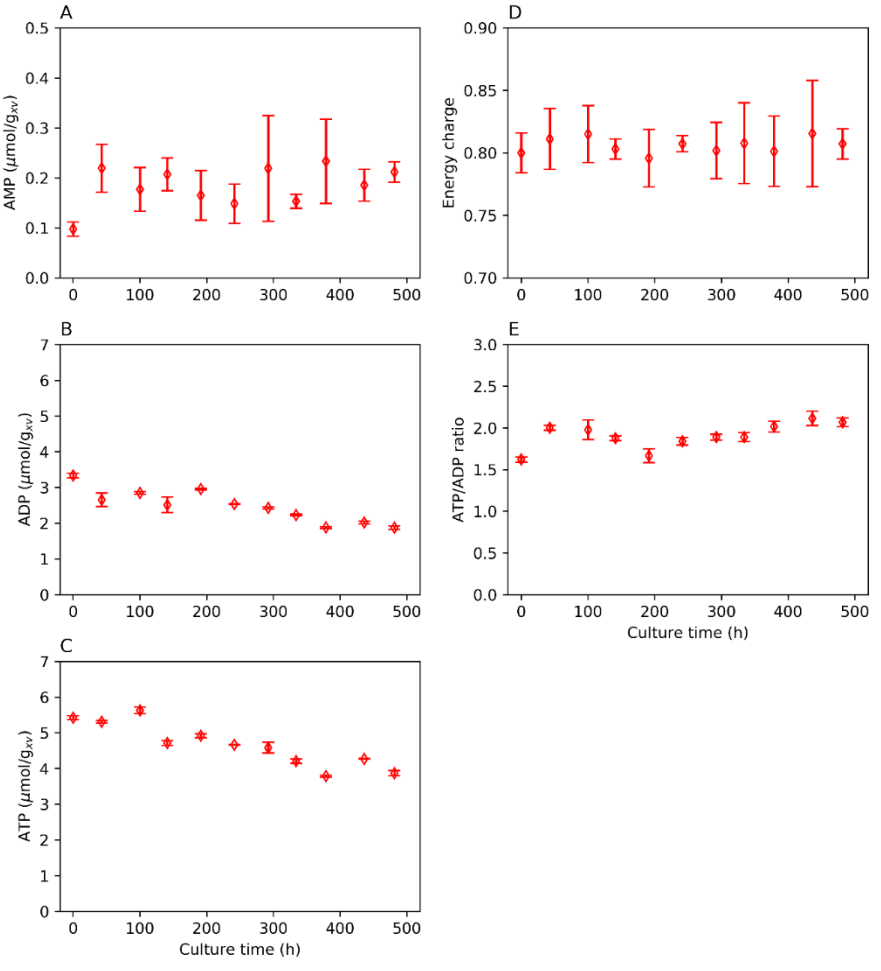

Figure 4.5 Intracellular adenosine phosphate level (A,B,C), adenylate energy charge (D) and ATP/ADP ratio (E) during aerobic, ammonium limited retentostat cultivation of *S. cerevisiae* SUC632. Retentostat cultures were grown on glucose, at pH 3 and were sparged with a 1:1 mixture of air and CO_2. Specific growth rates at the time points indicated are shown in Figure 4.1H. The data at time point t = 0 also represent the results in the preceding steady-state chemostat cultures at μ = 0.034 h^{-1}. Data represent the averages and standard errors of measurements from duplicate cultures.

To investigate the energy status of the SA-producing strain at near-zero growth rates, under the severe nitrogen limitation in low-pH retentostat cultures, intracellular levels of adenine nucleotides (ATP, ADP and AMP), as well as the

corresponding adenylate energy charge and ATP/ADP ratios were analysed (Figure 4.5). During retentostat cultivation, intracellular levels of ATP and ADP slowly decreased (Figure 4.5B and C) and stabilized after about 350 h. Retentostat cultures showed a stable intracellular AMP level that approximately two-fold higher than observed in the preceding chemostat culture (Figure 4.5A). Despite these differences in the concentrations of individual adenine nucleotides, the energy charge did not change upon the switch from chemostat to retentostat cultivation and remained at a stable value of approximately 0.8 throughout the retentostat experiments (Figure 4.5D). The ATP/ADP ratio slowly increased from a value of 1.5 to 2.0 at the end of the retentostat cultivation (Figure 4.5E).

Levels of the TCA cycle metabolites during retentostat cultivation

The target product in this study, succinic acid, as well as the most important by-product, malate, are both intermediates of the TCA cycle. To assess how SA production correlated with intracellular levels of other TCA-cycle intermediates, intracellular metabolite analyses were performed on the retentostat cultures (Figure 4.6A-F). Levels of all quantified TCA-cycle intermediates increased during retentostat cultivation of the engineered strain, but followed distinct dynamic patterns. Intracellular levels of citrate, isocitrate and succinate increased linearly with time during retentostat cultivation, levels of α-ketoglutarate and fumarate decreased until 150 h and increased thereafter, while the malate level increased until 300 h and then decreased. Intracellular levels of citrate, succinate and malate were two orders of magnitude higher than those of other TCA-cycle intermediates. When compared to a wild-type strain grown at similar glucose consumption rates in aerobic, glucose-limited chemostat cultures (Canelas et al. 2011) levels of citrate, succinate and malate were 5, 90 and 25 fold higher, respectively, towards the end of the nitrogen-limited retentostat cultures. Remarkably, the mass action ratio of the fumarase reaction (Figure 4.6G) was far above the apparent *in vivo* equilibrium constant of 5.2 (Canelas et al. 2011). This observation suggests that the overall flux was from malate to fumarate, with a low fumarate level resulting from the action of the heterologous, cytosolically expressed NADH-dependent fumarate reductase (FRDg) from *Trypanosoma brucei* (Jansen et al. 2013). Succinate formation via this reaction is highly

exergonic, thus providing a plausible explanation for the high intracellular succinate and low fumarate levels. The expression of isocitrate lyase (KIICL1) from *Kluyveromyces lactis* (Jansen et al. 2013) may be responsible for the high intracellular citrate levels as this enzyme, together with aconitase, allows for conversion of succinate via isocitrate to citrate and vice versa. The observation that the mass action ratio for the aconitase reaction was well below the estimated *in vivo* K_{eq}, (Figure 4.6H), indicate that net flux through this enzyme was in the direction of isocitrate.

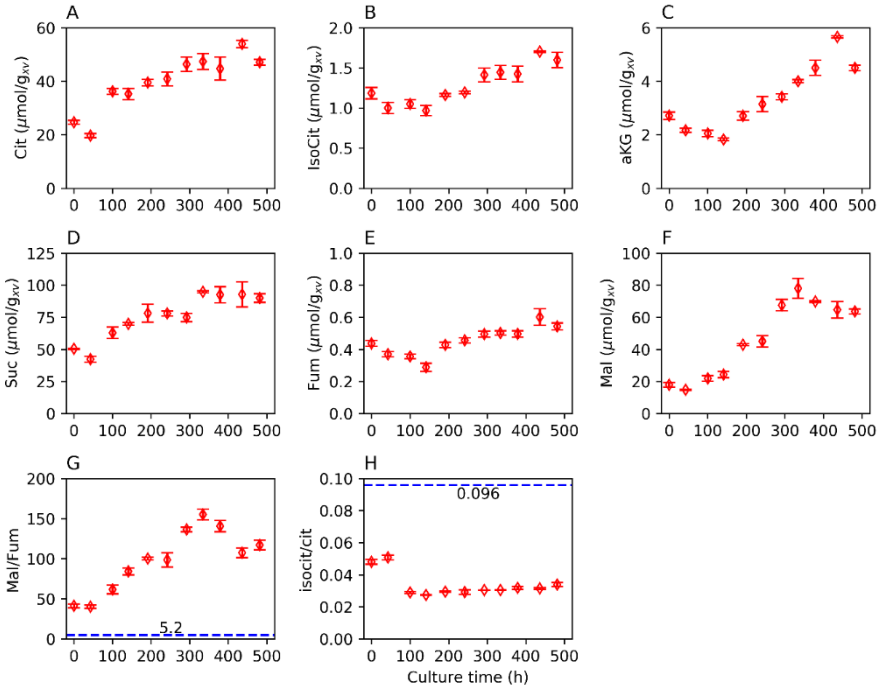

Figure 4.6 Intracellular levels of the TCA cycle metabolites (A-F) and mass action ratio's of fumarase and aconitase (G-H) during aerobic, ammonium limited retentostat cultivation of SUC632. Retentostat cultures were grown on glucose, at pH 3 and were sparged with a 1:1 mixture of air and CO_2. Specific growth rates at the time points indicated are shown in Figure 4.1H. The data at time point t = 0 also represent the results in the preceding steady-state chemostat cultures at $\mu = 0.034\ h^{-1}$. Dashed blue lines in figures G and H represent the apparent *in vivo* equilibrium constants determined for *S. cerevisiae* (Canelas et,al, 2011). Data represent the averages and standard errors of measurements from duplicate cultures.

Discussion

In this study, we explored the feasibility of applying cultivation at near-zero growth rate for high-yield production of chemicals from renewable feedstocks. As a model system we used an engineered industrial strain of *S. cerevisiae*, capable of producing succinic acid from glucose. To simulate industrial process conditions, growth studies were performed at low pH and at an elevated CO_2 concentration.

Fermentation processes at near-zero growth rate theoretically allow for highly efficient conversion of substrate to product, as no carbon- and energy source is required for biomass formation. However, long-term cultivation of *S. cerevisiae* at near-zero growth rate in retentostat cultures has been reported to result in accumulation of non-viable, non-producing cells (Boender et al. 2009; Vos et al. 2016). A previous study with the non-producing laboratory reference strain CEN.PK113-7D (Hakkaart et al. 2020) showed that, at pH 3, the specific death rates (k_d) in glucose- and ammonium-limited retentostat cultures (respectively 0.0039 ± 0.0005 and 0.0030 ± 0.0004 h^{-1}) were approximately eight-fold higher than in corresponding cultures grown at pH 5. However, cultivation of the reference strain at near-zero growth rate as such did not cause an increased k_d, since the death rates in glucose- and ammonium-limited retentostat cultures performed at pH 3 were two-fold and tenfold lower, respectively, than in corresponding chemostat cultures grown at a specific growth rate of 0.025 h^{-1} (Hakkaart et al. 2020).

In the present study, ammonium-limited steady-state chemostat cultivation at a dilution rate of 0.025 h^{-1}, under industrially relevant conditions (pH 3 and 50 % CO_2), indicated that the industrial SA-producing strain *S. cerevisiae* SUC632 was more robust than the congenic laboratory strain CEN.PK113-7D, as the k_d of the industrial strain was about 3-fold lower than that of the laboratory strain (Hakkaart et al. 2020). At near-zero growth rates in low-pH retentostat cultures, k_d values of the two strains were not significantly different (0.0030 ± 0.0004 and 0.0030 ± 0.0006 h^{-1}, respectively) (Hakkaart et al. 2020).

In the ammonium-limited chemostat and retentostat cultures, biomass-specific rates of SA production decreased asymptotically with decreasing growth rate to an essentially constant value of 3 ± 0.1 mCmol/(g viable biomass)/h at specific

growth rates below 0.02 h^{-1} (Figure 4.2B). This productivity was maintained until, after 525 h (3 weeks) the retentostat cultures were terminated. These results demonstrated that cell retention in ammonium-limited cultures can result in sustained, stable SA production in the virtual absence of growth. The combined chemostat and retentostat data showed that biomass-specific SA production rates increased linearly with glucose consumption rate (Figure 4.7). This observation strongly suggests that a coupling between the SA production rate and the flux through primary metabolism, possibly as a consequence of altered intracellular metabolite concentrations or altered expression of key enzymes. Further research is required to elucidate the underlying mechanisms and identify metabolic engineering targets for boosting SA production rates in the absence of growth.

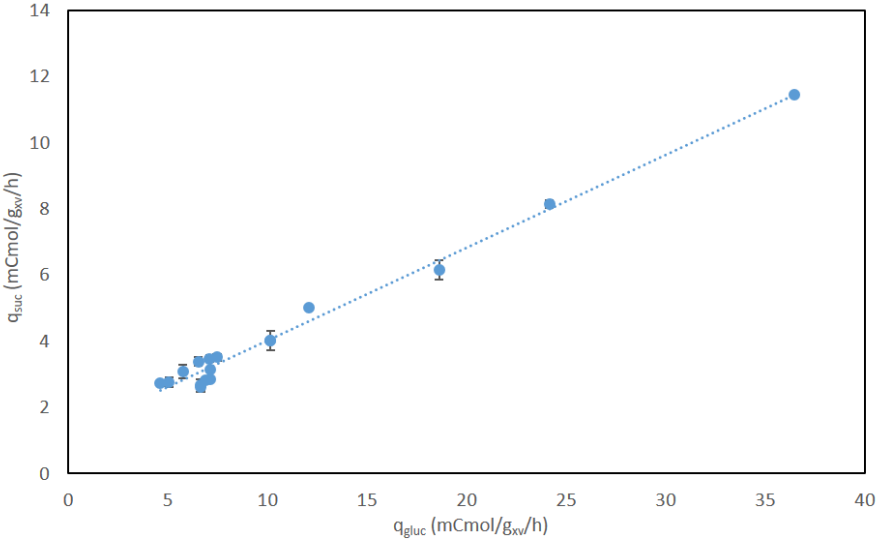

Figure 4.7 Specific succinic acid production rate plotted as a function of specific glucose consumption rate in aerobic, ammonium-limited chemostat and retentostat cultures of *S. cerevisiae* SUC632. Cultures were grown on glucose, at pH 3 and were sparged with a 1:1 mixture of air and CO_2. All data represent averages with standard errors obtained from duplicate chemostat and retentostat cultivations.

Use of membrane filters to achieve cell retention might be less feasible on an industrial scale as blocking of effluent filters could prevent long-time operation. Alternative means of cell retention could involve use of fast-sedimenting yeast mutants (Oud et al. 2013) or immobilization (Gulli et al. 2019; Nagarajan et al.

2014) might be explored. Near zero growth conditions can also be achieved by controlling the feed of a limiting nutrient in fed-batch processes. Due to the absence of a liquid outflow, fed-batch cultivation results in high final product titers, which are beneficial for the downstream processing. Wahl and coauthors (Wahl et al. 2017) studied growth of the same SA-producing *S. cerevisiae* strain in fed-batch cultures which, during the final phase of cultivation, were starved for ammonium. In contrast to our observation on nitrogen-limited retentostat cultures, the specific SA production rate observed after ammonium depletion was not stable but declined to a very low value within 90 h. As the authors expressed specific SA productivity per total amount of biomass and did not measure culture viability, this result may have reflected a loss of culture viability cause by the low cultivation pH (Hakkaart et al. 2020), complete nitrogen starvation and/or high SA concentrations. The SA yield on glucose in the N-starved fed-batch cultures declined from 0.64 ± 0.01 to 0.53 ± 0.01 mol SA per mol glucose during the final phase of fermentation (Wahl et al. 2017). In contrast, our ammonium-limited retentostat cultures the SA yield on glucose stabilized to a value of 0.60 mol SA per mol glucose, which was maintained until the end of the three-week retentostat runs (Figure 4.4). The lower SA yield in the fed-batch cultures may be related to the much higher SA concentrations (up to 0.6 mol/L, as compared to 63 ± 3 mmol/L in the retentostat cultures). A high SA titer at a low cultivation pH will result in entry of undissociated SA across the plasma membrane by passive diffusion, followed by active export by the DCT02 transporter. Experiments with ^{13}C-SA demonstrated the relevance of such a futile cycle, which necessitates an increased rate of glucose dissimilation to CO_2 and water and, consequently, causes a lower SA yield on glucose (Wahl et al. 2017).

Measurements of intracellular succinate and other TCA-cycle intermediates in N-limited retentostat cultures showed levels consistent with the genetic makeup of the industrial strain, whose metabolism has been rewired towards reductive conversion of oxaloacetate to succinate in the yeast cytosol by high-level expression of native and heterologous enzymes (Jansen et al. 2013). Similar intracellular metabolite levels were reported for ammonium-starved fed-batch cultures of the same strain (Wahl et al. 2017). The very high mass action rations of the fumarase reaction that were observed in both studies

indicate a strong driving force in the direction of fumarate synthesis and thus SA production. However, ^{13}C flux analysis in the fed-batch cultures showed that the oxidative TCA cycle flux was significantly higher than the reductive flux towards succinate. The net fumarase flux was therefore in the direction of malate, which would require a *in vivo* mass action ratio below K_{eq}. Wahl et al. explained the high value of the mass action ratio from subcellular compartmentation of malate (Wahl et al. 2017). The high malate to fumarate ratio then suggests a possible limitation of cytosolic fumarase for use of the reductive pathway towards SA, which could potentially be relieved by modifying *in vivo* kinetic and/or regulatory characteristics of this key enzyme .

With this work we have shown that long-term extreme limitation by a nutrient other than the carbon- and energy source enable stable conversion of substrate into product in the virtual absence of growth. Although we have used retentostat systems in this research, a similar concept could be applied in repeated fed-batch cultivations, in which the producing strain is used as a biocatalyst for prolonged periods of time and conversion of substrate into biomass is minimized. Further strain optimization should focus on improving glucose conversion rates at near-zero growth rates and, in particular, on increasing cell viability during prolonged cultivation at low pH.

Acknowledgement

This research was financed by the Netherlands BE-Basic research program (BE-Basic project: FS10-04 Uncoupling of microbial growth and product formation). We thank Dr. Alrik Los and Dr. Mickel Jansen at DSM for making the industrial strain available for this study. We thank Cor Ras and Patricia van Dam for analytical support.

Supporting information

Table S4.1 Residual $NH4^+$ and glucose conc. in the effluent of aerobic, ammonium-limited chemostat and retentostat cultures of *S. cerevisiae* SUC632. Cultures were grown on glucose, at pH 3 and were sparged with a 1:1 mixture of air and CO_2. All the Data represent the averages and standard errors of calculations on duplicate chemostat/retentostat cultures. "BDL" represents below the detection limit.

Chemostats		
μ	$NH4^+$	glucose
h^{-1}	g/L	g/L
0.085	BDL	7.35 ± 0.00
0.067	BDL	1.24 ± 0.12
0.055	BDL	0.72 ± 0.05
0.042	0.00033 ± 0.00022	0.81 ± 0.07
0.034	0.00081 ± 0.00012	0.46 ± 0.00
Retentostats		
Culture time	$NH4^+$	glucose
h	g/L	g/L
0	0.00081 ± 0.00012	0.46 ± 0.00
41	0.00072 ± 0.00001	0.44 ± 0.02
99	0.00045 ± 0.00001	0.71 ± 0.08
142	0.00024 ± 0.00009	1.07 ± 0.16
190	0.00010 ± 0.00003	1.42 ± 0.30
243	0.00011 ± 0.00008	1.69 ± 0.30
288	0.000014 ± 0.000010	1.99 ± 0.27
334	0.000014 ± 0.000010	2.13 ± 0.31
379	0.000014 ± 0.000010	2.08 ± 0.34
435	0.000012 ± 0.000008	1.87 ± 0.34
477	0.000036 ± 0.000020	1.84 ± 0.37
525	BDL	1.35 ± 0.00

Table S4.2 The specific production rates of ethanol, glycerol, lactate, acetate, malate based on per gram of viable biomass in aerobic, ammonium-limited chemostat and retentostat cultures of *S. cerevisiae* SUC632. Cultures were grown on glucose, at pH 3 and were sparged with a 1:1 mixture of air and CO_2. All the Data represent the averages and standard errors of calculations on duplicate chemostat/retentostat cultures. Lactate in retentostat samples were far below the limit of quantification method, so the corresponding q rates are not applicable (NA).

Chemostats					
μ	$q_{ethanol}$	$q_{glycerol}$	$q_{lactate}$	$q_{acetate}$	q_{malate}
h^{-1}	mCmol/g_{xv}/h	mCmol/g_{xv}/h	mCmol/g_{xv}/h	mCmol/g_{xv}/h	mCmol/g_{xv}/h
0.085	6.21 ± 0.00	1.37 ± 0.00	0.015 ± 0.000	0.048 ± 0.00	4.56 ± 0.00
0.067	2.95 ± 0.82	0.54 ± 0.13	0.033 ± 0.020	0.015 ± 0.008	0.79 ± 0.17
0.055	1.24 ± 0.05	0.62 ± 0.17	0.012 ± 0.004	0.014 ± 0.003	0.30 ± 0.02
0.042	0.27 ± 0.19	0.24 ± 0.05	0.001 ± 0.000	0.004 ± 0.001	0.23 ± 0.01
0.034	0.000 ± 0.000	0.084 ± 0.025	0.000 ± 0.000	0.003 ± 0.000	0.12 ± 0.00
Retentostats					
Culture time	$q_{ethanol}$	$q_{glycerol}$	$q_{lactate}$	$q_{acetate}$	q_{malate}
h	mCmol/g_{xv}/h	mCmol/g_{xv}/h	mCmol/g_{xv}/h	mCmol/g_{xv}/h	mCmol/g_{xv}/h
0	0.000 ± 0.000	0.084 ± 0.025	NA	0.003 ± 0.000	0.12 ± 0.00
41	0.000 ± 0.000	0.045 ± 0.014	NA	0.002 ± 0.000	0.11 ± 0.02
99	0.000 ± 0.000	0.12 ± 0.01	NA	0.004 ± 0.001	0.17 ± 0.04
142	0.008 ± 0.006	0.13 ± 0.01	NA	0.027 ± 0.003	0.30 ± 0.09
190	0.16 ± 0.05	0.20 ± 0.01	NA	0.038 ± 0.017	0.48 ± 0.15
243	0.34 ± 0.02	0.28 ± 0.01	NA	0.009 ± 0.001	0.63 ± 0.19
288	0.38 ± 0.03	0.30 ± 0.01	NA	0.009 ± 0.000	0.76 ± 0.17
334	0.35 ± 0.04	0.28 ± 0.02	NA	0.010 ± 0.001	0.76 ± 0.13
379	0.35 ± 0.00	0.26 ± 0.00	NA	0.008 ± 0.001	0.75 ± 0.20
435	0.30 ± 0.01	0.24 ± 0.02	NA	0.008 ± 0.000	0.63 ± 0.16
477	0.30 ± 0.02	0.24 ± 0.01	NA	0.008 ± 0.001	0.63 ± 0.19
525	0.28 ± 0.00	0.26 ± 0.00	NA	0.006 ± 0.000	0.38 ± 0.00

Chapter 5 Outlook

With this work it was demonstrated that near-zero growth can be successfully achieved through limited supply of a nutrient other than the carbon and energy source. This was shown by applying retentostat regimes, both to a non-producing yeast strain (CENPK113-7D) and an engineered succinic acid (SA) producing yeast strain (SUC632), whereby the growth was limited by either the nitrogen or the phosphorus source and the carbon source glucose was present in excess. Uncoupling of yeast growth and SA production was achieved in the producing strain under industrially relevant conditions (low pH and high CO_2) with a considerable SA yield on glucose. Main challenges were the increased death rate of both strains at low cultivation pH and the decreased SA productivity at low to near-zero growth rates. In this chapter, we pinpoint a few scientific questions that remain undiscussed or unsolved in this thesis, as well as some suggestions for potential follow-up research on near-zero growth conditions with large scale industrial applications in mind.

Technical limitations of retentostat cultivation

A retentostat is in fact a modified chemostat, wherein an internal or external filtration unit is installed to retain the cells in the bioreactor. Over the years, retentostat cultivation has been applied as a useful tool to study microbial physiology at extremely low to near-zero growth rates. For the research described in this thesis, we applied a commercial filtration probe assembly fitted with tubular 0.22 µm pore size polypropylene membranes. This experimental setup worked well without clogging for carbon-limited anaerobic and aerobic cultures during cultivation periods of about three weeks, whereby biomass concentrations of more than 20 g/L were reached. However, using the same experimental setup, nitrogen-limited cultures could only be operated for a period of approximately 9 days, reaching a biomass concentration of ca. 14 g/L, after which fouling caused the filters to clog. Membrane fouling was not observed in the phosphorus-limited retentostats, which could be operated without clogging for about 16 days (Chapter 2). Fortunately, the biomass concentrations of the N- and P-limited cultivations both reached stable values in spite of the different cultivation times, which still enabled the physiological analysis of these cultures during near-zero growth rates. The reason for the differences in lifespan of the filtration units under the different cultivation

conditions is unknown and might be related to differences in the characteristics of secreted proteins and/or other compounds.

Two other kinds of filters were also tested (experiment results were not shown in this thesis): a ceramic filter unit embedding 0.5 µm nanomaterials in the internal surface and a Millipore LAGL04TP6 hydrophilic PVDF filter cartridge (0.22 µm pore size). Unfortunately both of them clogged very quickly (after less than 5 days during N-limited cultivation). Therefore, searching a filtration set up, which can be more widely applied for different cultivation conditions, should be preferentially considered in the perspective of technical improvement of the retentostat setup.

Compared with full biomass retention in a retentostat, a partial cell recycling chemostat (PCRC) cultivation mode would be easier to operate at higher biomass concentrations, as it is less affected by filter clogging issues. Specifically, a PCRC is also a modified chemostat in which biomass can be partially remained in the bioreactor by either filtration, centrifugation or sedimentation (van Mastrigt et al. 2019). Such a system is culture time independent and can reach low or near-zero growth of a microorganism by controlling the feed rate and the recycle ratio. In practice, such a system is much easier and more economical to scale-up for an industrial fermentation processes. Therefore, a PCRC culture is highly recommended to reach microbial near-zero growth for fundamental research as well as industrial applications.

Estimation of maintenance energy requirement (m_s) and specific death rate (k_d)

According to the Herbert-Pirt equation, the biomass-specific substrate consumption rate (q_s) during carbon- and energy-limited near-zero growth cultivation is equal to the maintenance coefficient m_s in case no anabolic products are produced. This is based on the assumption that m_s is growth rate-independent. However, such an assumption has been debated intensively over the years (van Bodegom 2007). Boender (Boender et al. 2009) showed that m_s is independent of the specific growth rate in anaerobic glucose limited chemostat cultures of *S. cerevisiae*. Vos (Vos et al. 2016) applied a regression model, by using data from aerobic glucose limited retentostats of *S. cerevisiae*, to estimate m_s which assumed a first-order death rate (K_d), a constant biomass

yield $Y_{X/S}$ and a growth rate-independent m_s. A good fit of the regression model to the retentostat data was obtained. However, in case of the aerobic low pH carbon-limited cultures described in this thesis (Chapter 3), such a regression model could not fit the biomass data anymore after 10 days of retentostat cultivation, most probably due to a dynamic of the death rate K_d during the cultivation. Obviously, the estimated m_s based on the first 10 days of the cultivation cannot represent the entire culture process. During the carbon excess, N- and P-limited cultures (Chapter 2 and Chapter 3), the non-growth associated energy requirements were estimated from a stoichiometric model which was applied to the data from the pseudo-steady-state towards the end of the retentostat cultivations. Similarly, this does not represent the entire retentostat cultivation either. Both m_s and K_d are important physiological parameters, as accurate values of these two parameters is essential to design a proper process to reach near-zero growth smoothly, meanwhile guaranteeing sufficient nutrient supply for cellular survival. However, for the different retentostat regimes not only large differences in K_d were observed but its value also appeared to change during the cultivations. This hampers the proper estimation of the non-growth associated energy requirements. To further improve the regression model a variable death rate could be introduced. However, this requires knowledge about the underlying mechanisms which is currently not available. Further study on stress related regulation of autophagy and apoptosis is therefore required to elucidate these mechanism and allow extension of the model.

It was observed that the non-growth associated energy requirements in aerobic, non-energy-limited cultures were significantly higher than in aerobic and anaerobic energy-limited retentostats, using the same CENPK113-7D strain (Chapter 2). This may partially be due to futile cycling of $NH4^{+}$ and $PO4^{3-}$ in extreme nitrogen- and phosphorus-limitation, respectively (Cueto-Rojas et al. 2017; Gerasimaitė and Mayer 2016; Marini et al. 1997; Ogawa et al. 2000). Therefore, ^{15}N and ^{32}P labelling experiments could be applied to nitrogen- and phosphorous-limited cultures, respectively, whereby such studies could focus on investigating the extent of cycling of these nutrient and possibly their compartmentalization over cytoplasm and mitochondria. It was found that the maintenance coefficient estimated from carbon-limited aerobic chemostat

cultures was higher at pH 3 than at pH 5. This may have been caused by increased energy requirement to maintain the intracellular pH homeostasis (Martinez-Munoz and Kane 2008), but the underlying mechanism remains unknown and needs further study.

Robustness of yeast microbial host and strain engineering strategies

In general, *S. cerevisiae* is an acidophilic microorganism with an optimal range for growth between pH 4 and 6. We observed that *S. cerevisiae* CENPK113-7D maintained a culture viability above 80 % and a relatively high metabolic activity in carbon-, nitrogen- and phosphorus-limited retentostats at a cultivation pH of 5 (Boender et al. 2009; Vos et al. 2016) (Chapter 2). During similar cultivations at pH 3 the viability was significantly lower (Chapter 3). The transcriptional analysis indicated, in the carbon-limited chemostat cultures, low pH stress triggered genome-wide transcriptional regulation via common (MAPK-) signalling pathways, notably the cell wall integrity (CWI), high osmolality glycerol (HOG) and calcineurin pathways (Chapter 3).

The Engineered SA producing yeast strain (SUC632) also only maintained 25 % culture viability during near-zero growth rate retentostats at pH3. Although this engineered strain appeared capable of producing succinic acid at low to near zero growth rates, the specific production rate was much lower than at higher specific growth rates and seems linearly related to the specific glucose consumption rate. Wahl et al. (Wahl et al. 2017) also observed a significant decreases in SA productivity during near-zero growth conditions in low pH nitrogen starved fed-batch cultivations.

This highlights the needs: (1) to investigate the mechanism through which low pH affects yeast physiology, in particularly cell death; (2) further to increase robustness of yeast cell factories at low pH condition for carboxylic-acid production.

We suggest that corresponding global proteome analysis could be performed to reveal the physiological responses from the protein expression perspective, as well as to investigate whether the previously described transcriptional reprogramming is accompanied by similar changes at the proteome level. The proposed omics analysis by comparing different pH conditions (pH 5 and pH 3), different growth regimes (slow and near-zero) and different nutrient limitations

(C-, N- and P-limitation) could accelerate our understanding of the impact of the cultivation conditions on the physiology of *S. cerevisiae* and provide further leads for strain engineering to improve its robustness at low pH.

A low extracellular pH contributes to a large proton gradient across the cell membrane. Therefore, establishing a solid quantification method of the intracellular pH can demonstrate the proton influx via passive diffusion, ex/intracellular pH homeostasis/heterogeneity, and simultaneously understand the observed physiological responses caused by low extracellular pH. This may also inspire the strategies of strain engineering to improve microbial host robustness.

Single-cell technologies enables to improve the knowledge of the molecular basis of physiology at the level of the population. Therefore, development of proper single cell reporter systems and monitoring equipment (microscopes, microfluidics, sorters) is essential and urgently needed for single cell physiological analysis. Such insights could subsequently guide the directions for rational strain improvement via metabolic engineering.

Bibliography

Abbott DA, Knijnenburg TA, de Poorter LMI, Reinders MJT, Pronk JT, van Maris AJA. 2007. Generic and specific transcriptional responses to different weak organic acids in anaerobic chemostat cultures of *Saccharomyces cerevisiae*. FEMS Yeast Res 7(6):819-833.

Abbott DA, Suir E, van Maris AJA, Pronk JT. 2008. Physiological and Transcriptional Responses to High Concentrations of Lactic Acid in Anaerobic Chemostat Cultures of *Saccharomyces cerevisiae*. Appl Environ Microbiol 74(18):5759-5768.

Abbott DA, Zelle RM, Pronk JT, van Maris AJ. 2009. Metabolic engineering of *Saccharomyces cerevisiae* for production of carboxylic acids: current status and challenges. FEMS Yeast Res 9(8):1123-1136.

Acquisti C, Kumar S, Elser JJ. 2009. Signatures of nitrogen limitation in the elemental composition of the proteins involved in the metabolic apparatus. Proc Biol Sci 276(1667):2605-2610.

Aguilera J, Petit T, de Winde JH, Pronk JT. 2005. Physiological and genome-wide transcriptional responses of *Saccharomyces cerevisiae* to high carbon dioxide concentrations. FEMS Yeast Res 5(6-7):579-593.

Ahn JH, Jang YS, Lee SY. 2016. Production of succinic acid by metabolically engineered microorganisms. Curr Opin Biotechnol 42:54-66.

Ahuja S. 2015. Food, Energy, and Water: The Chemistry Connection. Ahuja S, editor: Elsevier

Alba-Lois L, Segal-Kischinevzky C. 2010. Yeast Fermentation and the Making of Beer and Wine. Nature Education 3(9):17.

Ameen SM, Caruso G. 2017. Lactic acid in food industry. Parisi S, editor: Springer.

Anders S, Pyl PT, Huber W. 2014. HTSeq-a Python framework to work with high-throughput sequencing data. Bioinformatics 31(2):166-169.

Attfield PV. 1997. Stress tolerance: The key to effective strains of industrial baker's yeast. Nat Biotechnol 15:1351-1357.

Baeshen NA, Baeshen MN, Sheikh A, Bora RS, Ahmed MMM, Ramadan HAI, Saini KS, Redwan EM. 2014. Cell factories for insulin production. Microb Cell Fact 13:141.

Bajmoczi M, Sneve M, Eide DJ, Drewes LR. 1998. TAT1 Encodes a Low-Affinity Histidine Transporter in *Saccharomyces cerevisiae*. Mol Cell Biol Res Commun 243:205–209.

Beauprez JJ, De Mey M, Soetaert WK. 2010. Microbial succinic acid production: Natural versus metabolic engineered producers. Process Biochem 45(7):1103-1114.

Becker J, Lange A, Fabarius J, Wittmann C. 2015. Top value platform chemicals: bio-based production of organic acids. Curr Opin Biotechnol 36:168-175.

Beekwilder J, Wolswinkel R, Jonker H, Hall R, de Vos CH, Bovy A. 2006. Production of resveratrol in recombinant microorganisms. Appl Environ Microbiol 72(8):5670-5672.

Bisschops MM, Luttik MA, Doerr A, Verheijen PJ, Bruggeman F, Pronk JT, Daran-Lapujade P. 2017. Extreme calorie restriction in yeast retentostats induces uniform non-quiescent growth arrest. Biochim Biophys Acta 1864(1):231-242.

Bisschops MM, Vos T, Martinez-Moreno R, Cortes PT, Pronk JT, Daran-Lapujade P. 2015. Oxygen availability strongly affects chronological lifespan and thermotolerance in batch cultures of *Saccharomyces cerevisiae*. Microb Cell 2(11):429-444.

Bisschops MM, Zwartjens P, Keuter SG, Pronk JT, Daran-Lapujade P. 2014. To divide or not to divide: a key role of Rim15 in calorie-restricted yeast cultures. Biochim Biophys Acta 1843(5):1020-1030.

Boender LGM, de Hulster EAF, van Maris AJA, Daran-Lapujade PAS, Pronk JT. 2009. Quantitative Physiology of *Saccharomyces cerevisiae* at Near-Zero Specific Growth Rates. Appl Environ Microbiol 75(17):5607-5614.

Boender LGM, van Maris AJA, de Hulster EAF, Almering MJH, van der Klei IJ, Veenhuis M, de Winde JH, Pronk JT, Daran-Lapujade P. 2011. Cellular responses of *Saccharomyces cerevisiae* at near-zero growth rates: transcriptome analysis of anaerobic retentostat cultures. FEMS Yeast Res 11(8):603-620.

Boer VM, Crutchfield CA, Bradley PH, Botstein D, Rabinowitz JD. 2010. Growth-limiting intracellular metabolites in yeast growing under diverse nutrient limitations. Mol Biol Cell 21(1):198-211.

Boer VM, de Winde JH, Pronk JT, Piper MD. 2003. The genome-wide transcriptional responses of *Saccharomyces cerevisiae* grown on glucose in aerobic chemostat cultures limited for carbon, nitrogen, phosphorus, or sulfur. J Biol Chem 278(5):3265-3274.

Boles E, Hollenberg CP. 1997. The molecular genetics of hexose transport in yeasts. FEMS Microbiol Rev 21(1):85-111.

Boorsma A, Nobel Hd, Riet Bt, Bargmann B, Brul S, Hellingwerf KJ, Klis FM. 2004. Characterization of the transcriptional response to cell wall stress in *Saccharomyces cerevisiae*. Yeast 21(5):413-427.

Borodina I, Nielsen J. 2014. Advances in metabolic engineering of yeast *Saccharomyces cerevisiae* for production of chemicals. Biotechnol J 9(5):609-620.

Botstein D, Fink GR. 2011. Yeast: An Experimental Organism for 21st Century Biology. Genetics 189(3):695-704.

Bozell JJ, Petersen GR. 2010. Technology development for the production of biobased products from biorefinery carbohydrates - the US Department of Energy's "Top 10" revisited. Green Chemistry 12(4).

Brandberg T, Gustafsson L, Franzén CJ. 2007. The impact of severe nitrogen limitation and microaerobic conditions on extended continuous cultivations of *Saccharomyces cerevisiae* with cell recirculation. Enzyme Microb Technol 40(4):585-593.

Brauer MJ, Huttenhower C, Airoldi EM, Rosenstein R, Matese JC, Gresham D, Boer VM, Troyanskaya OG, Botstein D. 2008. Coordination of Growth Rate, Cell Cycle, Stress Response, and Metabolic Activity in Yeast. Mol Biol Cell 19(1):352-367.

Brice C, Cubillos FA, Dequin S, Camarasa C, Martinez C. 2018. Adaptability of the *Saccharomyces cerevisiae* yeasts to wine fermentation conditions relies on their strong ability to consume nitrogen. PLoS One 13(2):e0192383.

Buck J, Levin LR. 2011. Physiological sensing of carbon dioxide/bicarbonate/pH via cyclic nucleotide signaling. Sensors 11(2):2112-2128.

Burgard AP, Dien SJV, Burk M; 2011. Methods and organisms for the growth-coupled production of 1,4-butanediol. United States.

Canelas AB, Ras C, ten Pierick A, van Gulik WM, Heijnen JJ. 2011. An *in vivo* data-driven framework for classification and quantification of enzyme

kinetics and determination of apparent thermodynamic data. Metab Eng 13(3):294-306.

Carmelo V, Bogaerts P, Sá-Correia I. 1996. Activity of plasma membrane H^+-ATPase and expression of PMA1 and PMA2 genes in *Saccharomyces cerevisiae* cells grown at optimal and low pH. Arch Microbiol 166:315-320.

Chemler JA, Yan Y, Koffas MA. 2006. Biosynthesis of isoprenoids, polyunsaturated fatty acids and flavonoids in *Saccharomyces cerevisiae*. Microb Cell Fact 5:20.

Chen RE, Thorner J. 2007. Function and regulation in MAPK signaling pathways: lessons learned from the yeast *Saccharomyces cerevisiae*. Biochim Biophys Acta 1773(8):1311-1340.

Chen Y, Nielsen J. 2013. Advances in metabolic pathway and strain engineering paving the way for sustainable production of chemical building blocks. Curr Opin Biotechnol 24(6):965-972.

Chen Y, Nielsen J. 2016. Biobased organic acids production by metabolically engineered microorganisms. Curr Opin Biotechnol 37:165-172.

Cheng TH, Kok BC, Uttraphan C, Yee MH. 2020. Study of yeast and sugar in bio-energy generation. Bulletin of Electrical Engineering and Informatics 9(2):443-451.

Choi D, Gao Z, Jiang W. 2020. Attention to Global Warming. Rev Financ Stud 33(3):1112-1145.

Cipollina C, ten Pierick A, Canelas AB, Seifar RM, van Maris AJ, van Dam JC, Heijnen JJ. 2009. A comprehensive method for the quantification of the non-oxidative pentose phosphate pathway intermediates in *Saccharomyces cerevisiae* by GC-IDMS. J Chromatogr B Analyt Technol Biomed Life Sci 877(27):3231-3236.

Clayton RA, White O, Ketchum KA, Venter JC. 1997. The first genome from the third domain of life. Nature 387:459-462.

Conesa A, Nueda MJ, Ferrer A, Talón M. 2006. maSigPro: a method to identify significantly differential expression profiles in time-course microarray experiments. Bioinformatics 22(9):1096-1102.

Cueto-Rojas HF, Maleki Seifar R, Ten Pierick A, Heijnen SJ, Wahl A. 2016. Accurate Measurement of the *in vivo* Ammonium Concentration in *Saccharomyces cerevisiae*. Metabolites 6(2):12.

Cueto-Rojas HF, Milne N, van Helmond W, Pieterse MM, van Maris AJA, Daran JM, Wahl SA. 2017. Membrane potential independent transport of NH_3 in the absence of ammonium permeases in *Saccharomyces cerevisiae*. BMC Syst Biol 11(1):49.

Daran-Lapujade P, Jansen ML, Daran JM, van Gulik W, de Winde JH, Pronk JT. 2004. Role of transcriptional regulation in controlling fluxes in central carbon metabolism of *Saccharomyces cerevisiae*. A chemostat culture study. J Biol Chem 279(10):9125-9138.

De Deken RH. 1966. The Crabtree Effect: A Regulatory System in Yeast. J Gen Microbiol 44:149-156.

De la Fuente IM, Cortes JM, Valero E, Desroches M, Rodrigues S, Malaina I, Martinez L. 2014. On the dynamics of the adenylate energy system: homeorhesis vs homeostasis. PLoS One 9(10):e108676.

de Lucena RM, Elsztein C, de Barros Pita W, de Souza RB, de Sa Leitao Paiva Junior S, de Morais Junior MA. 2015. Transcriptomic response of *Saccharomyces cerevisiae* for its adaptation to sulphuric acid-induced stress. Antonie Van Leeuwenhoek 108(5):1147-1160.

Della-Bianca BE, de Hulster E, Pronk JT, van Maris AJA, Gombert AK. 2014. Physiology of the fuel ethanol strain *Saccharomyces cerevisiae* PE-2 at low pH indicates a context-dependent performance relevant for industrial applications. FEMS Yeast Res 14(8):1196-1205.

Della-Bianca BE, Gombert AK. 2013. Stress tolerance and growth physiology of yeast strains from the Brazilian fuel ethanol industry. Antonie Van Leeuwenhoek 104(6):1083-1095.

Demain AL, Adrio JL. 2008. Contributions of microorganisms to industrial biology. Mol Biotechnol 38(1):41-55.

Deprez MA, Eskes E, Wilms T, Ludovico P, Winderickx J. 2018. pH homeostasis links the nutrient sensing PKA/TORC1/Sch9 menage-a-trois to stress tolerance and longevity. Microb Cell 5(3):119-136.

Dessie W, Xin F, Zhang W, Jiang Y, Wu H, Ma J, Jiang M. 2018. Opportunities, challenges, and future perspectives of succinic acid production by *Actinobacillus succinogenes*. Appl Microbiol Biotechnol 102(23):9893-9910.

DiCarlo JE, Norville JE, Mali P, Rios X, Aach J, Church GM. 2013. Genome engineering in *Saccharomyces cerevisiae* using CRISPR-Cas systems. Nucleic Acids Res 41(7):4336-4343.

Dobin A, Davis CA, Schlesinger F, Drenkow J, Zaleski C, Jha S, Batut P, Chaisson M, Gingeras TR. 2012. STAR: ultrafast universal RNA-seq aligner. Bioinformatics 29(1):15-21.

Dolz-Edo L, van der Deen M, Brul S, Smits GJ. 2019. Caloric restriction controls stationary phase survival through Protein Kinase A (PKA) and cytosolic pH. Aging Cell 18(3):e12921.

Doney SC, Fabry VJ, Feely RA, Kleypas JA. 2009. Ocean Acidification: The Other CO2 Problem. Annu Rev Mar Sci 1(1):169-192.

Dupres V, Alsteens D, Wilk S, Hansen B, Heinisch JJ, Dufrene YF. 2009. The yeast Wsc1 cell surface sensor behaves like a nanospring *in vivo*. Nat Chem Biol 5(11):857-862.

Eigenstetter G, Takors R. 2017. Dynamic modeling reveals a three-step response of *Saccharomyces cerevisiae* to high CO2 levels accompanied by increasing ATP demands. FEMS Yeast Res 17(1).

Engel SR, Dietrich FS, Fisk DG, Binkley G, Balakrishnan R, Costanzo MC, Dwight SS, Hitz BC, Karra K, Nash RS and others. 2014. The Reference Genome Sequence of *Saccharomyces cerevisiae*: Then and Now. G3 4(3):389-398.

Entian K-D, Kötter P. 2007. 25 Yeast Genetic Strain and Plasmid Collections. Yeast Gene Analysis - Second Edition. p 629-666.

Eraso P, Gancedo C. 1987. Activation of yeast plasma membrane ATPase by acid pH during growth. FEBS Lett 224(1):187-192.

Ercan O, Bisschops MM, Overkamp W, Jorgensen TR, Ram AF, Smid EJ, Pronk JT, Kuipers OP, Daran-Lapujade P, Kleerebezem M. 2015. Physiological and Transcriptional Responses of Different Industrial Microbes at Near-Zero Specific Growth Rates. Appl Environ Microbiol 81(17):5662-5670.

Ercan O, Smid EJ, Kleerebezem M. 2013. Quantitative physiology of *Lactococcus lactis* at extreme low-growth rates. Environ Microbiol 15(8):2319-2332.

Fuchs BB, Mylonakis E. 2009. Our Paths Might Cross: the Role of the Fungal Cell Wall Integrity Pathway in Stress Response and Cross Talk with Other Stress Response Pathways. Eukaryot Cell 8(11):1616-1625.

Fujita K, Matsuyama A, Kobayashi Y, Iwahashi H. 2006. The genome-wide screening of yeast deletion mutants to identify the genes required for tolerance to ethanol and other alcohols. FEMS Yeast Res 6(5):744-750.

Garcia R, Bravo E, Diez-Muniz S, Nombela C, Rodriguez-Pena JM, Arroyo J. 2017. A novel connection between the Cell Wall Integrity and the PKA pathways regulates cell wall stress response in yeast. Sci Rep 7(1):5703.

Gerasimaitė R, Mayer A. 2016. Enzymes of yeast polyphosphate metabolism: structure, enzymology and biological roles. Biochem Soc Trans 44(1):234-239.

Ghaddar K, Krammer EM, Mihajlovic N, Brohee S, Andre B, Prevost M. 2014. Converting the yeast arginine can1 permease to a lysine permease. J Biol Chem 289(10):7232-7246.

Goffin P, van de Bunt B, Giovane M, Leveau JHJ, Höppener-Ogawa S, Teusink B, Hugenholtz J. 2010. Understanding the physiology of *Lactobacillus plantarum* at zero growth. Mol Syst Biol 6(1):413.

Gohil N, Panchasara H, Patel S, Ramírez-García R, Singh V. 2017. Book Review: Recent Advances in Yeast Metabolic Engineering. Front Bioeng Biotechnol 5(71).

Gong Z, Nielsen J, Zhou YJ. 2017. Engineering Robustness of Microbial Cell Factories. Biotechnol J 12(10):1700014.

Goodenough P. 2014 UN Climate Panel Phase Out Fossil Fuels Almost Entirely by 2100. CNSNews.

Gournas C, Evangelidis T, Athanasopoulos A, Mikros E, Sophianopoulou V. 2015. The *Aspergillus nidulans* proline permease as a model for understanding the factors determining substrate binding and specificity of fungal amino acid transporters. J Biol Chem 290(10):6141-6155.

Gournas C, Prévost M, Krammer E-M, André B. 2016. Function and regulation of fungal amino acid transporters: insights from predicted structure. In: Ramos J, Sychrová H, Kschischo M, editors. Yeast membrane transport. Cham: Springer International Publishing. p 69-106.

Gulli J, Cook E, Kroll E, Rosebrock A, Caudy A, Rosenzweig F. 2019. Diverse conditions support near-zero growth in yeast: Implications for the study of cell lifespan. Microb Cell 6(9):397-413.

Guo M. 2020. The Global Scenario of Biofuel Production and Development. In: Mitra M, Nagchaudhuri A, editors. Practices and Perspectives in

Sustainable Bioenergy: A Systems Thinking Approach. New Delhi: Springer India. p 29-56.

Gutteridge A, Pir P, Castrillo JI, Charles PD, Lilley KS, Oliver SG. 2010. Nutrient control of eukaryote cell growth a systems: biology study in yeast. BMC Biology 8(68).

Hakkaart X, Liu Y, Hulst M, el Masoudi A, Peuscher E, Pronk J, Gulik W, Daran-Lapujade P. 2020. Physiological responses of *Saccharomyces cerevisiae* to industrially relevant conditions: slow growth, low pH and high CO_2 levels. Biotechnol Bioeng 117(3):721-735.

Hazelwood LA, Walsh MC, Luttik MA, Daran-Lapujade P, Pronk JT, Daran JM. 2009. Identity of the growth-limiting nutrient strongly affects storage carbohydrate accumulation in anaerobic chemostat cultures of *Saccharomyces cerevisiae*. Appl Environ Microbiol 75(21):6876-6885.

Hensing MCM, Rouwenhorst RJ, Heijnen JJ, van Dijken JP, Pronk JT. 1995. Physiological and technological aspects of large-scale heterologous-protein production with yeasts. Antonie Van Leeuwenhoek 67:261-279.

Hewitt CJ, Nienow AW. 2007. The Scale-Up of Microbial Batch and Fed-Batch Fermentation Processes. Adv Appl Microbiol 62:105-135.

Hong KK, Nielsen J. 2012. Metabolic engineering of *Saccharomyces cerevisiae*: a key cell factory platform for future biorefineries. Cell Mol Life Sci 69(16):2671-2690.

Ibstedt S, Stenberg S, Bagés S, Gjuvsland AB, Salinas F, Kourtchenko O, Samy JKA, Blomberg A, Omholt SW, Liti G and others. 2015. Concerted Evolution of Life Stage Performances Signals Recent Selection on Yeast Nitrogen Use. Mol Biol Evol 32(1):153-161.

Inagaki M, Schmelzle T, Yamaguchi K, Irie K, Hall MN, Matsumoto K. 1999. PDK1 Homologs Activate the Pkc1–Mitogen-Activated Protein Kinase Pathway in Yeast. Mol Cell Biol 19(12):8344-8352.

Isnard A-D, Thomas D, Surdin-Kerjan Y. 1996. The Study of Methionine Uptake in *Saccharomyces cerevisiae* Reveals a New Family of Amino Acid Permeases. J Mol Biol 262:473-484.

Jamalzadeh E. 2013. Transport of Dicarboxylic Acids in *Saccharomyces cerevisiae*. Delft: Delft University of Technology.

Jansen ML, Heijnen JJ, Verwaal R; 2013. Process for preparing dicarboxylic acids employing fungal cells. The Netherlands.

Jansen ML, van Gulik WM. 2014. Towards large scale fermentative production of succinic acid. Curr Opin Biotechnol 30:190-197.

Jørgensen TR, Nitsche BM, Lamers GE, Arentshorst M, van den Hondel CA, Ram AF. 2010. Transcriptomic Insights into the Physiology of *Aspergillus niger* Approaching a Specific Growth Rate of Zero. Appl Environ Microbiol 76(16):5344-5355.

Kaur J, Bachhawat AK. 2007. Yct1p, a novel, high-affinity, cysteine-specific transporter from the yeast *Saccharomyces cerevisiae*. Genetics 176(2):877-890.

Kazemi Seresht A, Cruz AL, de Hulster E, Hebly M, Palmqvist EA, van Gulik W, Daran JM, Pronk J, Olsson L. 2013. Long-term adaptation of *Saccharomyces cerevisiae* to the burden of recombinant insulin production. Biotechnol Bioeng 110(10):2749-2763.

Kolouchova I, Matatkova O, Sigler K, Masak J, Rezanka T. 2016. Lipid accumulation by oleaginous and non-oleaginous yeast strains in nitrogen and phosphate limitation. Folia Microbiol (Praha) 61(5):431-438.

Kuhnert P, Scholten E, Haefner S, Mayor D, Frey J. 2010. *Basfia succiniciproducens* gen. nov., sp. nov., a new member of the family *Pasteurellaceae* isolated from bovine rumen. Int J Syst Evol Microbiol 60(Pt 1):44-50.

Lahtvee P-J, Kumar R, Hallström BM, Nielsen J. 2016. Adaptation to different types of stress converge on mitochondrial metabolism. Mol Biol Cell 27(15):2505-2514.

Lameiras F, Heijnen JJ, van Gulik WM. 2015. Development of tools for quantitative intracellular metabolomics of *Aspergillus niger* chemostat cultures. Metabolomics 11(5):1253-1264.

Lange HC, Eman M, Zuijlen Gv, Visser D, Dam JCv, Frank J, Mattos MJTd, Heijnen JJ. 2001. Improved rapid sampling for in vivo kinetics of intracellular metabolites in *Saccharomyces cerevisiae*. Biotechnol Bioeng 75(4):406-415.

Lange HC, Heijnen JJ. 2001. Statistical reconciliation of the elemental and molecular biomass composition of *Saccharomyces cerevisiae*. Biotechnol Bioeng 75(3):334-344.

Larsson C, Nilsson A, Blomberg A, Gustafsson L. 1997. Glycolytic flux is conditionally correlated with ATP concentration in *Saccharomyces cerevisiae:* a chemostat study under Carbon- or Nitrogen-Limiting conditions. J Bacteriol 179(23):7243-7250.

Larsson C, Stockar Uv, Marison I, Gustafsson L. 1993. Growth and metabolism of *Saccharomyces cerevisiae* in chemostat cultures under carbon, nitrogen, or carbon and nitrogen-limiting conditions. J Bacteriol 175(15):4809-4816.

Lee RA, Lavoie J-M. 2013. From first- to third-generation biofuels: Challenges of producing a commodity from a biomass of increasing complexity. Anim Front 3(2):6-11.

Lesage G, Bussey H. 2006. Cell Wall Assembly in *Saccharomyces cerevisiae*. Microbiol Mol Biol Rev 70(2):317-343.

Levin DE. 2005. Cell Wall Integrity Signaling in *Saccharomyces cerevisiae*. Microbiol Mol Biol Rev 69(2):262-291.

Lidén G, Persson A, Gustafsson L, Niklasson C. 1995. Energetics and product formation by *Saccharomyces cerevisiae* grown in anaerobic chemostats under nitrogen limitation. Appl Microbiol Biotechnol 43(6):1034-1038.

Lindahl L, Genheden S, Faria-Oliveira F, Allard S, Eriksson LA, Olsson L, Bettiga M. 2017. Alcohols enhance the rate of acetic acid diffusion in *S. cerevisiae*: biophysical mechanisms and implications for acetic acid tolerance. Microb Cell 5(1):42-55.

Liu Y, El Masoudi A, Pronk JT, van Gulik WM. 2019. Quantitative Physiology of Non-Energy-Limited Retentostat Cultures of *Saccharomyces cerevisiae* at Near-Zero Specific Growth Rates. Appl Environ Microbiol 85(20):e01161-19.

Longo VD, Shadel GS, Kaeberlein M, Kennedy B. 2012. Replicative and chronological aging in *Saccharomyces cerevisiae*. Cell Metab 16(1):18-31.

Lu C, Brauer MJ, Botstein D. 2009. Slow Growth Induces Heat-Shock Resistance in Normal and Respiratory-deficient Yeast. Mol Biol Cell 20(3):891-903.

Luthfi AAI, Manaf SFA, Illias RM, Harun S, Mohammad AW, Jahim JM. 2017. Biotechnological route for sustainable succinate production utilizing oil palm frond and kenaf as potential carbon sources. Appl Microbiol Biotechnol 101(8):3055-3075.

Madeira A, Leitão L, Soveral G, Dias P, Prista C, Moura T, Loureiro-Dias MC. 2010. Effect of ethanol on fluxes of water and protons across the plasma membrane of *Saccharomyces cerevisiae*. FEMS Yeast Res 10(3):252-258.

Magocha TA, Zabed H, Yang M, Yun J, Zhang H, Qi X. 2018. Improvement of industrially important microbial strains by genome shuffling: Current status and future prospects. Bioresour Technol 257:281-289.

Mans R, Daran JG, Pronk JT. 2018. Under pressure: evolutionary engineering of yeast strains for improved performance in fuels and chemicals production. Curr Opin Biotechnol 50:47-56.

Mans R, van Rossum HM, Wijsman M, Backx A, Kuijpers NGA, van den Broek M, Daran-Lapujade P, Pronk JT, van Maris AJA, Daran J-MG. 2015. CRISPR/Cas9: a molecular Swiss army knife for simultaneous introduction of multiple genetic modifications in *Saccharomyces cerevisiae*. FEMS Yeast Res 15(2).

Marini AM, Soussi-Boudekou S, Vissers S, Andre B. 1997. A family of ammonium transporters in *Saccharomyces cerevisiae*. Mol Cell Biol 17(8):4282-4293.

Martinez-Munoz GA, Kane P. 2008. Vacuolar and plasma membrane proton pumps collaborate to achieve cytosolic pH homeostasis in yeast. J Biol Chem 283(29):20309-20319.

Mascaraque V, Hernáez ML, Jiménez-Sánchez M, Hansen R, Gil C, Martín H, Cid VJ, Molina M. 2013. Phosphoproteomic Analysis of Protein Kinase C Signaling in *Saccharomyces cerevisiae* Reveals Slt2 Mitogen-activated Protein Kinase (MAPK)-dependent Phosphorylation of Eisosome Core Components. Mol Cell Proteomics 12(3):557-574.

Maurer M, Kuhleitner M, Gasser B, Mattanovich D. 2006. Versatile modeling and optimization of fed batch processes for the production of secreted heterologous proteins with *Pichia pastoris*. Microb Cell Fact 5:37.

Melnykov AV. 2016. New mechanisms that regulate *Saccharomyces cerevisiae* short peptide transporter achieve balanced intracellular amino acid concentrations. Yeast 33(1):21-31.

Mendes F, Sieuwerts S, de Hulster E, Almering MJH, Luttik MAH, Pronk JT, Smid EJ, Bron PA, Daran-Lapujade P. 2013. Transcriptome-Based Characterization of Interactions between *Saccharomyces cerevisiae* and *Lactobacillus* in Lactose-Grown Chemostat Cocultures. Appl Environ Microbiol 79(19):5949-5961.

Miller-Fleming L, Giorgini F, Outeiro TF. 2008. Yeast as a model for studying human neurodegenerative disorders. Biotechnol J 3(3):325-338.

Mohd Azhar SH, Abdulla R, Jambo SA, Marbawi H, Gansau JA, Mohd Faik AA, Rodrigues KF. 2017. Yeasts in sustainable bioethanol production: A review. Biochem Biophys Rep 10:52-61.

Mohr A, Raman S. 2013. Lessons from first generation biofuels and implications for the sustainability appraisal of second generation biofuels. Energy Policy 63(100):114-122.

Monod J. 1949. The growth of bacterial cultures. Annu Rev Microbiol 3:371-394.

Nagarajan S, Kruckeberg AL, Schmidt KH, Kroll E, Hamilton M, McInnerney K, Summers R, Taylor T, Rosenzweig F. 2014. Uncoupling reproduction from metabolism extends chronological lifespan in yeast. PNAS:201323918.

Naik SN, Goud VV, Rout PK, Dalai AK. 2010. Production of first and second generation biofuels: A comprehensive review. Renew Sustain Energy Rev 14(2):578-597.

Negishi T, Ohya Y. 2010. The cell wall integrity checkpoint: coordination between cell wall synthesis and the cell cycle. Yeast 27(8):513-519.

Niedenfuhr S, ten Pierick A, van Dam PT, Suarez-Mendez CA, Noh K, Wahl SA. 2016. Natural isotope correction of MS/MS measurements for metabolomics and (13)C fluxomics. Biotechnol Bioeng 113(5):1137-1147.

Nielsen J, Keasling JD. 2016. Engineering Cellular Metabolism. Cell 164(6):1185-1197.

Nijkamp JF, van den Broek M, Datema E, de Kok S, Bosman L, Luttik MA, Daran-Lapujade P, Vongsangnak W, Nielsen J, Heijne WH and others. 2012. De novo sequencing, assembly and analysis of the genome of the laboratory strain *Saccharomyces cerevisiae* CEN.PK113-7D, a model for modern industrial biotechnology. Microb Cell Fact 11:36.

Nueda MJ, Tarazona S, Conesa A. 2014. Next maSigPro: updating maSigPro bioconductor package for RNA-seq time series. Bioinformatics 30(18):2598-2602.

Ogawa N, DeRisi J, Brown PO. 2000. New Components of a System for Phosphate Accumulation and Polyphosphate Metabolism in

Saccharomyces cerevisiae Revealed by Genomic Expression Analysis. Mol Biol Cell 11:4309-4321.

Omura F, Hatanaka H, Nakao Y. 2007. Characterization of a novel tyrosine permease of lager brewing yeast shared by *Saccharomyces cerevisiae* strain RM11-1a. FEMS Yeast Res 7(8):1350-1361.

Orij R, Postmus J, Ter Beek A, Brul S, Smits GJ. 2009. *In vivo* measurement of cytosolic and mitochondrial pH using a pH-sensitive GFP derivative in *Saccharomyces cerevisiae* reveals a relation between intracellular pH and growth. Microbiology 155(1):268-278.

Orij R, Urbanus ML, Vizeacoumar FJ, Giaever G, Boone C, Nislow C, Brul S, Smits GJ. 2012. Genome-wide analysis of intracellular pH reveals quantitative control of cell division rate by pHc in *Saccharomyces cerevisiae*. Genome Biol 13:R80.

Otero JM, Panagiotou G, Olsson L. 2007. Fueling Industrial Biotechnology Growth with Bioethanol. In: Olsson L, editor. Biofuels. Berlin, Heidelberg: Springer Berlin Heidelberg. p 1-40.

Oud B, Guadalupe-Medina V, Nijkamp JF, de Ridder D, Pronk JT, van Maris AJA, Daran J-M. 2013. Genome duplication and mutations in *ACE2* cause multicellular, fast-sedimenting phenotypes in evolved *Saccharomyces cerevisiae*. PNAS 110(45):E4223-E4231.

Overkamp W, Ercan O, Herber M, van Maris AJA, Kleerebezem M, Kuipers OP. 2015. Physiological and cell morphology adaptation of *Bacillus subtilis* at near-zero specific growth rates: a transcriptome analysis. Environ Microbiol 17(2):346-363.

Palma M, Guerreiro JF, Sá-Correia I. 2018. Adaptive Response and Tolerance to Acetic Acid in *Saccharomyces cerevisiae* and *Zygosaccharomyces bailii*: A Physiological Genomics Perspective. Front Microbiol 9(274).

Parrou JL, François J. 1997. A simplified procedure for a rapid and reliable assay of both glycogen and trehalose in whole yeast cells. Anal Biochem 248(1):186–188.

Petitjean M, Teste MA, Francois JM, Parrou JL. 2015. Yeast tolerance to various stresses relies on the Trehalose-6P synthase (Tps1) protein, not on trehalose. J Biol Chem 290(26):16177-16190.

Pfeiffer T, Schuster S, Bonhoeffer S. 2001. Cooperation and competition in the evolution of ATP-producing pathways. Science 292:504-507.

Pinazo JM, Domine ME, Parvulescu V, Petru F. 2015. Sustainability metrics for succinic acid production: A comparison between biomass-based and petrochemical routes. Catalysis Today 239:17-24.

Piper MD, Daran-Lapujade P, Bro C, Regenberg B, Knudsen S, Nielsen J, Pronk JT. 2002. Reproducibility of oligonucleotide microarray transcriptome analyses. An interlaboratory comparison using chemostat cultures of *Saccharomyces cerevisiae*. J Biol Chem 277(40):37001-37008.

Piper P, Mahé Y, Thompson S, Pandjaitan R, Holyoak C, Egner R, Mühlbauer M, Coote P, Kuchler K. 1998. The Pdr12 ABC transporter is required for the development of weak organic acid resistance in yeast. EMBO J 17(15):4257-4265.

Piper PW. 1995. The heat shock and ethanol stress responses of yeast exhibit extensive similarity and functional overlap. FEMS Microbiol Lett 134(2-3):121-127.

Pirt SJ. 1982. Maintenance energy: a general model for energy-limited and energy-sufficient growth. Arch Microbiol(133):300-302.

Pirt SJ. 1997. The maintenance energy of bacteria in growing cultures. Proc R Soc Lond B 163:224-231.

Pohlers S, Martin R, Krüger T, Hellwig D, Hänel F, Kniemeyer O, Saluz HP, Van Dijck P, Ernst JF, Brakhage A and others. 2017. Lipid Signaling via Pkh1/2 Regulates Fungal CO_2 Sensing through the Kinase Sch9. mBio 8(1):e02211-16.

Postma E, Verduyn C, Scheffers WA, van Dijken JP. 1989. Enzymic analysis of the crabtree effect in glucose-limited chemostat cultures of *Saccharomyces cerevisiae*. Appl Environ Microbiol 55(2):468-477.

Ramsay A, Douglas L. 1979. Effects of phosphate limitation of growth on the cell-wall and lipid composition of *Saccharomyces cerevisiae*. J Gen Microbiol 110(1):185-191.

Reifenberger E, Boles E, Ciriacy M. 1997. Kinetic Characterization of Individual Hexose Transporters of *Saccharomyces Cerevisiae* and their Relation to the Triggering Mechanisms of Glucose Repression. Eur J Biochem 245(2):324-333.

Richard L, Guillouet SE, Uribelarrea J-L. 2014. Quantification of the transient and long-term response of *Saccharomyces cerevisiae* to carbon dioxide stresses of various intensities. Process Biochem 49(11):1808-1818.

Robak K, Balcerek M. 2018. Review of Second Generation Bioethanol Production from Residual Biomass. Food Technol Biotechnol 56(2):174-187.

Robinson MD, McCarthy DJ, Smyth GK. 2009. edgeR: a Bioconductor package for differential expression analysis of digital gene expression data. Bioinformatics 26(1):139-140.

Rodríguez-Peña JM, García R, Nombela C, Arroyo J. 2010. The high-osmolarity glycerol (HOG) and cell wall integrity (CWI) signalling pathways interplay: a yeast dialogue between MAPK routes. Yeast 27(8):495-502.

Roelants FM, Torrance PD, Bezman N, Thorner J. 2002. Pkh1 and Pkh2 Differentially Phosphorylate and Activate Ypk1 and Ykr2 and Define Protein Kinase Modules Required for Maintenance of Cell Wall Integrity. Mol Biol Cell 13(9):3005-3028.

Ruiz SJ, van 't Klooster JS, Bianchi F, Poolman B. 2017. Growth inhibition by amino acids in *Saccharomyces cerevisiae*. biorxiv.

Sáenz DA, Chianelli MS, Stella CA. 2014. L-Phenylalanine Transport in *Saccharomyces cerevisiae*: Participation of GAP1, BAP2, and AGP1. J Amino Acids 2014:9.

Sauer UU. 2001. Evolutionary Engineering of Industrially Important Microbial Phenotypes. Metab Eng 73(129):129-169.

Schmelzle T, Helliwell SB, Hall MN. 2002. Yeast Protein Kinases and the RHO1 Exchange Factor TUS1 Are Novel Components of the Cell Integrity Pathway in Yeast. Mol Cell Biol 22(5):1329-1339.

Schmitt ME, Brown TA, Trumpower BL. 1990. A rapid and simple method for preparation of RNA from *Saccharomyces cerevisiae*. Nucleic Acids Res 18(10):3091-3092.

Schreve J, Garrett JM. 1997. The Branched-Chain Amino Acid Permease Gene of *Saccharomyces cerevisiae*, BAP2, Encodes the High-Affinity Leucine Permease (S1). Yeast 13:435-439.

Schwartz R, Ting CS, King J. 2001. Whole Proteome pI Values Correlate with Subcellular Localizations of Proteins for Organisms within the Three Domains of Life. Genome Res 11:703-709.

Seifar RM, Ras C, van Dam JC, van Gulik WM, Heijnen JJ, van Winden WA. 2009. Simultaneous quantification of free nucleotides in complex biological

samples using ion pair reversed phase liquid chromatography isotope dilution tandem mass spectrometry. Anal Biochem 388(2):213-219.

Shah MV. 2016. Dicarboxylic acids transport, metabolism and production in aerobic *Saccharomyces cerevisiae*. Delft: Delft University of Technology.

Silljé HHW, Paalman JWG, Schure EGt, Olsthoorn SQB, Verkleij AJ, Boonstra J, Verrips CT. 1999. Function of trehalose and glycogen in cell cycle progression and cell viability in *Saccharomyces cerevisiae*. J Bacteriol 181(2):396-400.

Sonnleitner B, Käppeli O. 1986. Growth of *Saccharomyces cerevisiae* is controlled by its limited respiratory capacity: Formulation and verification of a hypothesis. Biotechnol Bioeng 28:927-937.

Steel CC, Grbin PR, Nichol AW. 2001. The pentose phosphate pathway in the yeasts *Saccharomyces cerevisiae* and *Kloeckera apiculata,* an exercise in comparative metabolism for food and wine science students. Biochem Mol Biol Educ 29(6):245-249.

Steensels J, Gorkovskiy A, Verstrepen KJ. 2018. SCRaMbLEing to understand and exploit structural variation in genomes. Nat Commun 9(1):1937.

Tai SL, Boer VM, Daran-Lapujade P, Walsh MC, de Winde JH, Daran JM, Pronk JT. 2005. Two-dimensional transcriptome analysis in chemostat cultures. Combinatorial effects of oxygen availability and macronutrient limitation in *Saccharomyces cerevisiae*. J Biol Chem 280(1):437-447.

Taillandier P, Ramon Portugal F, Fuster A, Strehaiano P. 2007. Effect of ammonium concentration on alcoholic fermentation kinetics by wine yeasts for high sugar content. Food Microbiol 24(1):95-100.

Taniguchi M, Wakamiya K, Tsuchiya M, Matsuno R, Kamikubo T. 1983. Continuous ethanol production by cell-holding culture of yeasts. Appl Microbiol Biotechnol 18(4):201-206.

Tavoularis SN, Tazebay UH, Diallinas G, Sideridou M, Rosa A, Scazzocchio C, Sophianopoulou V. 2003. Mutational analysis of the major proline transporter (PrnB) of *Aspergillus nidulans*. Mol Membr Biol 20(4):285-297.

Taymaz-Nikerel H, Jamalzadeh E, Borujeni AE, Verheijen PJT, van Gulik WM, Heijnen JJ. 2013. A thermodynamic analysis of dicarboxylic acid production in microorganisms. In: von Stockar U, van der Wielen LAM,

editors. The Role of Thermodynamics in Biochemical Engineering. New York. p 547-579.

Thomas RC. 1976. The effect of carbon dioxide on the intracellular pH and buffering power of snail neurones. J Physiol 255(3):715-735.

Tijhuis L, Van Loosdrecht MCM, Heijnen JJ. 1993. A thermodynamically based correlation for maintenance gibbs energy requirements in aerobic and anaerobic chemotrophic growth. Biotechnol Bioeng 42(4):509-519.

Tretter L, Patocs A, Chinopoulos C. 2016. Succinate, an intermediate in metabolism, signal transduction, ROS, hypoxia, and tumorigenesis. Biochim Biophys Acta 1857(8):1086-1101.

Trip H, Evers ME, Driessen AJ. 2004. PcMtr, an aromatic and neutral aliphatic amino acid permease of *Penicillium chrysogenum*. Biochim Biophys Acta 1667(2):167-173.

Ullah A, Orij R, Brul S, Smits GJ. 2012. Quantitative Analysis of the Modes of Growth Inhibition by Weak Organic Acids in *Saccharomyces cerevisiae*. Appl Environ Microbiol 78(23):8377-8387.

van Bodegom P. 2007. Microbial maintenance: a critical review on its quantification. Microb Ecol 53(4):513-523.

van Dam JC, Eman MR, Frank J, Lange HC, van Dedem GWK, Heijnen SJ. 2002. Analysis of glycolytic intermediates in *Saccharomyces cerevisiae* using anion exchange chromatography and electrospray ionization with tandem mass spectrometric detection. Analytica Chimica Acta 460(2):209-218.

van Dijken PJ, Weusthuis AR, Pronk TJ. 1993. Kinetics of growth and sugar consumption in yeasts. Antonie van Leeuwenhoek 63:343-352.

van Gulik WM, Heijnen JJ. 1995. A metabolic network stoichiometry analysis of microbial growth and product formation. Biotechnol Bioeng 48(6):681-698.

van Hoek P, van Dijken JP, Pronk JT. 1998. Effect of Specific Growth Rate on Fermentative Capacity of Baker's Yeast. Appl Environ Microbiol 64(11):4226-4233.

van Maris AJ, Konings WN, van Dijken JP, Pronk JT. 2004. Microbial export of lactic and 3-hydroxypropanoic acid: implications for industrial fermentation processes. Metab Eng 6(4):245-255.

van Mastrigt O, Abee T, Lillevang SK, Smid EJ. 2018. Quantitative physiology and aroma formation of a dairy *Lactococcus lactis* at near-zero growth rates. Food Microbiol 73:216-226.

van Mastrigt O, Egas RA, Lillevang SK, Abee T, Smid EJ. 2019. Application of a partial cell recycling chemostat for continuous production of aroma compounds at near-zero growth rates. BMC Res Notes 12(1):173.

Vanrolleghem PA, de Jong-Gubbels P, van Gulik WM, Pronk JT, van Dijken JP, Heijnen S. 1996. Validation of a Metabolic Network for *Saccharomyces cerevisiae* Using Mixed Substrate Studies. Biotechnol Prog 12:434-448.

Varela C, Pizarro F, Agosin E. 2004. Biomass content governs fermentation rate in nitrogen-deficient wine musts. Appl Environ Microbiol 70(6):3392-3400.

Väremo L, Nielsen J, Nookaew I. 2013. Enriching the gene set analysis of genome-wide data by incorporating directionality of gene expression and combining statistical hypotheses and methods. Nucleic Acids Res 41(8):4378-4391.

Verduyn C, Postma E, Scheffers WA, van Dijken JP. 1990. Energetics of *Saccharomyces Cerevisiae* in Anaerobic Glucose-Limited Chemostat Cultures. J Gen Microbiol 136(3):405-412.

Verduyn C, Postma E, Scheffers WA, Van Dijken JP. 1992. Effect of benzoic acid on metabolic fluxes in yeasts: A continuous-culture study on the regulation of respiration and alcoholic fermentation. Yeast 8(7):501-517.

Verduyn C, Stouthamer AH, Scheffers WA, van Dijken JP. 1991. A theoretical evaluation of growth yields of yeasts. Antonie van Leeuwenhoek 59:49-63.

Verheijen PJT. 2000. Data reconciliation and error detection. Smolke C, editor: Boca Raton: CRC Press. p 8.1–8.13.

Vos T, Hakkaart XD, de Hulster EA, van Maris AJ, Pronk JT, Daran-Lapujade P. 2016. Maintenance-energy requirements and robustness of *Saccharomyces cerevisiae* at aerobic near-zero specific growth rates. Microb Cell Fact 15(1):111.

Wada M, Kato J, Chibata I. 1981. Continuous production of ethanol in high concentration using immobilized growthing yeast cells. Appl Microbiol Biotechnol 11(2):67-71.

Wahl SA, Bernal Martinez C, Zhao Z, van Gulik WM, Jansen MLA. 2017. Intracellular product recycling in high succinic acid producing yeast at low pH. Microb Cell Fact 16(1):90.

Werpy T, Petersen G. 2004. Top Value Added Chemicals from Biomass: Volume I - Results of Screening for Potential Candidates from Sugars and Synthesis Gas. National Renewable Energy Lab., Golden, CO (US).

Westfall PJ, Gardner TS. 2011. Industrial fermentation of renewable diesel fuels. Curr Opin Biotechnol 22(3):344-350.

Wu L, Mashego MR, van Dam JC, Proell AM, Vinke JL, Ras C, van Winden WA, van Gulik WM, Heijnen JJ. 2005. Quantitative analysis of the microbial metabolome by isotope dilution mass spectrometry using uniformly 13C-labeled cell extracts as internal standards. Anal Biochem 336(2):164-171.

Yin X, Li J, Shin HD, Du G, Liu L, Chen J. 2015. Metabolic engineering in the biotechnological production of organic acids in the tricarboxylic acid cycle of microorganisms: Advances and prospects. Biotechnol Adv 33:830-841.

Zeikus JG, Jain MK, Elankovan P. 1999. Biotechnology of succinic acid production and markets for derived industrial products. Appl Microbiol Biotechnol 51(5):545-552.

Zelle RM, de Hulster E, Kloezen W, Pronk JT, van Maris AJA. 2010. Key Process Conditions for Production of C_4 Dicarboxylic Acids in Bioreactor Batch Cultures of an Engineered *Saccharomyces cerevisiae*. Appl Environ Microbiol 76(3):744-750.

Zhu X, Garrett J, Schreve J, Michaeli T. 1996. GNP1, the high-affinity glutamine permease of *S. cerevisiae*. Curr Genet 30:107-114.

Publications

Liu Y, el Masoudi A, Pronk JT, van Gulik WM. 2019. Quantitative Physiology of Non-Energy-Limited Retentostat Cultures of *Saccharomyces cerevisiae* at Near-Zero Specific Growth Rates. Appl Environ Microbiol 85(20):e01161-19.

Hakkaart X*, **Liu Y***, Hulst M, el Masoudi A, Peuscher E, Pronk JT, van Gulik WM, Daran-Lapujade P. 2020. Physiological responses of *Saccharomyces cerevisiae* to industrially relevant conditions: slow growth, low pH and high CO2 levels. Biotechnol Bioeng 117(3):721-735. (*Joint first authorship)

Liu Y, Esen O, Pronk JT, van Gulik WM. Uncoupling growth and succinic acid production in an industrial *Saccharomyces cerevisiae* strain. Submitted to the journal Biotechnology and Bioengineering, under review.

Acknowledgement

The Ph.D. journey is far more than delivering this book. All the people that helped, supported, and joined me in this trip and all the good/tough moments that happened in the past 4 years made it a rich and colourful journey.

Jack, I am honoured that you are my promotor. Your critical thinking, perfectionism, and enthusiasm for science have influenced and shaped me to be a researcher. I really enjoyed those every six-weeks progress meetings/discussions in your office, which inspired and motivated me on doing research and tracked me in the right direction of finishing the project. You always timely commented on my manuscripts and polished the language. I appreciated your efforts in my thesis writing. Besides, a big thank you to the lunch walk you initiated for my career development.

Walter, thanks for giving me the opportunity to do a Ph.D. project with you. Your patience and friendliness in the email contact made me not hesitate to take the Ph.D. offer from more than 10 thousand km far away. Thanks for your effortless guide and support in the lab to build up the retentostat fermenters in the first year of my Ph.D. I admired your work style in the lab: precise, organized and patient. I also enjoyed the teaching time with you. We have spent three Easter holidays to correct the exam papers, and I loved those time. I also appreciated the meetings/discussions with you on science, and your efforts on correcting my manuscripts. You rare more than a scientific supervisor, as you have helped fix my broken bike, introduced me Dutch culture, and shared a lot of cooking recipes, etc.

Martin, it was such a nice experience to work with you on proteomic analysis. You always supplied first-time support in the lab as well as in front of the computer for data analysis. I appreciated your help and admired your passion for work.

The members of the Be-Basic FS10 “near-zero growth” project: Pascale, Xavier, Bas, Frank, Phillipp, Alrik, Mickel, and Viktor also contributed to the thesis. Every three months project meetings were always fruitful and inspiring. Pascale and Xavier, without your efforts and collaborations, our joint publication would

never become reality. I appreciated you both for the informative discussions, critical thinking, and writing.

Olga, it was a great scientific collaboration to host you in my Ph.D. project. Thanks for inviting me to Warwick and Exeter for the scientific discussions/presentations. I am motivated to make our collaboration work as a scientific paper in the near future. Besides, you and Iliya were so friendly that hosting me in your lovely home.

Cor, Patricia, Carol, Johan, Silvia, Reza, Angie, thanks for analysing my samples. The work from you has guaranteed the delivery of this thesis.

Dirk and Rob, my amazing fermentation buddies, you were always around whenever my fermenters went wrong. Apart from the professional support, you both were nice to help me so many times to lift my heavy fermenters and move the 50 kg medium vessels.

Eric and Marijke, thanks for hosting me in the IMB lab. Eric, you always kindly helped whenever I encountered an issue in the lab. Marijke, thanks for teaching me to use the flow cytometer and the Z2 counter.

Apilena, Astrid and Jannie, my lovely kitchen ladies, thanks for autoclaving my fermentation stuff, introducing the Dutch culture during lunch break and giving me those nice Dutch and Indonesian recipes.

Marcel, thanks for making the rapid sampling device and filtration device for my experiments, as well as fixed the crippled legs of my fermenters countless times.

My lovely students: Rik, Alexandro, Anissa, and Osman, I enjoyed the lab work, the scientific talks, and meetings with each of you. Anissa, without your contributions, it was impossible to make two articles published.

Adrie, working with you on the live and virtual Chemical Biotechnology bachelor course for three years was a fantastic teaching experience. I have learned a lot from it. Thanks for trusting me and giving me the opportunity.

Jenifer and Anka, our super sufficient moms, thanks for taking care of so many tricky issues outside science during my Ph.D.

Florence, Mariana, and Song, my dearest colleagues and friends, I am so lucky to meet you in Delft. Thanks for your share, care, support, and friendship. I enjoyed our collaborations in the lab, countless talks in a corner of BT building, hangouts and trips, etc.

A big thank you to the CSEers: Francisca, Lucas, Eleni, Koen, Jinrui, Karel, Maxime, Carla, Agi, Joan, Hugo Kleikamp, Aljoscha, Hugo Federico, Mihir, Sushil, Leonor, Robin, Camilo, and Sofia. I enjoyed the scientific as well as social moments with you guys in the last four years: random scientific chats, group meetings, breakfast, cakes, treats, lab cleaning, group hangout, the retreat to Faro, Friday drinks, Santa gift exchange, Xmas Market, etc. Francisca and Julien, thanks for hosting me in Stockholm and organizing the trip to Norway, the 22km hiking to meet Trolltunga was amazing. Lucas, I liked the tennis-playing with you, and your special Brazilian recipe to make a stone bread. Eleni, thanks for your tips for my Greece trip. Hugo Federico, thanks for your help and suggestions on my job hunting.

The joys of the Ph.D. journey also share with other colleagues in BT building: Joana and Susana from BPE, Monica, Emma, Ana Maria, Yimeng, Yuemei and Ingrid from EBT, Pablo and Zhizhen from BTS.

A big thank also goes to the lovely friends I have met during the Ph.D. Lorrie, it is unbelievable that I met you when I travelled alone to Barcelona. We became close friends in one day, it just seemed that we have known each other for years. Those trips with you (the pleasant as well as the thrilling ones), the countless talks, and shared joys and sadness made my Ph.D. life. Ru and Yujie, my best friends in Delft, the laughs, tears, joys, sadness, gossips, arguments, food, wine, short/long trips with you highlighted my life in Delft. My appreciation also goes to two lovely families who have hosted me countless food and joys: Neil, Xiangfen and my lovely little Bubble; Jin and Yun. Sixue and Chunyan, my dearest neighbours and friends in Michiel building, thanks for your care and share, as well as the food, snacks, and wine. Dr. Wang (Zhejian), you were not just a good friend who taught me so many Chinese recipes in my first year Ph.D., but also a supportive colleague. Yuting, my best Dutch classmate and friend. Shupan, Xiaomingming, and Sur.J, it is great to have you around in the Netherlands.

I also want to say thank you to a group of best friends in China, who always contact me by WeChat to share life.

感谢我的父母在我的求学生涯中给与的关爱和帮助。无论在我的学业还是工作中，他们总是一如既往的鼓励，尊重和支持。这本论文的完成也属于他们的功劳。谢谢你们，爸爸妈妈！同时也感谢弟弟一直以来对我学业和择业的支持，并替我承担了很多家庭责任。

Last, it is my dear Nie. Thanks for loving me, always encouraging and convincing me, being patient with me and standing with me. The shared happy/sad moments, the escapes, trips, holidays, adventures make my life. I am prepared for our coming journey.

Curriculum Vitae

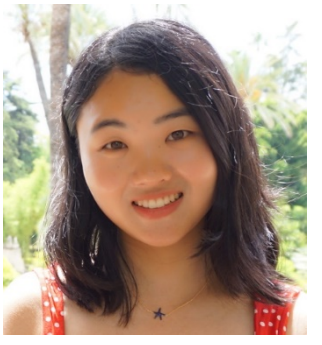

Yaya Liu was born in the Autumn of 1990 in Xinyang, China. After 18 years, Yaya left her hometown and enrolled in the bachelor program Bioengineering in China Three Gorges University, Yichang, China. She received a national scholarship in the second year of her bachelor study. Her early research interest was inspired by her Bachelor research project, in which she studied optimization of the fermentation process of microbial oil production by oleaginous yeast. Subsequently, Yaya performed a bachelor internship at Angel Yeast Co. Ltd in Yichang, China.

In 2012, Yaya moved to East China University of Science and Technology in Shanghai, China for a Biochemical Engineering Master program. During this study, she developed an active interest in biopharmaceutical applications, as reflected by her MSc thesis, which was entitled “Process optimization of antibodies production with DHFR-CHO cells”. The work described in this thesis were the basis for publication in a scientific journal. Yaya was honoured as the “best graduate” of her Master program in the summer of 2015.

In August 2015, Yaya moved to Delft University of Technology to start the Ph.D. project of which the results are described in this thesis and which focused on the subject of uncoupling yeast cell growth and succinic acid production. The project was funded by BE-Basic and the research work was performed in the Cell System Engineering section under the supervision of Dr. Walter van Gulik and Prof. Jack Pronk.

After completing her Ph.D. project, Yaya decided to move from academia to the pharmaceutical industry. Since October 2019, she works at Janssen Pharmaceuticals in Leiden, the Netherlands.